Anomalous Magnetic Moment of the W Boson in Different Models.

by

Gilles Couture

B.Sc., Université Laval, 1980
M.Sc., University of Arizona, 1983
M.Sc., University of Arizona, 1984

A THESIS SUBMITTED IN PARTIAL FULFILLMENT OF

THE REQUIREMENT FOR THE DEGREE OF

DOCTOR OF PHILOSOPHY

in

THE FACULTY OF GRADUATE STUDIES

Department of Physics

We accept this thesis as conforming

to the required standard

THE UNIVERSITY OF BRITISH COLUMBIA

September 1987

In presenting this thesis in partial fulfilment of the requirements for an advanced degree at the University of British Columbia, I agree that the Library shall make it freely available for reference and study. I further agree that permission for extensive copying of this thesis for scholarly purposes may be granted by the head of my department or by his or her representatives. It is understood that copying or publication of this thesis for financial gain shall not be allowed without my written permission.

Department of Physics

The University of British Columbia
1956 Main Mall
Vancouver, Canada
V6T 1Y3

Date 29 September 1987

Abstract.

We consider the anomalous magnetic moment of the W boson, κ, from an experimental and from a theoretical point of view. In the first chapter,we consider five experiments where this parameter could in principle be measured. Our results show that the W pair-production remains the best process to measure κ. Single W production is very sensitive to κ, but it is plagued by very small cross-sections. Photon-electron colliders can also be valuable for measuring κ through single W production. In the second chapter, we consider a composite model where κ is essentially free. We found that it is impossible to rule out such a model from a single measurement of κ. We give detailed production rates for these processes.

In the second half of the thesis, we set limits on the corrections to κ at the one loop level; first in the minimal SM and then in a two-Higgs-doublet model. The main results are that measured corrections of 0.1 would clearly indicate non-perturbative physics while the minimal SM can accommodate corrections up to 0.02. Possible extensions of the SM cannot increase this figure by much: unless one is willing to introduce several extra weakly interacting families, it remains that 75%, or more, of the corrections will arise from the minimal SM.

Table of Contents.

List of Tables.

List of Figures.

Acknowledgement.

It is my pleasure to thank my research supervisor, Dr. J.N. Ng, whose guidance and enthusiasm over the past three years made these calculations, and others, possible.

Many thanks are due to Jean Holt for her help on some of the Feynman diagrams. I wish to thank Brenda Watson for many valuable comments to improve the use of the english language.

This research is supported in part by NSERC of Canada under grant no. A8428.

INTRODUCTION.

Our current understanding of nature recognizes four forces: gravity, experienced by all particles on all scales, the weak and the strong forces that act on the nuclear scales, and the electromagnetic force that acts between charged particles on all scales. One of the greatest achievements of the past forty years has been to build an understanding of the last three forces on a microscopic level. In building the theories to describe the interactions, what became known as the "gauge principle" emerged as the most powerful guideline. The gauge principle can be summarized as follows: by requiring the theories to be invariant under local phase transformations (i.e. transformations that are functions of space and time.) one is naturally led to introduce a vector field, called gauge field. This vector field is seen as the carrier of the force between two particles. Starting from a noninteracting Lagrangian, interaction terms will be generated by the gauge fields. In essence, the gauge principle generates a dynamical theory from a noninteracting one by a suitable choice of gauge fields.

The gauge principle proved extremely successful for quantum electrodynamics (QED), which describes the EM interaction through the common electric charge. In fact, QED was the first quantum theory based on the gauge principle. Many years later, the same technique was used to described the strong interaction between quarks via another charge called colour. This theory is known as quantum chromodynamics (QCD). More important, a unified theory of the weak and EM interactions has been built on the gauge principle by Glashow[1], Weinberg[2], and Salam[3]. Together, QCD and this unified model now form what is known as the Standard Model (SM). The SM is then a gauge theory.

A potential problem that arises in using the gauge principle is that gauge

bosons must be massless because explicit mass terms in the initial Lagrangian spoil gauge invariance, the very essence of the theory. In QED, this is not a problem because electromagnetism is a long range force and requires massless photons. In the case of the weak interaction, the gauge bosons must be very massive in order to explain the short range of the interaction; this mass problem baffled physicists for a long time. The problem was finally solved in a very elegant way using the concepts of internal symmetries and spontaneous symmetry breaking (SSB); this was the work of Goldstone, Higgs and Kibble.

Quite independently, in doing calculations of actual processes, one encounters many divergences. It took many years to find a consistent way to handle these divergences via renormalization involving a careful interpretation of a measurement. This was accomplished mainly by Feynman and Tomonaga in a QED context.

It now appears that nature, for some reasons, is better described by gauge theories.

Except for gravity, we describe nature as being made of Fermions (particle with half integer units of spin.) of two types: the leptons and the quarks. There are three families of each category. Furthermore, the leptons are divided into massive ones (electron, muon, and τ.) and massless ones (their neutrinos.) Massless leptons interact only weakly; massive ones interact weakly and electromagnetically. There are six quarks (up to now, five quarks have manifested themselves in processes.) grouped into three families of two. They carry the colour charge and interact strongly through it. They also interact weakly and electromagnetically. Quarks will bind to form hadrons: either three together to form baryons like the proton or the neutron, or two together to form mesons like the π or the ρ mesons. The forces are carried by the gauge particles, or gauge bosons (the bosons have integer units of spin.) required by the gauge principle. Today's theories require three types of

gauge bosons: the photon for the EM interaction, the W^+, W^-, Z^0 for the weak interaction and eight gluons for the strong force.

As mentioned before, the strong, weak and EM interactions are described by gauge theories. The hope to describe gravity by a gauge theory is partly based on the deep connection between the Christoffel symbol and the gauge fields: they are both introduced to take into account the change of local frames at each space-time point when one wants to compare two vectors or tensors at different space-time points[4]. The Christoffel symbol refers to four-dimensional space while the gauge boson refers to some internal space. The gauge fields or Christoffel symbol tell us how much the coordinate frames change between the two points where we compare the two fields.

The unification of all four forces in a single framework is a grandiose scheme and would crown our understanding of nature. A lot of effort in particle physics is devoted to this project and some recent developments in superstring theories[5] are very promising. However, one may wonder if such a goal will ever be reached, even through a gauge principle, with such disparate forces. Recall that the forces are in the following strength ratio:

$$strong \sim 1$$

$$EM \sim 1/137$$

$$weak \sim 1 \times 10^{-6}$$

$$gravity \sim 1 \times 10^{-40}$$

In spite of this tremendous range, there are reasons to believe in unified theories; one of them being the fact that the strengths are not constant as a function of energy! The theories used to describe the forces refer to internal spaces denoted

by $SU(3)_C \otimes SU(2)_W \otimes U(1)_Y$ where the C stands for colour, W for weak and Y for hypercharge. $SU(3)_C$ describes the strong force and $SU(2)_W \otimes U(1)_Y$ is for the electro-weak model. The SU(N) and U(N) labels describe the gauge group used in the theory. It is the coupling constants of these gauge groups that we can calculate as a function of energy; as they are related to the above-mentioned couplings, these will also change. The use of renormalization group equations shows that the strong coupling of SU(3) decreases when the energy increases. So does the SU(2) coupling. This is known as asymptotic freedom and is cherished by theorists since it has been known for a while that the constituents of the protons seem to behave as "less bound" particles when the energy increases[6,7]. This arises from the fact that the gauge particles also carry the charge: the gluons carry colour, the weak bosons carry the weak hypercharge. Such theories are called non-Abelian. On the other hand, U(1) electromagnetic is Abelian since the photon is neutral. (It is worth mentioning that a group is called Abelian when all its generators commute.) The effect is to increase this coupling constant with energy. So we have two "stronger" coupling constants that get weaker and a "weaker" one that gets larger with increasing energy. Thus, there is justification to think that at some fantastically high energy they will be equal. In fact, the theories predict that they meet at $\sim 10^{15}$ GeV where they are roughly 1/40. One could then treat them as one, single force. It is reasonable to extrapolate and assume that, at still higher energy, gravity will unify with the other three and thereby complete the grand unification of all known nature. This unification will occur at the Planck scale ($\sim 10^{-33} cm$) where the strength of gravity is of order one, definitively out of the perturbative regime.

There is still a very long way to go along this path but a major step was accomplished when the weak and electromagnetic interactions were unified in a single framework by Glashow, Weinberg, and Salam. As mentioned before, QCD and this

model now form the Standard Model (SM). The SM can describe adequately all low energy experiments of today. QCD had its successes, but to the historians of sciences, the seventies and early eighties will appear as the epoch of triumph of the unified model of the EM and weak interactions. This period of fifteen years saw the experimental confirmation of a theory that started more than fifty years ago. Indeed, in 1934 Fermi proposed his theory of the β decay ($n \rightarrow p + e + \bar{\nu}$). In the following years, decays such as $\pi - \mu$, and $\mu - e$ were discovered and found, like β decay, to have a long lifetime. The concept of a distinct class of interactions slowly emerged: the weak interaction. However, the theory proposed by Fermi had major problems: being a point interaction, it has a bad high energy behaviour. (in today's terminology, we would say that the theory is nonrenormalizable.) Nevertheless, at low energy it proved very useful.

After a few years of theoretical meandering, where the form of the coupling was thought to be of tensor type ($\sigma^{\mu\nu}$), a major breakthrough came in 1957 when Wu et al. discovered that parity was violated in weak interactions[8]. The year before, Lee and Yang[9] had discussed this possibility from a theoretical point of view. This crucial experiment led to the famous V-A (vector minus axial vector) formulation of the theory in 1958. (The axial vector part leads to P violation)

At the same period (1957), Schwinger proposed the idea that electromagnetism and the weak interaction (both of vector form) could be unified. The vector form of both theories is very profound and a good clue that unification is sensible. Indeed, a vector boson can lead to attractive and repulsive interactions while a scalar boson, for example, allows attractive interactions only. Therefore, this connection refers to the very essence of an interaction. Besides, QED had proved extremely successful already and the idea was certainly appealing. In the weak ineraction *à la* QED, one would have gauge bosons that mediate the force, the analog of the photon in

QED. These vector bosons, contrary to the photon, would have to be very massive to account for the very short range of the weak interaction. However, mass terms are highly undesirable in the initial Lagrangian because they spoil renormalizability and gauge invariance. Glashow, in 1961, proposed a unified model based on the $SU(2) \otimes U(1)$ symmetry. His model did not have any mechanism to generate masses for the gauge bosons; the mass terms were explicitly included in the initial Lagrangian. His model was therefore nonrenormalizable and could not predict the relative strength of the vector boson interactions. This mass problem made impossible a satisfying unification of the weak and E.M. interactions for many years. One had to wait for the idea of spontaneous symmetry breaking (SSB) by Goldstone[10] and the Higgs-Kibble mechanism[11]. Goldstone showed that SSB generates a massless boson (Goldstone boson) for each broken symmetry. The Higgs-Kibble mechanism, on the other hand, allows the massless gauge bosons of the initial Lagrangian to absorb these Goldstone bosons and become massive. One can then start from a Lagrangian that has no explicit mass terms for the gauge bosons and end up with massive ones while preserving renormalizability and gauge invariance.

It was Weinberg in 1967 and Salam, independently in 1968, who made good use of these ideas and built a "satisfying" model of the electro-weak theory. They introduced a complex doublet of scalar fields whose goal was uniquely to break the symmetry of the ground state and give masses to the other particles. The model was not quite satisfying because renormalizability remained to be proved. This was done in a very general manner in 1971 by 't Hooft[12] who proved that Yang-Mills type gauge theories, with unbroken gauge symmetries or SSB, are renormalizable. So, the model built by Weinberg and Salam was renormalizable. Later on, it was also shown explicitly that the anomaly term originating from the lepton sector was

exactly cancelled by the quarks' contribution! (See Appendix VI for a discussion of the anomaly.) Note here that this anomaly cancellation was used later as a requirement for a third quark family, following the discovery of a third lepton family; another requirement for a third family stems from CP violation[13]. The model also has strong predictive power because all the vertices are well defined (through the well measured Fermi constant). The fundamental unknowns of the model are the mass of the Higgs boson (the field that is not absorbed by the original gauge bosons) and the mixing angle between the gauge bosons, expressed as $sin^2(\theta_W)$. This last angle measures the amount of P violation in the theory and is a measure of the relative strengths of different gauge boson interactions. These two paramters *must* be determined experimentally.

So, a self-consistent, renormalizable model that unifies the E.M. and weak interactions was available in 1971. Still, the most important question remained. Does this model have anything to do with nature? All that was known about the weak interaction was that only left-handed particles participate in the weak interaction and one unit of electric charge is exchanged during the process. A lot of models can fit this description!

The first strong experimental confirmation of the SM came in 1973 from the Gargamelle collaboration (Hasert et al.)[14]. This experiment, for the first time, observed some weak neutral current effects and experimental results agreed with the SM. It also ruled out a model by Georgi and Glashow where the Z^0 boson was absent.

Although the SM was a very strong candidate after the Gargamelle experiment, its phenomenological parameter $sin^2(\theta_W)$ remained to be measured. This was quickly understood to be a critical test of the model because it can be measured from a variety of experiments and must be universal to all of them. Indeed,

this parameter will appear in all couplings that involve weak bosons and fermions. Therefore, lepton or hadron experiments are candidates to measure it. For the following ten years, experimentalists measured $sin^2(\theta_W)$ as accurately as possible. One should mention the Gargamelle, Aachen-Padua, Columbia-Brookhaven, and CHARM collaborations. Some of the results are listed in Table I [ref. 15]. This table spans more than ten years of hard work. The values of $sin^2(\theta)$ are all consistent within the errors. This is certainly a confirmation of the universality of the parameter and a very strong indirect confirmation of the SM – indirect, because one measures the effects of the $W^{\pm}$ and Z^0 bosons without really observing them.

These gauge bosons are the essential, new feature of the SM. In order to definitely confirm the SM, one would have to observe them directly. The main problem is their masses: the $W^{\pm}$ was predicted to be approximately $83GeV/c^2$ and the Z^0 to be approximately $94GeV/c^2$. Carlo Rubbia understood this clearly and undertook the task of producing such heavy particles; pioneering the beam colliders idea and technology. The discovery in 1983 at CERN of these particles[16] gave him and Simon van der Meer the Noble prize of physics of 1984. This dicovery was the most spectacular confirmation of the SM and provided the statement that the SM relates to nature.

Future experiments to measure very precisely the anomalous magnetic moment of the muon could also show the weak interaction effects; although the theoretical calculations are plagued by large uncertainties in the hadron sector[17].

Given all of this, one might be misled to think that everything is fine with the SM and that we understand what is happening in these reactions. As we will describe next, there are many fundamental problems with the SM as it now stands.

The most serious problem lies in the Higgs sector. The Higgs particles are very successful means of breaking the symmetry and giving masses to other par-

TABLE I

$Sin^2(\theta_W)$ from different experiments.

Processes	$Sin^2(\theta_W)$
$\nu_\mu + N \rightarrow \nu_\mu + ANY$	0.229 ± 0.090 0.230 ± 0.023
$\nu_\mu + p \rightarrow \nu_\mu + p$	0.26 ± 0.06
$\nu_\mu + N \rightarrow \nu_\mu + N + \pi^0$	0.22 ± 0.09
$\bar{\nu}_\mu + N \rightarrow \bar{\nu}_\mu + N + \pi^0$	$0.15 - 0.52$
$e^- + d \rightarrow e^- + ANY$	0.224 ± 0.020
$\bar{\nu}_\mu + e^- \rightarrow \bar{\nu}_\mu + e^-$	$0.23 \left\{ \begin{matrix} +0.09 \\ -0.23 \end{matrix} \right.$
$\nu_\mu + e^- \rightarrow \nu_\mu + e^-$	$0.22 \left\{ \begin{matrix} +0.08 \\ -0.05 \end{matrix} \right.$
$\bar{\nu}_e + e^- \rightarrow \bar{\nu}_e + e^-$	0.29 ± 0.05
$e^+ + e^- \rightarrow (e^+e^-) \quad (\mu^+\mu^-)$	0.25 ± 0.15

Different values of $Sin^2(\theta_W)$ from different processes. All values agree within errors. This suggests universality of the weak mixing angle and confirms the SM.

ticles but they seem *extra* in the sense that they do not carry any force and do not form any normally observed matter. Their only *raison d'être* is to break the symmetry. Besides, the SM cannot predict the mass of the Higgs boson (remnant of the original symmetry.) and this corner stone of the model has not been observed yet. The combination of SSB and Higgs-Kibble mechanism is the only way we know to generate masses for gauge particles without breaking gauge symmetry; so the Higgs particles will appear in any renormalizable gauge theory. One solution to this problem is to assume that the Higgs are composites; made of more fundamental particles called preons[18]. This is the philosophy of models like technicolour. However, these models have problems on their own and no successful one has been built yet.

Another important question refers to the mixing of the gauge bosons: why is $sin^2(\theta_W) \approx 0.215$? It would be nice to have an explanation for this small (large ?) value. The grouping of the fermions in three families seems also *ad hoc*. Again one would like to know why to group them in this way except "because it works" and why there are only three families; maybe there are more than three... Some Grand Unified Theories (GUT) can answer these questions but another important problem arises: the hierarchy problem[19]. The GUT scale is typically $10^{14} - 10^{16}$ GeV; this is the scale where the strong and the electro-weak forces unify into a single force. The question regards these two scales. If one wants to use perturbation theory and obtain a reliable answer, the mass of the Higgs particles must be less than $1TeV/c^2$. (See Appendix VIII.) The GUT scale is $\sim 10^{15}$ Gev so that the GUT scalar particles have masses of this order. The question is then to explain why some scalar particles are super-heavy while another one is rather light. Besides, if we suppose that some mechanism can give a very small mass to one of the scalar particles, higher order corrections require to tune some parameters of the theory to

$\sim 12 - 14$ significant figures. This is not very satisfying.

One elegant way to solve the "extra" character of the scalars and the hierarchy problem is to work with supersymmetries (SUSY)[20]. These theories treat the fermions and bosons on the same footing and postulate a SUSY partner for every particle of the SM. Thus the appearance of scalars is natural, being associated with the fermions of spin-1/2. The hierarchy problem is solved by some critical cancellations that occur between the fermions and bosons partners.

Another important problem regards CP-violation. Since its discovery[21] in 1964 it is still waiting for a "natural" explanation in the SM framework[22,23]. One possible solution was proposed by Kobayashi and Maskawa[13]. Their suggestion is very similar to the Cabibbo mixing process[4] where one postulates mixing between the d and s quarks in order to explain some strangeness-violating processes. In order to explain CP-violation, the Kobayashi-Maskawa mechanism requires three families of quarks. This third family of quarks seems *ad hoc* in the sense that its only justifications are some experiments that one tries to explain. It is not required by any symmetry or basic principle of the model. This goes back to the question as to how many families of fermions there are; the model cannot answer this question. From a consistency point of view, a stronger requirement for a third family of quarks is the discovery of a third family of leptons: one must require a third family of quarks in order to have anomaly cancellation. This argument is not entirely satisfying because one cannot use it to obtain a limit on the number of fermion families.

Finally, one starts with so many initial parameters (~ 20), including two coupling constants, that one cannot escape a "bitter aftertaste". These two coupling constants mean that the model is not really a unification of the two interactions: a satisfying unified model would have one coupling constant. Here, they are re-

lated through the weak mixing angle but the fact that the angle *must* be obtained experimentally makes them irreconcilable.

All those considerations have led most physicists to see the SM as a low energy limit of a more global theory. This global theory, hopefully, will deal with only one coupling constant, very few initial parameters and answer the previous questions. As of now, the price to pay on those more global theories is a lot of freedom in the initial parameters and a very weak predictive power. There is no experimental evidence to support any of the models and a handful of experiments ,such as proton decay, neutrino oscillation and neutrino masses, are relevant for these theories. The non-observation of proton decay has ruled out models based on minimal SU(5) [ref. 24]; neutrino oscillations experiments have been negative up to now[25] and neutrino masses have been very controversial[26]. There is some hope however that data from the new supernova, SN1987A, will set tight limits on neutrino masses[27].

From this point of view, it becomes relevant to probe the SM in its fine details and hopefully find some experimental discrepancy with the next generation of accelerators. The new machines, planned to start to run in the late eighties and early nineties (LEP, SLC, SSC), are designed to study in detail the W and Z bosons that were only glimpsed at by the CERN teams, and possibly to discover heavier particles. The first experiments will obviously measure the mass and width of the W and Z as precisely as possible. The mass is a good probe of the SM since it is well defined and involves non negligible radiative corrections[28]. Similarly, the width depends on the number of fermion families available, their masses and the couplings; all well defined quantities in the SM.

A more sensitive probe of the SM is the mass ratio[29] $\rho \equiv M_W^2/M_Z^2 cos^2(\theta_W)$ where θ_W is the weak mixing angle. In the SM this ratio is identically 1. Any deviation from 1 is a drawback for the SM. As of now, the experimental value of

$\rho = 0.992 \pm 0.020$ is in good agreement with the model.

Another sensitive probe of the SM are the three-boson vertices[30,31]: γW^+W^- and $Z^0W^+W^-$. They are very important because their ratio depends on properties like renormalizability. The couplings arise from the following terms of the Lagrangian:

$$\mathcal{L} = -\frac{1}{4}F^i_{\mu\nu}F^{i\mu\nu} + (\mathcal{D}_\mu\Phi)(\mathcal{D}_\mu\Phi) \qquad (I.1)$$

where

$$F^i_{\mu\nu} \equiv \partial_\nu A^i_\mu - \partial_\mu A^i_\nu + g\varepsilon_{ijk}A^j_\mu A^k_\nu$$

and

$$\mathcal{D}_\mu \equiv \partial_\mu - i\frac{g'}{2}B_\mu - i\frac{g}{2}\vec{\tau}\cdot\vec{A}_\mu$$

with A_μ and B_μ being the SU(2) and U(1) gauge fields, respectively.

From this, using the definitions of the real γ, Z^0, and $W^\pm$ fields in terms of the SU(2) and U(1) fields, one derives the couplings in momentum space (i.e. Fourier transform of the Lagrangian density.) as:

$$\Gamma^{\mu\nu\lambda} = -ie\Big\{(k_1-k_2)^\lambda g^{\mu\nu} + (k_2-k_3)^\mu g^{\nu\lambda} + (k_3-k_1)^\nu g^{\lambda\mu}\Big\} \qquad (I.2)$$

and

$$Z^{\mu\nu\lambda} = -igcos(\theta_W)\Big\{(k_1-k_2)^\lambda g^{\mu\nu} + (k_2-k_3)^\mu g^{\nu\lambda} + (k_3-k_1)^\nu g^{\lambda\mu}\Big\} \qquad (I.3)$$

where k_1, k_2, k_3 are the momentum of the incoming photon,(or Z^0)W^+, W^- bosons, respectively, as shown on fig. 1. These vertices are obviously well defined as are their relative strengths: $\sim cotg(\theta_W)$. Since the W boson is a spin-1 particle, it will interact[32] via its charge (e), its magnetic moment ($\mathcal{M}$), and also its electric

Figure 1. Three-boson vertex.

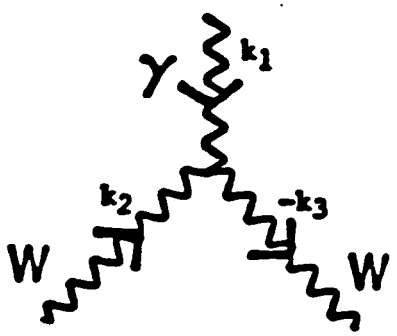

Vertex that involves three gauge bosons. This vertex depends on the magnetic moment of the W boson, κ, when the neutral boson is the photon. The neutral gauge boson could also be the Z^0 boson.

quadrupole moment (Q_E). From the previous form of $\Gamma^{\mu\nu\lambda}$, one derives[33] the magnetic moment of the W boson to be:

$$\mathcal{M} = 2\left(\frac{e}{2M_W}\right)$$

and its quadrupole moment:

$$Q_E = -\frac{e}{M_W^2}.$$

If one allows for an anomalous magnetic moment parameter, κ, following Lee and Yang[34], (which amounts in our case to writing κ in front of the photon momentum.) these quantities become:

$$\mathcal{M} = (1+\kappa)\left(\frac{e}{2M_W}\right) \qquad Q_E = -\frac{e\kappa}{M_W^2}$$

We emphasize again that $\kappa \equiv 1$ at tree level in the SM. These two vertices are crucial to the SM because all the parameters are well defined and, above all, they probe the gauge sector of the theory. The gauge sector also involves four-boson vertices but those are higher order and will be much more difficult to measure. For example, the $W^+W^-\gamma Z^0$ vertex would appear to lowest order in a W boson collision process! So, the three-boson vertices are essentially the first probe of the gauge sector of the SM. In the same way, κ is the ideal probe of the vertices since it is identically one at tree level. Therefore, one should think of ways to measure this variable. The Penning trap methods[35] used for the measurement of (g-2) of the electron or the precession methods[36] used for the measurement of (g-2) of the muon will not work here, because of the very short life of the W boson: $\tau \sim 10^{-24} sec.$ We will not consider the possible extension of τ via a time dilation factor. Only one possibility remains: to measure carefully processes that involve the γW^+W^- or the $Z^0W^+W^-$ vertices and see how one can extract κ from rates or angular distributions.

In principle, one could also extract κ from a precise measurement of the electric quadrupole moment of the W. However, such a measurement would be highly non trivial since the W is charged and the quadrupole moment interacts with the electric field gradient. We will not consider this possibility any further.

Certainly, κ is one at tree level in the SM. Also certainly, this parameter will be altered by loop corrections. (By tree level we mean a diagram where all internal momenta are well defined given all external momenta as opposed to a loop diagram where some of the internal momenta remain free and imply an integral over the allowed range.) The SM being a weakly interacting theory, the corrections are expected to be of order (α/π) so that κ will become $1 + \mathcal{O}(\alpha/\pi)$. This is in strong contrast with composite models, for example, where κ can be as large as 4 or 5 [ref. 37]. Besides, in these models (composite) the γW^+W^- and the $Z^0W^+W^-$ vertices are in principle independent and do not have to appear in a well defined ratio as in the SM.

It is the goal of this thesis to study these vertices and more particularly the anomalous magnetic moment of the W-boson in the SM and beyond. One of the main goals is to set some limits on its value in different models and see the implications of any experimental discrepancy. Of course, if some experimentalists were to measure $\kappa \approx 2$, it would be a big setback for the SM. But how would a measured value of 1.08 be assessed? Could the SM account for it? Could some other models also explain such a value for κ? Such questions will be addressed in the thesis. We will also discuss some experiments where one could measure the strengths of the three-boson vertices and κ.

The thesis is divided as follows. In chapter I, we will describe a few experiments where the three-boson couplings could be measured. We will first emphasize three processes that we calculated in the SM framework. Then, we will extend the

discussion to other reactions investigated by others. As we will see, very few processes are available to measure these vertices. These cross-sections and other results become our benchmarks for future comparisons. In chapter II, following a model by Hung and Sakurai, we will consider a non-standard γW^+W^- and $Z^0W^+W^-$ coupling model. This model is very close to composite models where κ is essentially free and the two types of vertices are unrelated. We will see that this model can mimic very well the SM; making its identification all the more difficult. From other predictions of such models, unaddressed in this work, one should be able to rule out or confirm these models.

The first two chapters consider κ from an experimental point of view; the next two will be purely theoretical. In chapter III, we calculate one-loop corrections to κ in the SM context. This again will be our benchmark for other models. The new feature here is to consider massive loop particles. As we will see, the mass of the top quark is a very important parameter and one can at best give a range for κ until the mass is well known. In chapter IV, we extend the model by adding one Higgs doublet and calculate the same type of corrections. This is the minimal extension of the SM; and is the first step towards supersymmetry. As we will see later, these models have to obey some nontrivial constraints and are certainly interesting in their own rights. As it turns out, they do not change the results obtained in the SM by much.

The main point of the last two chapters is to set limits on the corrections to κ in different models and anticipate the meaning of possible future experimental discrepancies with the SM. It is hoped that these discrepancies will be precise enough and large enough to give us a good clue as to where to look for physics beyond the SM. There will be conclusions at the end of each chapter and in a last section, we will summarize and highlight the most important results of the thesis.

Chapter I

Some Experiments to Measure κ.

1.1 Introduction

In this chapter, we will describe a few experiments where κ could in principle be measured. We will mainly concentrate on electron colliders since these machines have very little background compared to hadron colliders. Besides, our results are very relevant since the new generation of such machines will start running this year or within the next few years: SLC will start running in the fall of 1987, LEPI will follow in the spring of 1988 and LEPII should be ready for 1990.

The processes we will discuss are the following:

$$e_R^- \; e^+ \rightarrow W^- \; e^+ \; \nu_e$$

$$e^\pm \; \gamma \rightarrow W^\pm \; \nu_e$$

$$e^+ \; e^- \rightarrow W^+ \; \bar{\nu}_e \; e^-$$

$$e^+ \; e^- \rightarrow W^+ \; W^-$$

radiative zeros

where we have investigated the first three processes in detail and will present our results. As these calculations were performed in the SM framework, the reader is referred to Appendix I for a review of the model and a list of the relevant couplings. The fourth process has been investigated very extensively and one can say that it is the process that everyone will study with the new machines. We will quote the main results of other groups. The radiative zeros cover a whole class of processes where an interesting zero of radiation of intensity occurs. This zero depends critically on

κ – therefore is relevant to us. The last two processes are included for completeness, as we did not perform any calculations on these.

In order to avoid any confusion, we note here that when we write "left-handed particle" we mean a particle whose state is obtained by the projection operator $(1 - \gamma_5)/2$; a state where the spin is antiparallel to the momentum[38]. In the ultrarelativistic limit, this is a good quantum number.

1.2 $e_R^- \; e^+ \rightarrow W^- \; e^+ \; \nu_e$

Here, we study a polarized $e^- \; e^+$ beam in a reaction whose rate is dependant on κ. The purpose of polarizing the beam[39−41] is to get rid of all t-channel diagrams, due to the left-handedness of the theory. Hopefully this will enhance the effect of κ. The only remaining diagrams are s-type and shown on fig. 2. The advantage of looking for a single W production is to lower the threshold of the process. The obvious drawback is having to deal with three vertices, and therefore a greatly reduced cross-section. Since there are no t-channel diagrams, there is no hope of increasing the rate via a particle exchange pole in the amplitude. Therefore, one expects very small cross-section but hopefully large effects due to κ.

In working on this process, it proved very useful to group the diagrams as shown in fig. 2. The reader is referred to Appendix II for some details of the calculation. Since the photon and Z^0 boson have the same type of couplings, one can enlarge the effective coupling and treat these two particles as a single one with a mixed coupling. Thus, one really deals with three diagrams instead of five. This greatly reduces the effort; only three squared terms and six interference ones. We worked in the unitarity gauge: all physical fields, no ghost, but difficult propagators for the gauge bosons. The calculation is straightforward but very tedious.

The polarization vectors we used for the gauge bosons were the following:

$$\begin{aligned}
\varepsilon_1 &= \big(0, cos(\theta)\ cos(\phi), cos(\theta)\ sin(\phi), -sin(\theta)\big) \\
\varepsilon_2 &= \big(0, -sin(\phi), cos(\phi), 0\big) \\
\varepsilon_3 &= \big(P, E\ sin(\theta)\ cos(\phi), E\ sin(\theta)\ sin(\phi), E\ cos(\theta)\big)/M
\end{aligned} \tag{1.1}$$

where the angles are the standard spherical coordinates angles. In addition, P

is the 3-momentum of the particle and E is the energy of the particle of mass M. This is a well known form for polarization vectors[42]. There was some interest in treating the polarizations independently since this can lead to useful information. Obviously, the summation of the three partial cross-sections lead to the total cross-section. One has some freedom in the choice of polarization vectors; all one really needs is $\varepsilon_i \cdot \varepsilon_j = -\delta_{ij}$ and $\varepsilon_i \cdot q = 0$ where q is the four momentum of the particle. Certainly, an appropriate choice will relate in an easier way to the experimental observables[30,43].

The final integrals were done numerically by Monte Carlo methods. The reader is referred to Appendix III for some details. The matrix element was calculated by hand and verified by a computer routine: REDUCE. This matrix element is then fed into the Monte Carlo routine. The expression for the matrix element is far too long to be written here.

In fig. 3, we give the total cross-section of the process as a function of the beam energy for different values of κ. Recall that $\kappa \equiv 1$ in the minimal SM. The main features are clear: the cross-section increases with κ but the fact that the values are paired on the range of energy studied will not make its unique determination an easy task. Due to constraints from (g-2) experiments on leptons[44], we limited the calculation to $|\kappa| \leq 3$. Note also that our results are for one lepton family. If the experiment were sensitive to all possible leptons, our answer should be multiplied by three. Obviously, this factor of three will not be enough to increase the cross-section to large values and σ will remain hopelessly small from an experimental point of view; due to lack of luminosity. The only relevance of fig. 3, is that any data point with reasonable error bars would give a very good idea of the numerical value of κ.

In fig. 4, we give the angular distribution of the outgoing particles. These

distributions are rather insensitive to the beam energy or κ; at best, the neutrino and the electron are exchanged in the distributions. Again, due to the smallness of the cross-section, one would not attempt to isolate such distributions but rather add all events. The main point here is to show that the particles are emitted at large angles, which should facilitate their detection. It is also a characteristic of s-channel diagrams.

Finally, one should note that the reaction proceeds via both the γW^+W^- and the $Z^0W^+W^-$ vertices. Therefore, the effect of κ is "contaminated" by the weak neutral vertex. One would have to know precisely the $Z^0W^+W^-$ coupling in order to extract the γW^+W^- coupling from this experiment. One could also proceed the other way around and extract the weak neutral vertex, given the electromagnetic one.

Figure 2. Feynman Diagrams in the Process $e_R^- \; e^+ \rightarrow W^- \; e^+ \; \nu_e$.

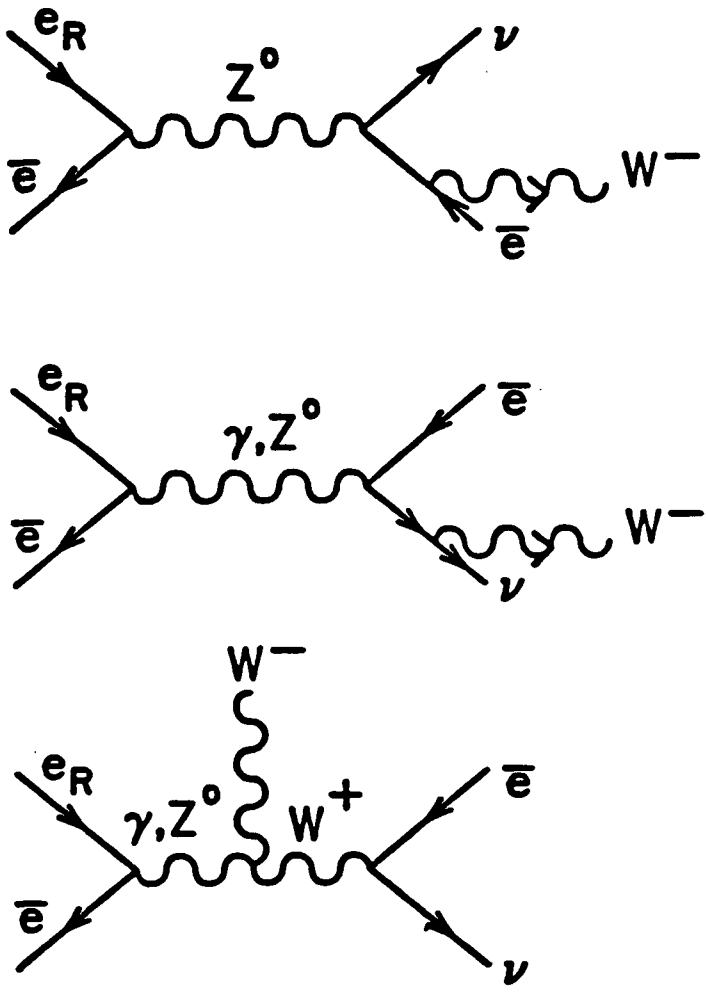

The five Feynman diagrams that represent the process $e_R^- \; e^+ \rightarrow W^- \; e^+ \; \nu_e$ can be grouped as shown here. The notation γ, Z^0 represents two diagrams: one diagram with the photon and one with the Z^0 boson. This grouping greatly reduces the algebra.

Figure 3. Cross-section for the Process $e_R^- \; e^+ \rightarrow W^- \; e^+ \; \nu_e$ in the SM.

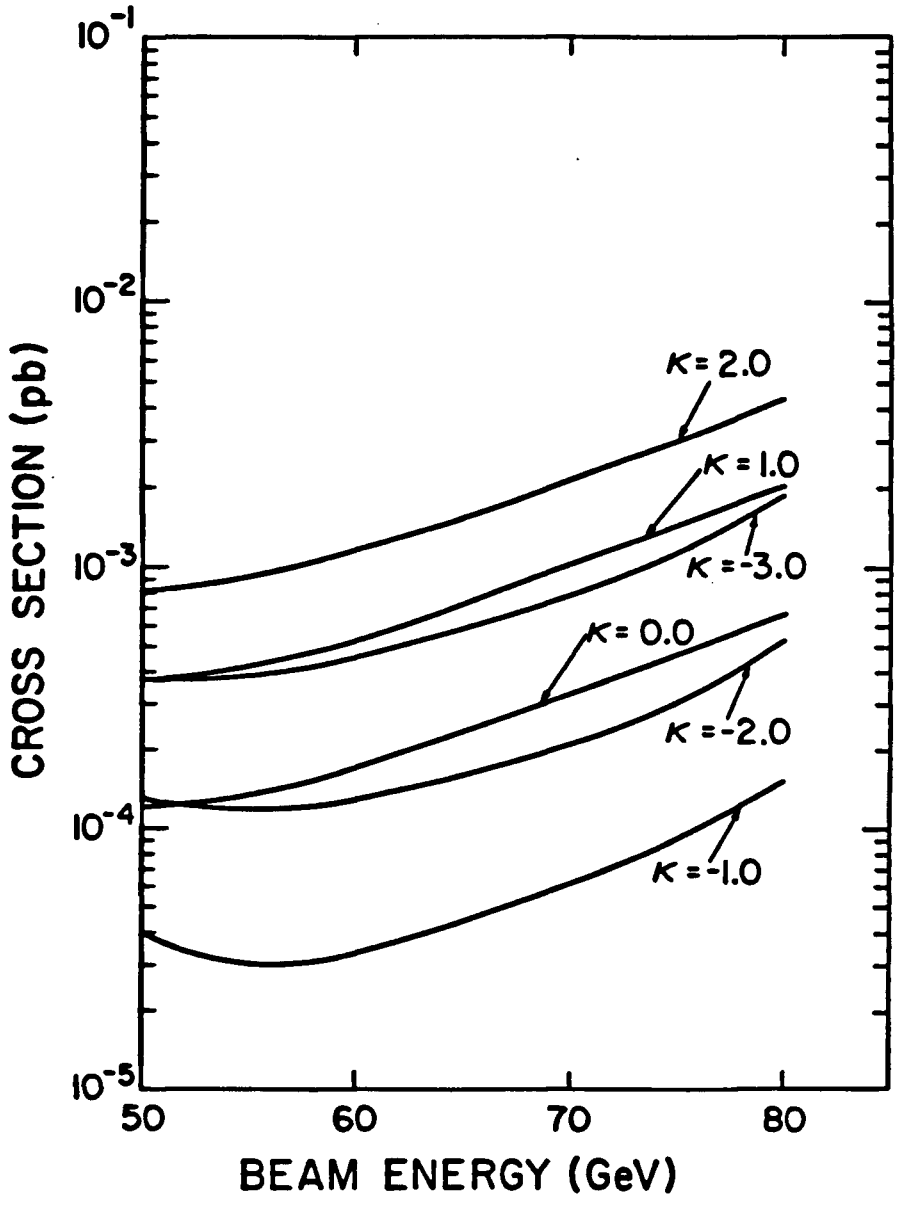

Cross-section of the process as a function of beam energy for different values of κ. Note the strong dependence of the cross-section on κ but also the very small cross-section. The results appear to be paired but on a larger range of beam energies, this pairing does not hold.

Figure 4. Angular distributions in the process $e_R^- \; e^+ \rightarrow W^- \; e^+ \; \nu_e$.

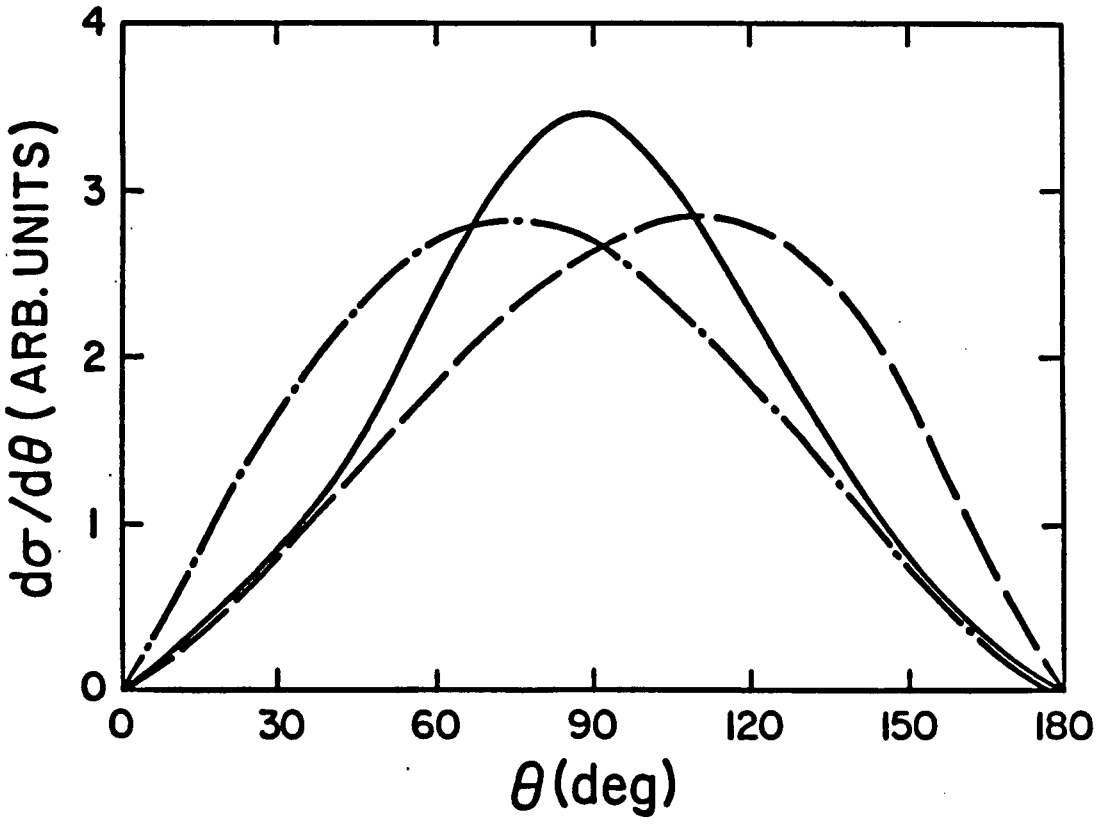

Angular distribution of the outgoing particles: the W^- (continuous line), the positron (dash line), and the neutrino (dash-dotted line). The neutrino would appear as missing energy. Note the large angles for all three particles; this would facilitate their detection. This distribution is rather static as a function of beam energy or κ.

1.3 $e^{\pm}\ \gamma \rightarrow W^{\pm}\ \nu_e$

This experiment is very interesting for several reasons. As shown on fig. 5, it proceeds only through two diagrams. One of these involve known couplings and the other one the vertex we want to study. So the γW^+W^- is as "pure" as possible. Besides, as we will see later, the cross-sections are rather large and have a strong dependance on κ. Third, this process involves new technology by using an electron-photon collider. In principle, a high energy photon beam can be obtained by back-scattering a focused low energy laser beam from a high energy electron beam. However, in doing so, one has to deal with another factor α for this extra process; which reduces greatly the cross-section. Here, we will assume that a high luminosity, high energy photon beam is available. Some calculations along these lines are rather encouraging: a luminosity as high as 10^{30} has been claimed[45,46] possible!

This cross-section can be evaluated completely analytically. After a tedious but straightforward calculation, one obtains[39]:

$$\begin{aligned}\sigma = \frac{\pi\alpha^2}{8x^2 M_W^2 sin^2(\theta_W)}\Bigg\{ & 12 - 4\bar{\kappa} + (1/4)(\bar{\kappa}-2)^2 - 14/x \\ & + x\Big\{10 - 4\bar{\kappa} - (1/2)(\bar{\kappa}-2)^2\Big\} \\ & + x^2\Big\{\bar{\kappa}^2 + 4\bar{\kappa} - 4 - (3/4)(\bar{\kappa}-2)^2\Big\} \\ & - ln(x)\Big\{8 + x\{\bar{\kappa}^2 + 8\bar{\kappa} - 4\} - x^2(\bar{\kappa}-2)^2 - 8/x\Big\}\Bigg\}\end{aligned} \tag{1.2}$$

where

$$x \equiv s/M_W^2, \qquad \bar{\kappa} \equiv 1 + \kappa$$

and the other constants are standard.

The result as a function of beam energy for different values of κ is given on fig. 6. One notices first the large value of σ and its strong dependence on κ. Our maximum value of 47 pb for $\kappa = 1$ agrees with previous calculations[46]. Note also the fast increase of the cross-section with beam energy just beyond threshold.

Thus, one could use this process to extract the γW^+W^- vertex and then use the previous process to extract the $Z^0W^+W^-$ vertex. In this way, one could verify their relative strength and test the SM.

Figure 5. **Feynman diagrams for the process: $e^+ \gamma \rightarrow \bar{\nu} W^+$.**

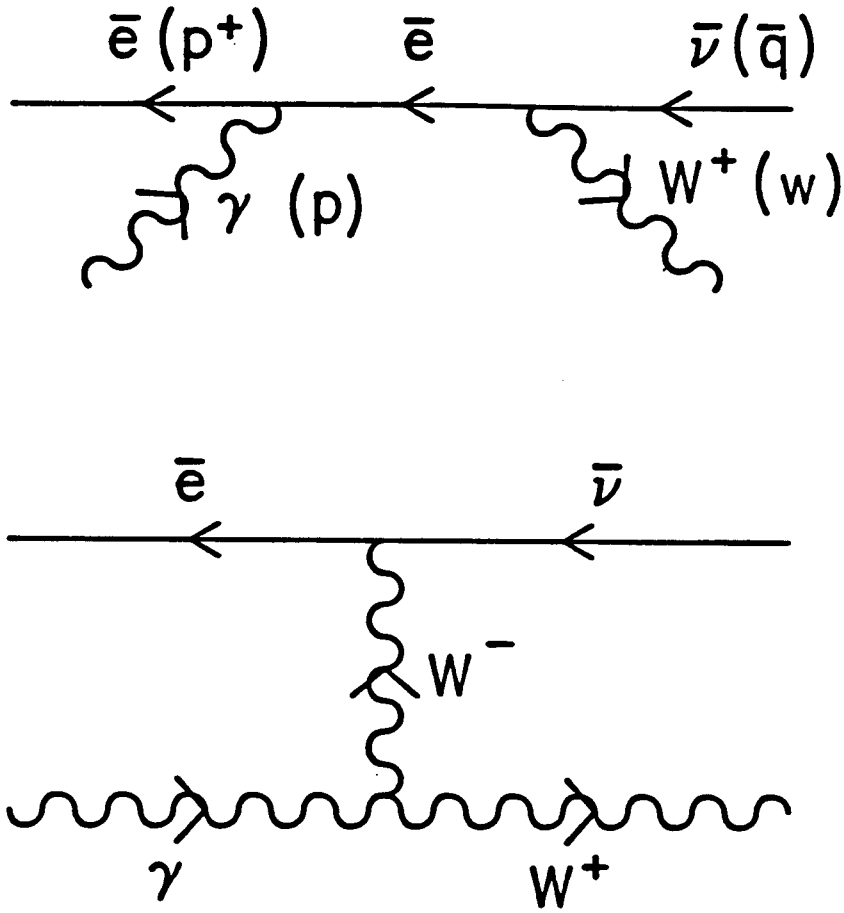

The two channels through which the process can proceed. Note that the $\gamma W^+ W^-$ vertex is as "pure" as possible.

Figure 6. Cross-section for the process: $e^+ \gamma \rightarrow \bar{\nu} W^+$.

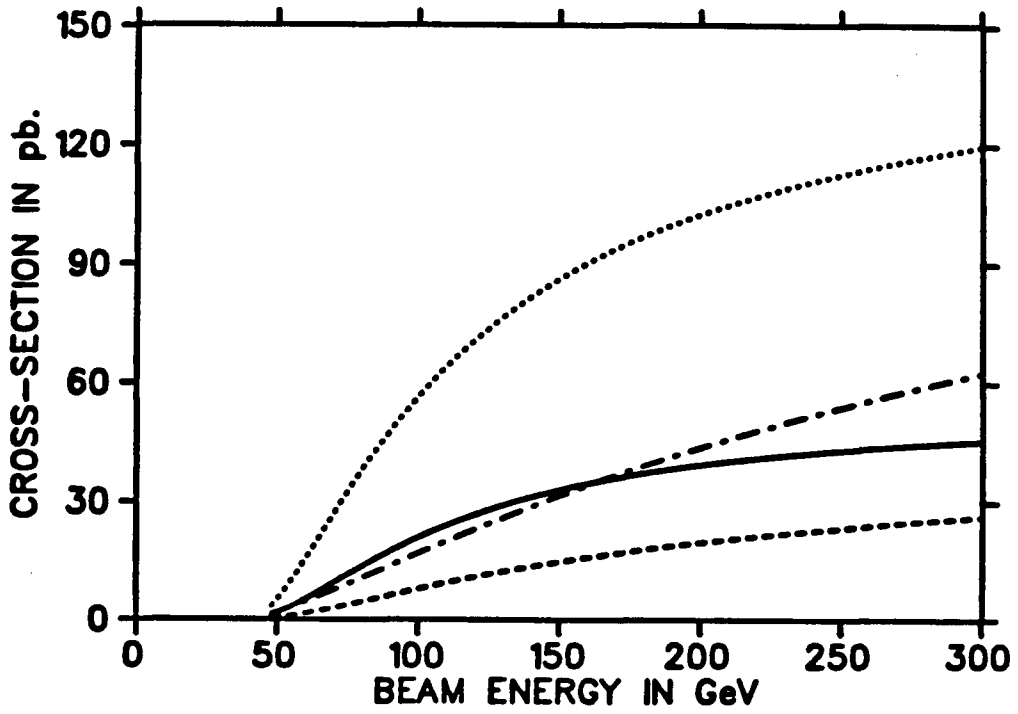

Cross-section of the process as a function of beam energy for different values of κ: -1 (dash-dotted line), 0 (dash line), 1 (solid line), 2 (dotted line)

1.4 $e^+ \; e^- \rightarrow W^+ \; \bar{\nu}_e \; e^-$

In principle, this reaction proceeds via t- and s-channel diagrams. However, because of the masslessness of the photon, the t-channel amplitudes that involve the exchange of a virtual photon will have a pole close to the region of physical kinematics, analogous to the Rutherford scattering. This pole will give the main contribution to the cross-section[47,39]. The pole occurs for grazing angles; when the outgoing electrons are collinear with the incoming ones. One then considers only the diagrams exhibiting this pole. They are shown on fig. 7. Moreover, because of this pole, one can use the Weiszäcker-Williams approximation (WWA); also known as the equivalent photon approximation. This allows one to perform a completely analytical calculation. See Appendix IV for some details about the WWA.

The WWA basically says that since the main contribution to the cross-section comes from the pole (which occurs when one has a real photon) one might as well set the photon on-shell and treat the subprocess:

$$e^+ \; \gamma \rightarrow W^+ \; \bar{\nu}_e$$

which is the calculation we did in the previous section. Then, in order to obtain a final answer, one multiplies by a flux factor arising from the e^- integration and integrates over the momentum range available to the photon. In this way, one gets a complete analytical answer for the whole process.

The final integrations one has to do look like[39]:

$$
\begin{aligned}
\sigma(s) =& \frac{\alpha^3}{8M_W^2 sin^2(\theta_W)} ln\Big(\frac{s}{m_e^2}\Big) \int_\rho^1 dy\Big(\frac{1}{y} - 1 + \frac{y}{2}\Big) \\
& \Big\{ (\bar{\kappa}^2 + 4\bar{\kappa} - 4 - (3/4)(\bar{\kappa} - 2)^2) + \frac{\rho}{y}(10 - 4\bar{\kappa} - (1/2)(\bar{\kappa} - 2)^2) \\
& + \frac{\rho^2}{y^2}(12 - 4\bar{\kappa} + (1/4)(\bar{\kappa} - 2)^2) - 14\frac{\rho^3}{y^3} \\
& - 8\Big(\frac{\rho^3}{y^3} + \frac{\rho^2}{y^2}\Big) ln\Big(\frac{y}{\rho}\Big) + (\bar{\kappa} - 2)^2 ln\Big(\frac{y}{\rho}\Big) \\
& - (\bar{\kappa}^2 + 8\bar{\kappa} - 4)\Big(\frac{\rho}{y}\Big) ln\Big(\frac{y}{\rho}\Big) \Big\}
\end{aligned}
\tag{1.3}
$$

where

$\bar{\kappa} \equiv 1+\kappa$, $\rho \equiv \frac{M_W^2}{s}$, $y \equiv \Big(\frac{s^\gamma}{s}\Big)$, where s^γ is now "s" of the previous process. For the previous process, s^γ had to be at least M_W^2 and could be at most the total "s"; these are the limits of our integral. We normalized everything so that the integrals are dimensionless.

These integrals are certainly tedious but rather straightforward. Numerically, the di- and tri-logarithms (otherwise known as Spence functions.) proved very easy to evaluate by their series expansion. In most cases, 25 terms were sufficient.

On fig. 8, we show the behaviour of σ as a function of beam energy for different values of κ. Note first the larger value of the cross-section; compared to the first process for example. This large value comes from the photon pole which enhances greatly the result. Notice also that on the range of energies studied here, the absolute value of κ will be much easier to obtain than its sign. Furthermore, this process involves only the γW^+W^- vertex and known electromagnetic vertices. This could also be used to measure this coupling alone. However, it is at the extreme experimental limit of feasibility.

Figure 7. Feynman diagrams for the process: $\bar{e}\ e \rightarrow e\ W^+\ \bar{\nu}$.

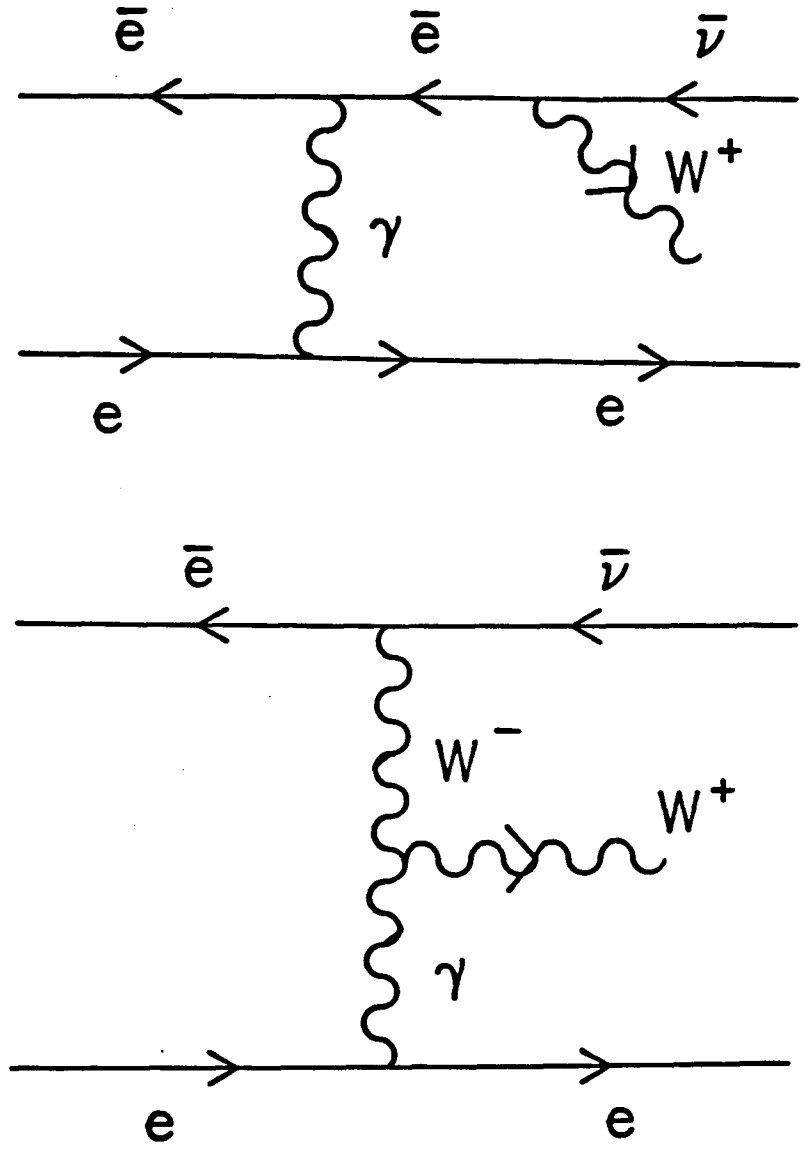

These two Feynman diagrams are the main contribution to the process because they proceed via virtual photon exchange; which leads to a pole and gives the main part of the cross-section.

Figure 8. Cross-section of the process: $e\ \bar{e} \rightarrow W^+\ e\ \bar{\nu}$.

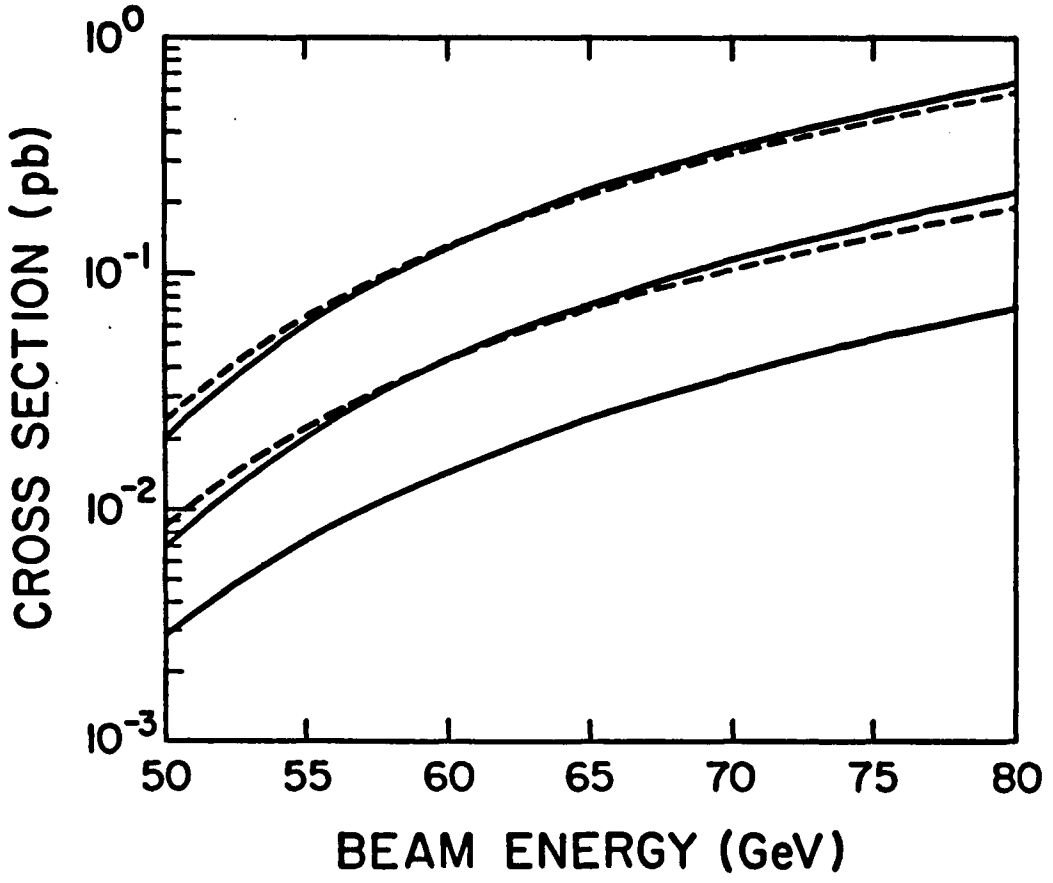

Cross-section of the process as a function of beam energy for different values of κ : 0, ± 1 ± 3. The cross-section increases with $|\kappa|$ and the negative values of κ correspond to the dotted lines. Note the relatively much larger values of σ compared to figure 3. This enhancement is due to the photon pole.

1.5 $e^+ e^- \rightarrow W^+ W^-$

This proces is certainly the most promising of all. It has been studied extensively and we shall only quote the most important results here[30,40,42,48]. We show in fig. 9 the contributions from the different Feynman diagrams. The calculation of the process is very straightforward and rather simple. We show on fig. 10 [ref. 49] the cross-section as a function of beam energy for different values of κ. Note the large value of the cross section: the peak is approximately 17 pb., which is obtained for $\sqrt{s} \approx 200 GeV/c^2$, where s is the standard Mandelstam variable. The only drawback of the process is its rather large threshold. The good point though is that the cross-section rises very quickly after threshold. However, to insure a large difference in the cross-section for different values of κ, one has to go to large beam energies.

Although there is a strong dependence of the cross-section on κ, the angular distribution is the most promising variable for a precise measurement of κ. Due to the large cross-section, one can afford to make such a measurement. We show on fig. 11 [ref. 49] the angular distribution for different values of κ. It is clear that a single data point would not uniquely determine κ very well but a distribution over a range of 45 degrees or more would do so.

This process can also help to measure the width of the W boson. Very close to threshold, the cross-section will have a tail that will be different depending on the width of the boson; of course the rates will be much smaller but with sufficient statistics, one could extract the width from such a measurement. This behaviour is shown on fig. 12 [ref. 46]. We see that the effect is noticeable and should lead to a measurement of the width within a factor 2; which would be an improvement over current data[50].

From the estimated luminosities at SLC and LEP it seems that a 10% measurement of κ will have to wait for LEPII ($\sim$ 1990) and that it will be very difficult, even for this machine. However, a 30% measurement is well within the possibilities of LEPII. We recall that the optimistic maximum luminosities and maximum beam energies for these e^+e^- colliders are [refs. 51, 52]

Collider	*Luminosity*	*BeamEnergy*
	$cm^{-2}sec^{-1}$	GeV
SLC	$\sim 5 \times 10^{30}$	~ 50
$LEPI$	$\sim 1 \times 10^{31}$	~ 55
$LEPII$	$\sim 5 \times 10^{31}$	~ 100

Figure 9. Feynman diagrams for the process: $e^+ \; e^- \rightarrow W^+ \; W^-$.

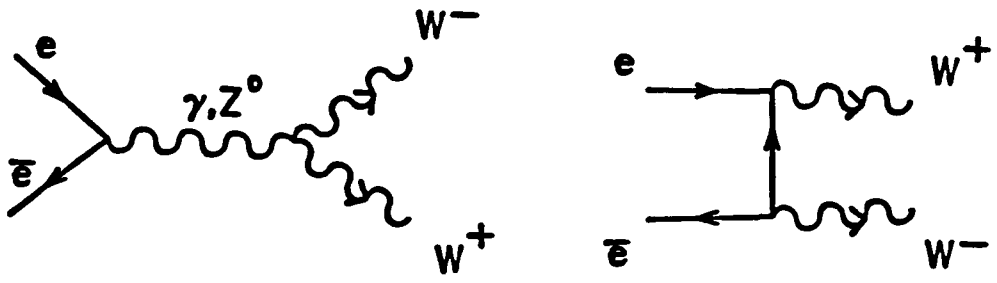

The three channels that contribute to the process: $e^+ \; e^- \rightarrow W^+ \; W^-$. Again, grouping of two of the diagrams that involve the exchange of a neutral gauge boson greatly reduces the algebra.

Figure 10. Cross-section for the process: $e^+ \; e^- \rightarrow W^+ \; W^-$.

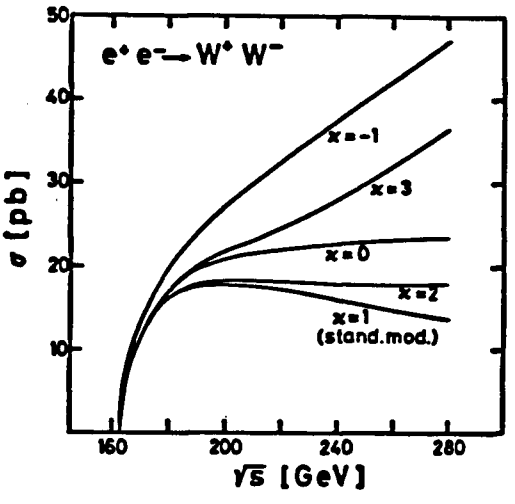

Cross-section of the process as a function of beam energy for different values of κ. Note the high threshold energy, the fast rise of σ beyond threshold, and the strong dependance on κ at higher energies. The cross-section is also very large.

Figure 11. Angular distribution.

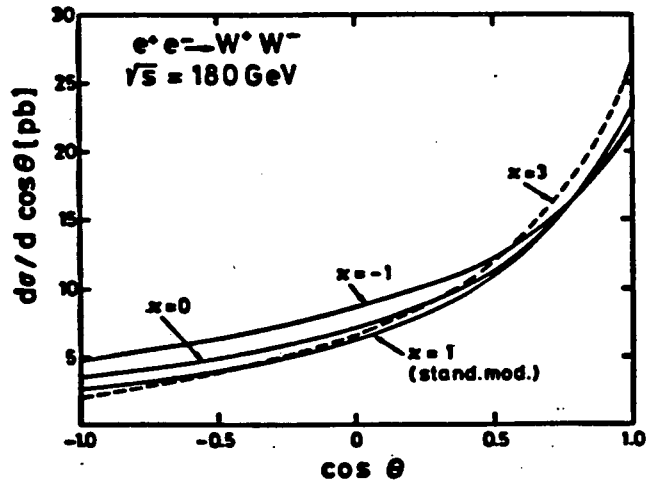

Angular distribution of the process. One sees that a single data point at any angle would not determine κ uniquely, unless it is very precise. However, a distribution over 45 degrees or more would do much better.

Figure 12. Width of the W boson.

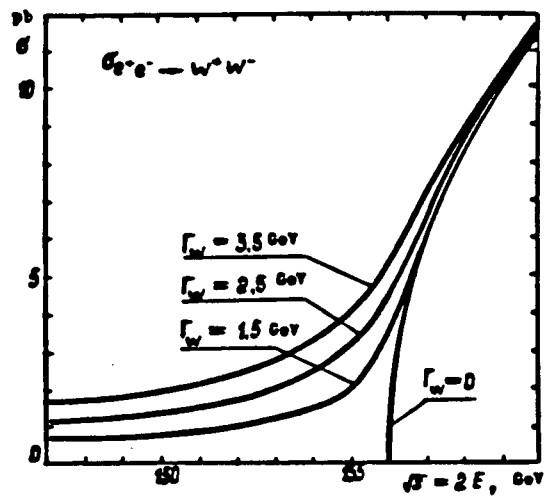

Total cross-section as a function of beam energy for different values of the width of the W boson. This shows clearly that the total cross-section at threshold or "just under" depends on the width of the W boson. From this, it seems possible to measure the width within a factor 2.

1.6 Radiative Zeros.

We now turn briefly to a whole class of processes that involve so-called "radiative zeros". As their name indicates, the processes are characterised by a particular angle where the outgoing particles simply cannot be emitted. This angle itself depends only on the charges of the particles involved. However, in order to obtain a "null zone", one must require all the spinning particles to have the canonical gyromagnetic ratio g=2 which translates into κ =1 for the W boson. Therein arises the relevance of the null zones to our problem.

The radiative zeros were discovered by Michaelian, Samuel and Sahdev in 1979 [ref. 53, 54]. They were looking at the process $p\ \bar{p} \rightarrow W^{\pm}\ \gamma\ X$. In their original paper, they found that the differential cross-section was identically zero at the specific angle $cos(\theta_{cm}) = -1/3$ and for $\kappa = 1$, where θ_{cm} is the angle between the γ and $\bar{u}$ in the γW^- center of mass. It is defined as $t = -(1/2)(s - M_W^2)(1 - cos(\theta_{cm}))$. They could relate the angle to the charges by the relation: $cos(\theta_{cm}) = -(1 + 2Q_i)$ where $Q_i = -1/3$. The main points are that the angle is momentum independent and *requires* κ to be one. Therefore, as noted by the authors, loop corrections will spoil the null zones and the process can lead to a possible measurement of κ. It is important to note that the null zones occur at a specific angle when looking at the constituent subprocess. When one takes into account the different quark constituents of the hadronic target, there is no zero anymore but a slight decrease in the cross-section from $\kappa = -1$ to $\kappa = 1$. Furthermore, when one integrates and gets the total cross-section, the difference is merely 7% from $\kappa = -1$ to $\kappa = 1$. These numbers suffice to show that the zeros of radiation will be very difficult to observe.

Later studies showed[55,56] the following conditions to be necessary and suffi-

cient to observe radiative zeros:

1– tree amplitude process

2– photon as an external particle

3– gauge theoretic vertices

4– spin of the particles ≤ 1

5– spinning external particles must have g=2

6– kinematically, all external particles of charge Q_i and momentum p_i must have the same ratio:

$$\rho \equiv \frac{Q_i}{p_i \cdot q}$$

where q is the photon momentum.

7– all charged particles in the initial and final states must have the same sign.

8– neutral particles must be massless and travel in the same direction as the photon.

When all these conditions are met, one will have radiative zeros. In our case, if κ is not 1, then the "null zone" will not exhibit an exact zero. Obviously, if $\Delta\kappa \ll 1$, then the signal will be very weak. Unfortunately, in $p\bar{p}$ colliders, these null zones are plagued by large backgrounds[57], which makes values of κ less than 4 or 5 unobservable. In lepton colliders, one must have three vertices at least to obtain the W and γ, so that hopelelessly small cross-sections are expected.

We show on fig. 13 [ref. 53] the behaviour of these null zones for hadron colliders. To our knowledge, no such calculations have been done for leptonic reactions. Some lepton-hadron processes have been calculated recently[58] and the results are very encouraging in the sense that a substantial decrease in the angular distributions could be observed. So these zeros of radiation could effectively be observed.

Figure 13. Radiative zeros.

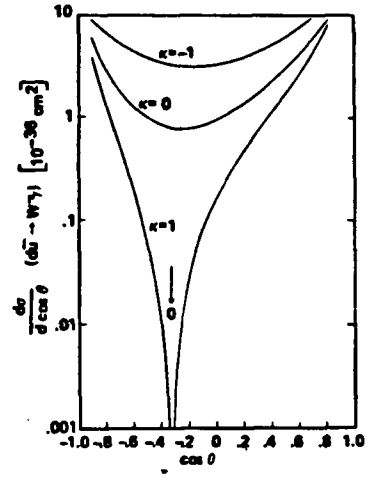

a) Differential cross-section of the process $d\ \bar{u} \rightarrow W^-\ \gamma$ in the c.m. frame. The parameters for this calculation were: $\sqrt{s} = 200GeV$, $M_W = 85GeV$ θ is the angle between the W^- and d or between the γ and $\bar{u}$. Note the drastic change from $\kappa = -1$ to $\kappa = 1$. This shows clearly what is meant by radiative zeros.

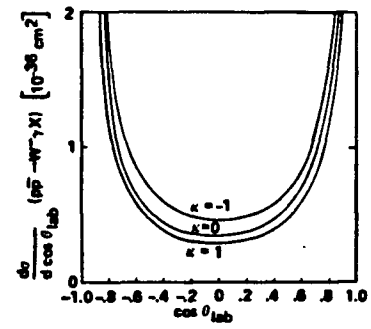

b) Differential cross-section of the process $p\ \bar{p} \rightarrow W^-\ \gamma\ X$ in the lab. frame. The parameters for this calculation were: $E_\gamma > 30GeV$, $M_W = 85GeV$, $\sqrt{s} = 540GeV$. θ_{lab} is the angle between the photon and the W boson in the laboratory. Note that there is only a slight decrease in the cross-section from $\kappa = -1$ to $\kappa = 1$ due to the inclusiveness of the cross-section.

1.7 Conclusions.

As should be clear now, there exists only one experiment where it will be possible to measure κ in the near future and obtain better than an order of magnitude precision. It is the double boson production:

$$e^+ \; e^- \rightarrow W^+ \; W^-$$

Unfortunately, it seems we will have to wait for LEPII for a 10% measurement, since this is the only machine designed to have sufficient energy. SLC ($\sim$ 1987), and LEPI ($\sim$ 1988) will focus on single W production; the cross-sections are too small for the projected luminosities ($\mathcal{L} \sim 5 \times 10^{31} cm^{-2} sec^{-1}$) to have any hope of a 50% measurement. (It seems that SLC will be short of its projected luminosity by almost an order of magnitude, at least for the first few years.) This does not mean that the task should not be undertaken. Such experiments should be carried on, keeping in mind that if one sees more events than expected, then $\kappa \gg 1$ and the SM is in deep trouble; opening the way to composite models, possibly.

In Table II, we summarize the processes and rates one can expect from the new generation of colliding machines.

TABLE II

Processes to measure κ.

Summary of the Processes.		
Process	$\sqrt{s}$ in GeV	Events in 100 days.
$e^{\pm}\ \gamma \rightarrow W^{\pm}\ \nu_e$	120	~ 450
$e^{+}\ e^{-} \rightarrow W^{+}\ e^{-}\ \bar{\nu}_e$	120	~ 2
$e^{+}\ e^{-} \rightarrow W^{+}\ W^{-}$	200	~ 700
$p\ \bar{p} \rightarrow W^{\pm}\ \gamma\ X$	200	~ 140

Different processes and their rates at a typical energy. We assumed a luminosity of $5 \times 10^{30} cm^{-2} sec^{-1}$, which is an average luminosity expected from the new accelerators. We do not include the first process that we investigated because the yield is less than one event in 100 days of beam time. The electron-photon collider has a large rate once we can have such a photon beam. As is clear from the table, the most promising process is the double boson production. The last process is representative of radiative zeros; the rate is misleading because it is plagued by very large backgrounds in hadrons colliders and very small rates in lepton colliders.

SO : 1) an order of magnitude estimate of κ is possible at SLC or LEPI,

2) a 30% measurement must wait for LEPII,

3) a 10% measurement is very difficult at LEPII.

Chapter II

Non Standard γWW and ZWW Couplings.

2.1 Introduction.

Up to now, we have restricted ourselves to the SM framework only. Even though the SM is now believed by most physicists to be an adequate description of nature up to a few hundred GeV's, some very important components of the model have not been tested yet; the most obvious one being the Higgs sector. Another one refers to the self coupling of the weak bosons. This sector is still unexplored from an experimental point of view and crucial to the model. In the SM, all the self couplings of the gauge bosons are well defined, due to the gauge structure of the theory. If one is willing to give up this gauge structure and work with an SU(2) *global* symmetry, one gains a lot of freedom in the couplings. Indeed, the γWW and ZWW couplings are free and independent; the same also applies for the four-boson vertices. The price to pay for this freedom is high though: one looses renormalizability. In fact, as soon as the vertices differ from their gauge theoretical values, the model becomes non renormalizable.

As we mentioned before, there exist models where the gauge bosons are not point particles but made of more fundamental constituents called preons[18]. In these models three- and four-boson vertices are free and independant; their value can differ from the gauge theoretical value. Therefore, these models are nonrenormalizable. We will refer to models where κ is free as composite models. This terminology is loosely used in the literature to refer to models where the gauge vertices are free.

In spite of the divergences above-mentioned, one can proceed by introducing a

cut-off, Λ, which represents the energy scale where one expects the model to break down and some new, unknown physics to enter and dampen the bad behaviour of the model. Certainly, these models are legitimate but not nearly as "elegant" as the renormalizable ones.

The freedom gained is not "infinite" however: there exist some phenomenological results that the models have to respect. For example, the factor $(g-2)$ for the muon involves the γWW vertex and can be used to set bounds on κ or $\Delta\kappa$. Using current data of $(g-2)_\mu$ one gets[59]:

$$|\Delta\kappa| ln\left(\frac{\Lambda^2}{M_W^2}\right) \leq 4.4 \tag{2.1}$$

where Λ is a cut-off energy in TeV.

This bound can be improved by a better measurement of $(g-2)_\mu$. The most recent measurement[60] is still a factor 5 or so larger than the weak interaction contribution. (i.e. the error in the measurement is still 5 times larger than the weak contribution.) The main problem lies in the hadronic sector whose experimental error is approximately the same as the weak signal. There are some proposals[17] to improve the measurement of $(g-2)_\mu$ to the level of the weak signal but in order to extract the weak interaction contribution, the calculation of the hadronic sector must be improved by almost an order of magnitude.

From another point of view, one can assume the W to be composite but the photon to remain a particle. Then, the photon propagator will be affected by virtual boson loops. This can lead to noticeable effects in $e^+e^- \to l^+l^-, q\bar{q}$ processes. From results at PETRA, it has been calculated that[61]:

$$|\Delta\kappa|\left(\frac{\Lambda}{M_W}\right) \leq 33 \tag{2.2}$$

where Λ is the cut-off.

This bound is not as tight as the other one at low energy, but is tighter for $\Lambda \geq 5$ TeV. Both of these bounds agree with what is known as the Veltman conjecture which says that an effective low energy theory of composite states with mass much less than the binding scale has to be renormalizable if it is to be described by perturbation theory. This is what one would expect intuitively: at low energy, the composite object behaves like a point particle. Similarly, the proton is a point-like object at low energy. In our case, the theorem translates into $\Delta\kappa \to 0$ as $\Lambda \to \infty$, since $\Delta\kappa \to 0$ in the gauge theoretical limit.

A tighter bound can be obtained from the process: $\gamma W \to \gamma W$. From partial-wave analysis and demanding that unitarity not be violated, one can get[59]:

$$|(\Delta\kappa + 1)^2 - 1| \leq 2.6/\Lambda^2 \tag{2.3}$$

where Λ is the cut-off in TeV. For $\Delta\kappa \ll 1$ this reduces to :

$$|\Delta\kappa| \leq 1.3/\Lambda^2.$$

By turning the argument around, if $\Lambda \leq 1$ TeV, then $|\Delta\kappa| \sim 1$; which is an extreme case. Note that this type of analysis is very close to the one performed by Lee, Quigg, Thacker in the Higgs particle case[62].

It should be pointed out that the ratio M_W/M_Z can be altered when the self-energy couplings differ from their gauge theoretic values, and can be used to set constraints on models.

The above discussion is intended to show that these composite models are not entirely free but still allow a range of possible parameters. Recently, such models have been studied[63–65] in processes like: $e^+e^- \to W^+W^-$, $p\bar{p} \to W^+W^-$. The main lesson was that for $\sqrt{s} \sim 180$ GeV (i.e. LEPII), one will be able to use experimental results to rule out or confirm "dramatic" departure from the SM. The point of these calculations is to try and find some experiments where a possible

strong departure from the SM could be explained by composite models. It seems that a single experiment will not be able to rule out composite models since their parameters can be tuned to "adapt" to an experimental result. On the other hand, a series of experiments could rule out such models by requiring their parameters to belong to two non-overlapping ranges.

In this chapter, we will study one such model, based on previous work by Hung and Sakurai[66] and Bjorken[67]. In a first step, we will describe the model and in a second one we will slightly constrain a free constant of the model. In the fourth section, we will consider this model for the process $e_R^- e^+ \to W^- e^+ \nu_e$ and see how it can differ from the previous calculation. The fifth section will be our conclusions.

2.2 Description of the Model.

The main features of the model are:

1) an assumed global SU(2) symmetry
2) postulated three massive weak bosons
3) assumed γZ^0 mixing

The main point here is that *all* the predictions of the SM verified experimentally up to now can also be recovered by this model. However, the model leads to tri- and quadrilinear terms that differ substantially from the SM. They can lead to drastically different behaviour at high energy while agreeing with the SM at low energy. This behaviour can rule out the model or confirm it.

Using a massive vector boson triplet, W^i_μ, coupled to a weak isospin fermionic current $J^{i\mu}$ and a primordial photon field $\tilde{A}_\mu$ coupled to the electromagnetic current J^μ_{em} and finally a γW^3 mixing of strength $\lambda_{\gamma W}$ we have[66]:

$$\begin{aligned}\mathcal{L} = &-\frac{1}{4}W^i_{\mu\nu}W^{i\mu\nu} - \frac{1}{2}\tilde{m}^2_W W^{i\mu}W^{i_\mu} - \frac{1}{4}\tilde{F}^{\mu\nu}\tilde{F}_{\mu\nu} \\ &+ \tilde{e}\tilde{A}_\mu J^\mu_{em} + gW^i_\mu J^i_\mu \\ &-\frac{1}{4}\lambda_{\gamma W}\left\{\tilde{F}_{\mu\nu}W^{3\mu\nu} + W^{3\mu\nu}\tilde{F}_{\mu\nu}\right\}\end{aligned} \tag{2.4}$$

where

$$\tilde{F}_{\mu\nu} \equiv \partial_\nu \tilde{A}_\mu - \partial_\mu \tilde{A}_\mu$$

$$W^i_{\mu\nu} \equiv \partial_\nu W^i_\nu - \partial_\mu W^i_\nu$$

with the latin indices being the SU(2) indices. The last term of the Lagrangian

represents the γW^3 mixing term. Notice that we associate the W^3 term with the neutral boson which will be associated with the Z^0 boson later on, within a constant.

In order to express the Lagrangian in terms of the physically observable photon and Z^0 boson fields, we use the following non-unitary transformation[39]:

$$\begin{pmatrix} \tilde{A}^\mu \\ W^{3\mu} \end{pmatrix} = \begin{pmatrix} 1 & -\frac{\lambda_{\gamma W}}{(1-\lambda_{\gamma W}^2)^{1/2}} \\ 0 & \frac{1}{(1-\lambda_{\gamma W}^2)^{1/2}} \end{pmatrix} \begin{pmatrix} A^\mu \\ Z^\mu \end{pmatrix} \tag{2.5}$$

From this, one can derive mass terms for the weak bosons which can be used to "fix" the $\lambda_{\gamma W}$ parameter. One gets:

$$M_W^2/M_Z^2 = 1 - \lambda_{\gamma W}^2$$

which implies that

$$\lambda_{\gamma W}^2 = sin^2(\theta_W) \tag{2.6}$$

in order to agree with the known phenomenology of the weak bosons. Note that the value does not have to be precisely the weak mixing angle, because of experimental uncertainties, but it has to be very close to it. In the model as first worked by Hung and Sakurai and Bjorken, this parameter was free and could certainly accommodate the SM. In the past few years, experimentalists have been able to fix this parameter to a value close to the weak mixing angle.

In our case, we extend the model by adding a triple vector boson term to the Lagrangian that is SU(2)-global invariant[39]. Namely, we add:

$$\omega \; \varepsilon_{ijk} \; W^{\mu\nu i} \; W_{\mu j} \; W^{\nu k}.$$

where ω is a free parameter that we will try to constrain from known phenomenology.

The next step is to calculate the couplings relevant to our process. This is done most easily by using the "extended minimal" substitution as suggested by Hung and Sakurai. Namely, we use:

$$\partial_\mu W^i_\nu \rightarrow \partial_\mu W^i_\nu + \frac{1}{2} g \varepsilon_{ijk} W^j_\mu W^k_\nu + e \varepsilon_{i3k} A_\mu W^k_\nu. \tag{2.7}$$

Using this substitution and the previous rotation, we can rewrite the gauge part of the Lagrangian as follows:

$$\begin{aligned}
\mathcal{L}_{eff} =& \frac{ie}{2} F_{\mu\nu}\left(W^{\mu+}W^{\nu-} - W^{\mu-}W^{\nu+}\right) \\
&+ ieA_\mu\left(W^{\mu\nu-}W^+_\nu - W^{\mu\nu+}W^-_\nu\right) \\
&+ \frac{i}{2cos(\theta_W)}(g-\omega) Z_{\mu\nu}\left(W^{\mu+}W^{\nu-} - W^{\mu-}W^{\nu+}\right) \\
&+ \frac{i}{cos(\theta_W)}(g-\omega) Z_\mu\left(W^{\mu\nu-}W^+_\nu - W^{\mu\nu+}W^-_\nu\right) \\
&+ \frac{ig}{2} cos(\theta_W) Z_{\mu\nu}\left(W^{\mu-}W^{\nu+} - W^{\nu-}W^{\mu+}\right)
\end{aligned} \tag{2.8}$$

The first two terms reproduce exactly their SM counterpart. By choosing ω to be $gsin^2(\theta_W)$, the third and fourth terms can also reproduce the SM. (We used this as a verification on our numerical calculations.) However, one is left with the fifth term. Therefore, this model reproduces exactly the γWW vertex of the SM but the ZWW vertex cannot coincide with the SM, except by numerical accident. This is a rather peculiar feature of the model.

The new vertex is now written as:

$$\begin{aligned}
Z^{\mu\nu\lambda} =& i(g-\omega)sec(\theta_W)\{(z-w^+)^\lambda g^{\mu\nu} + (w^+ - w^-)^\mu g^{\nu\lambda} + (w^- - z)^\nu g^{\lambda\mu}\} \\
&- igcos(\theta_W)\{z^\lambda g^{\mu\nu} - z^\nu g^{\mu\lambda}\}
\end{aligned} \tag{2.9}$$

This is the vertex that we will use in the process:

$$e_R^- \; e^+ \rightarrow W^- \; e^+ \; \nu_e$$

Before we study this process, we will try to constrain ω, which is still completely free.

2.3 Constraints on ω from the beta decay of the Z^0.

The process we will use to constrain ω is the Z^0 decay into a W boson and lepton pairs. This process increases the width of the Z^0 boson. As we expect this contribution to be a function of ω, we can use the experimental value to set a limit on ω. In the SM, this process has a contribution that is absolutely negligible; it is of the order of 10^{-7} GeV while the total width is roughly 3.0 GeV [ref. 50]. For large values of ω, this might not be the case and this process might increase the width by a fair amount. This is what we now calculate.

The calculation of the width is straightforward in the SM and this more involved coupling makes the calculation slightly more tedious. In the rest frame of the Z^0 boson, we get[39]:

$$\Gamma = \int_{M_W}^{\frac{M_Z^2+M_W^2}{2M_Z}} \frac{\alpha\sqrt{E^2-M_W^2}}{144\pi^2 M_Z^2 sin^2(\theta_W)} dE$$
$$\Bigg\{(2a+b)^2 M_Z^2 \Big\{E^2 + (\frac{E^2}{M_W^2}-1)(3M_Z^2 - 4EM_Z + 4M_W^2)\Big\}$$
$$+ 4a(2a+b)M_Z^2 \Big\{(M_W^2 - EM_Z)(\frac{E^2}{M_W^2}-1) - \frac{E^3(M_Z^2-M_W^2)}{M_Z M_W^2}\Big\}$$
$$+ 4a^2 M_W^2 \Big\{(3M_W^2 - 6EM_Z + M_Z^2)\Big(\frac{E^2}{M_W^2}-1\Big) + M_Z^2\Big(\frac{E^4}{M_W^4}-1\Big)\Big\}\Bigg\} \tag{2.10}$$

where E is the energy of the W boson and

$$a \equiv \frac{g-\omega}{cos(\theta_W)}, \quad b \equiv gcos(\theta_w)$$

The last integrals were done by numerical methods using the program DCADRE. The result is plotted on fig. 14 as a function of ω. With the current experimental value of $\Gamma_Z \leq 8.5GeV$ [ref. 50], we obtain $|\omega| \leq 1200$ where we have included decays into W^+, W^- plus all three families of fermions. We can be more conservative and subtract first the partial width due to pairs of known fermions (i.e. the SM width). This gives the slightly more stringent bound of $|\omega| \leq 900$. Obviously, these bounds are not very useful from a phenomenological point of view. We will then ignore them in our particular problem and limit ω to a range that seems "reasonable": less than 4 or 5.

As mentioned before, this decay process is practically nonexistent in the SM. Therefore, if it is seen at all at SLC or LEP, it implies a rather large value of ω and constitutes a big drawback for the SM.

Figure 14. Partial width of the Z^0 boson.

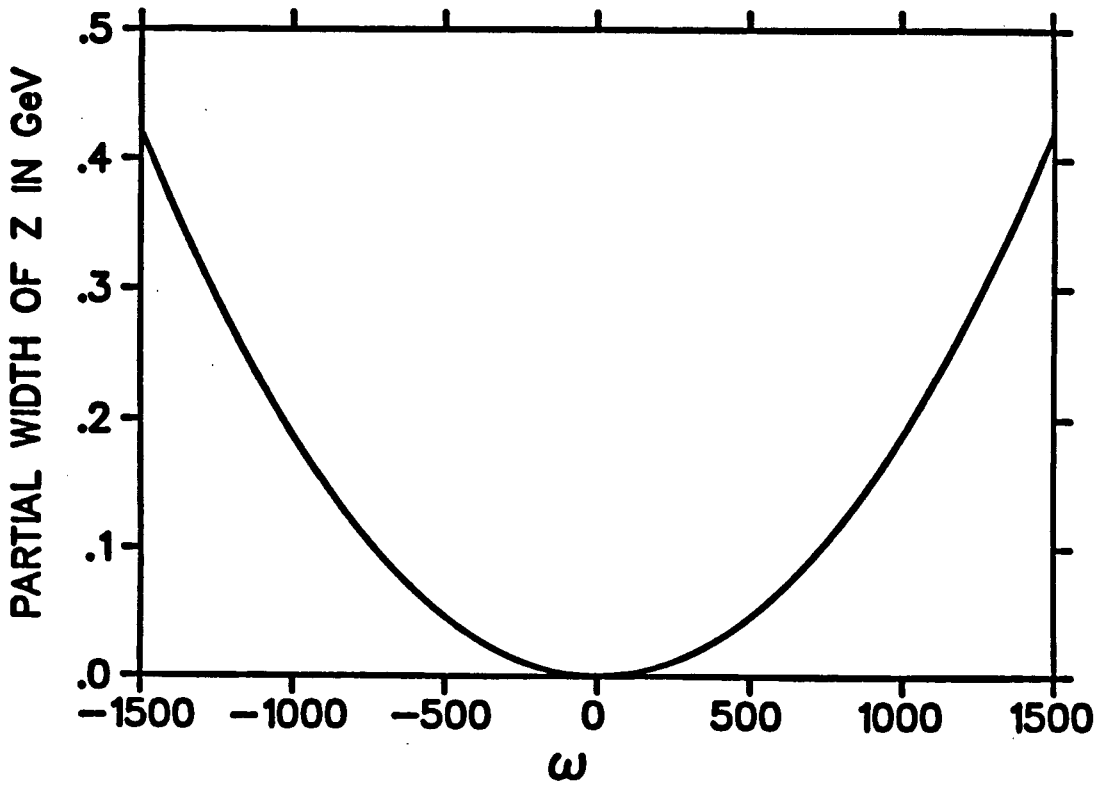

Partial width of the Z^0 boson as a function of ω. Note that we have to go to extremely large values of ω in order to reach an observable effect.

2.4 $e^-_R\ e^+ \to W^-\ e^+\ \nu_e$.

We now consider this vertex in the process analysed before. The reaction proceeds via the same channels as before and the calculation is essentially the same, but slightly more tedious. We used the same polarization vectors as before and the final integrals were done numerically by Monte Carlo. Again, the expression of the matrix element is far too lengthy to write here. We give the total cross-section as a function of beam energy for different values of ω in fig. 15 and fig. 16. We also give the SM value for comparison. One sees that for an appropriate choice of ω, the model can mimic the SM very well at low energy (i.e. on the range that we showed on the two figures). However, one sees that the two models begin to differ at the high limit of the range studied here; therefore if the fit is good at low energy, it is poor at high energy and vice versa. This is what we wanted. Note also the unexpected behaviour for the value $\omega = 1$; there is no easy way to explain this behaviour.

Note also the problem that we had before is recurrent here: the cross sections are very small and hopeless from an experimental point of view; unless ω is enormous. The angular distribution is also essentially the same as before and is stable.

Figure 15. Cross-section for the process $e_R^- \; e^+ \to W^- \; e^+ \; \nu_e$ for $\omega > 0$.

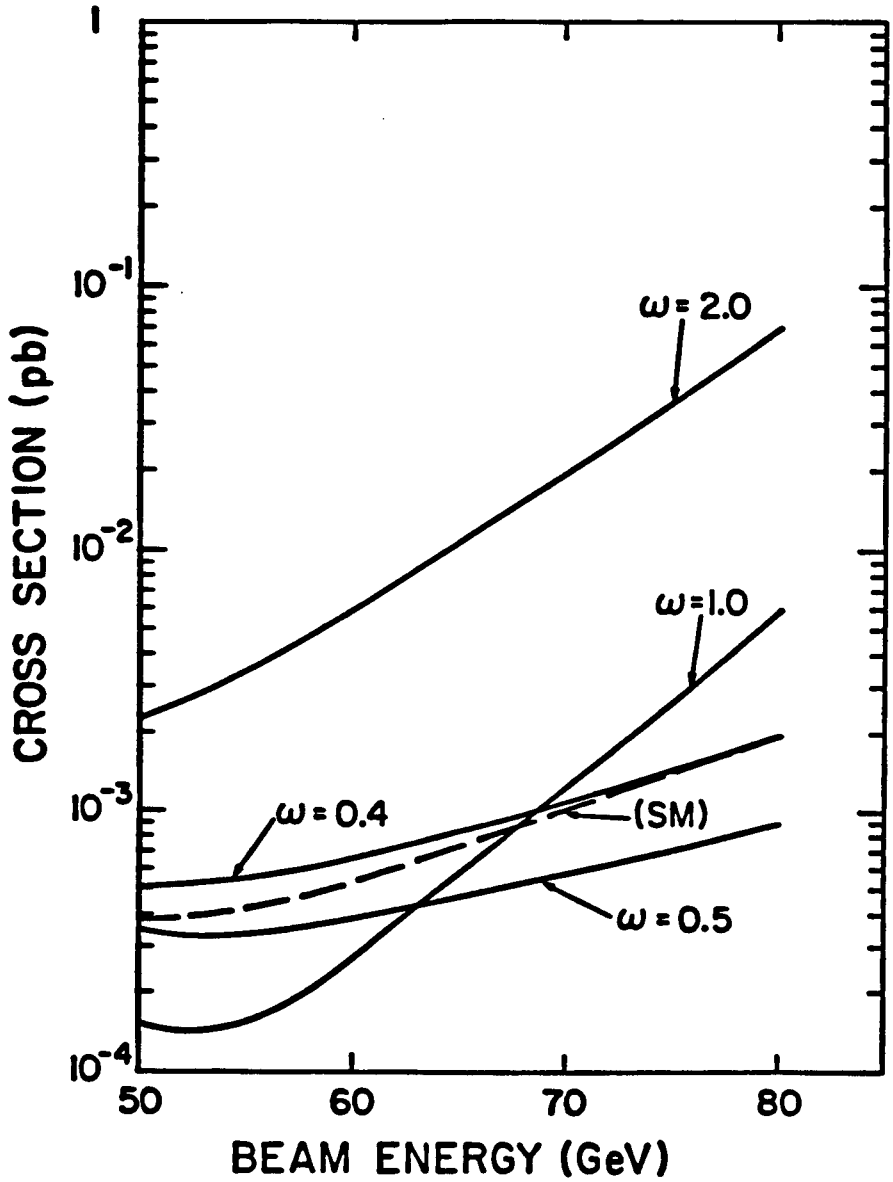

Cross-section of the process as a function of beam energy for positive values of ω. The SM value (dotted line) is also given for reference. We can reproduce the SM values on a range of energies for an appropriate choice of ω.

Figure 16. Cross-section for the process $e_R^- \; e^+ \rightarrow W^- \; e^+ \; \nu_e$ for $\omega \leq 0$.

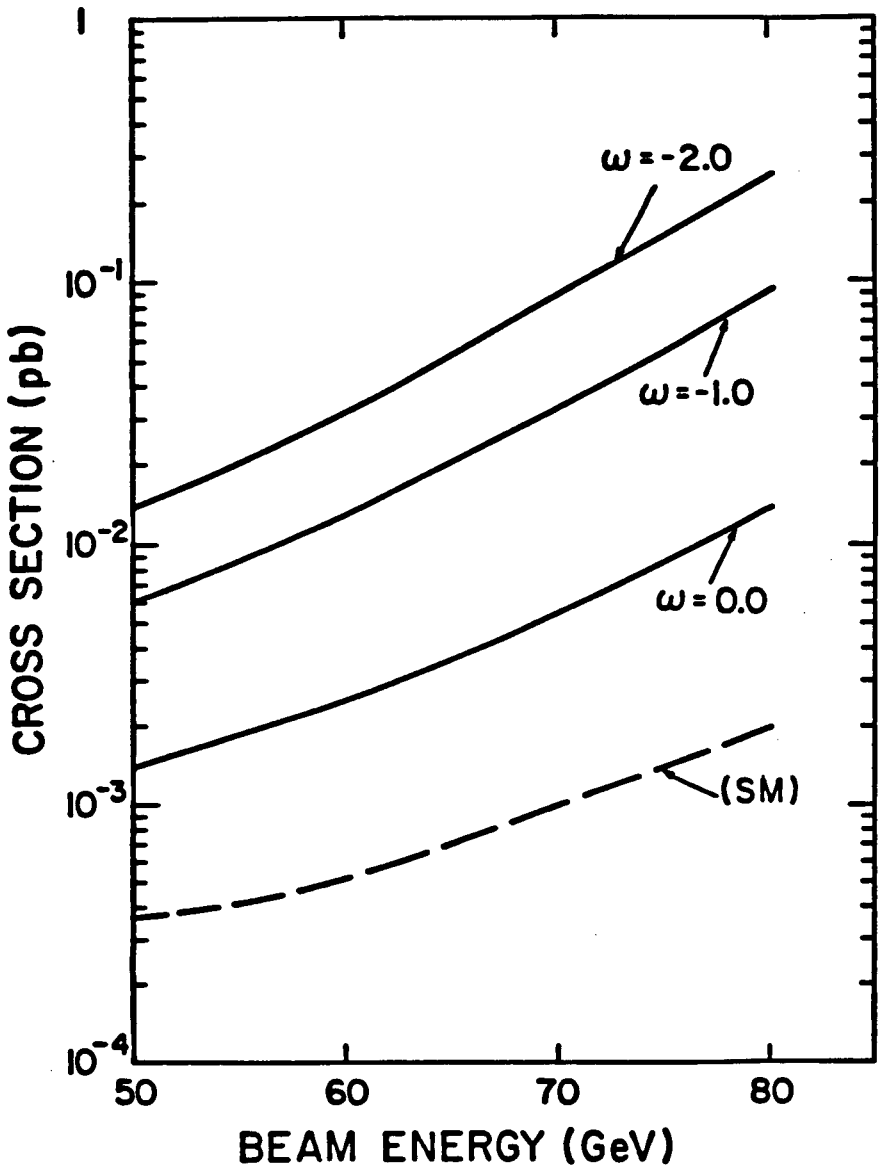

This figure is the same as figure 15 but for negative values of ω.

2.5 Conclusions.

In conclusion, we can say that it is very straightforward to build a composite model that can reproduce the SM at low energy and that a single measurement of κ could not rule out such a model. However, it seems very difficult to build such a model that will agree with the SM both at low and high energies. Therefore, it is likely that measurements of processes like the one investigated here will rule out or confirm composite models. The cross-section for this particular process being so small, it is unlikely that it will be measured in the near future. One would have to rely on the $e^+e^- \to W^+W^-$ process for example or on some other indirect contributions like the $(g-2)_\mu$ in order to constrain the models.

We have also seen that the widths of the particles can be substantially increased by non-standard couplings. Therefore, a precise measurement of the widths of the W and Z bosons becomes very relevant and important from a "model building" point of view. Experimentally, a precisely measured width that would be even slightly larger than its SM value would mean large non-standard parameters.

Chapter III
Loop Corrections to κ in the Standard Model.

3.1 Introduction

As seen in the previous chapters, one will have to wait for LEP II for a precise measurement of κ; a 10% measurement will be very difficult but a 30% one should be well within the possibilities of the machine. Such a measurement will be very useful in setting tight constraints on all models and could possibly rule out the SM. We have seen previously[9] that κ enters in the γW^+W^- vertex in the following way:

$$\Gamma^{\mu\nu\lambda} = -ie\Big\{(\kappa k_1 - k_2)_\nu g^{\lambda\mu} + (k_2 - k_3)_\lambda g^{\mu\nu} + (k_3 - \kappa k_1)_\mu g^{\lambda\nu}\Big\} \tag{3.1}$$

where the notation is defined on fig. 1. In the SM, κ must be identically 1 at tree level. This value is very well defined and closely related to properties like renormalizability. That this is so can be understood by noting that the terms of the Lagrangian where the γW^+W^- vertex comes from will also give rise to other 3- and 4-boson vertices. These vertices are all involved in renormalization where some fine cancellations are required. Therefore, any of those vertices is a direct test of the renormalizability of the model; therein arises the importance of the γW^+W^- vertex. Corrections will arise through higher order loops and are expected to be of order (α/π), as the SM is a weakly interacting theory. We define $\Delta\kappa \equiv \kappa - 1$. As of now[61], $\Delta\kappa \leq 1$ is certainly not ruled out by any experiment but a 30% measurement from LEP II would be a strong constraint on any model and a very good test for

the SM.

From this point of view, one sees the relevance of a precise calculation of $\Delta\kappa$ in the SM. One should calculate as precisely as possible the bounds of $\Delta\kappa$ in the SM to see the significance of future experiments. These corrections will involve loops of fermions and gauge bosons. Previous calculations[68–71] always assumed massless fermions on the loops. As we will see later, the masses enter as m_f^2/M_W^2 (in obvious notation). Therefore, the massless approximation is basically correct for leptons or the first two families of quarks but is certainly poor for the top quark, whose lower mass limit was of 23 GeV/c^2 [ref. 72] and has now been pushed to 50 GeV/c^2. [ref. 73]

The goal of this chapter is to set limits on κ in a SM framework. The new feature is to calculate the massive fermion loops contribution to $\Delta\kappa$; the massive gauge boson loops have been calculated and verified in the past and we shall use the known results. In our calculations we will assume all the leptons to be massless, which is debatable for a τ lepton of $\sim 1.5 GeV/c^2$; the first two families of quarks will also be assumed to be massless. Therefore, we will only consider the third family and see how $\Delta\kappa$ varies as a function of the mass of the top quark. In addition, we will assume the mass of the bottom quark to be 5 GeV/c^2.

3.2 Calculation.

As this section is performed in the SM framework, the reader is referred to Appendix I for a summary of the model and a list of the relevant couplings.

The notation defined in fig. 1 shows clearly where κ enters in the γW^+W^- vertex, but it is not very practical from a computational point of view. The most useful notation is defined in fig. 17. We shall assume CP invariance of the model and set all particles on the mass-shell. In this way, the most general CP invariant vertex can be written in the form[68]:

$$\Gamma^{\mu\nu\lambda} = ie\Big\{A\Big(2p^\lambda g^{\mu\nu} + 4(Q^\nu g^{\lambda\mu} - Q^\mu g^{\lambda\nu})\Big) + 2\Delta\kappa(Q^\nu g^{\lambda\mu} - Q^\mu g^{\lambda\nu}) + 4\frac{\Delta Q}{M_W^2}p^\lambda Q^\mu Q^\nu\Big\} \tag{3.2}$$

where A is a constant that will be absorbed into renormalizations, ΔQ is the anomalous electric quadrupole moment and the second term is the correction to the anomalous magnetic moment. At tree level, A$\equiv$ 1, $\Delta\kappa \equiv 0$, and $\Delta Q \equiv 0$.

The magnetic dipole moment and the electric quadrupole moment will be altered by these corrections. After some calculations[48] we derive that:

$$\mathcal{M} = \Big(1 + (\kappa + \Delta\kappa) + \frac{\Delta Q}{2}\Big))\Big(\frac{e}{2M_W}\Big)$$

and

$$Q_E = -\Big(\frac{e}{M_W^2}\Big)\Big((\kappa + \Delta\kappa) - \frac{\Delta Q}{2}\Big).$$

We see that both of these moments will have corrections that originate from $\Delta\kappa$ and ΔQ. This means that a precise measurement of $\mathcal{M}$ could not lead to a precise

Figure 17. Three-boson vertex.

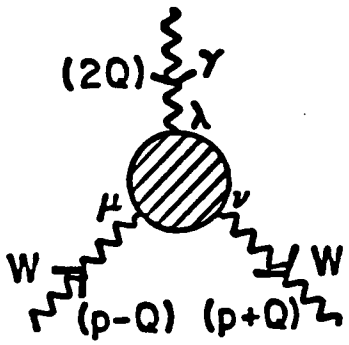

A more practical way to write the momenta in a three-boson vertex is given here. This can noticeably reduce the required algebra.

Figure 18. Heavy fermion loop.

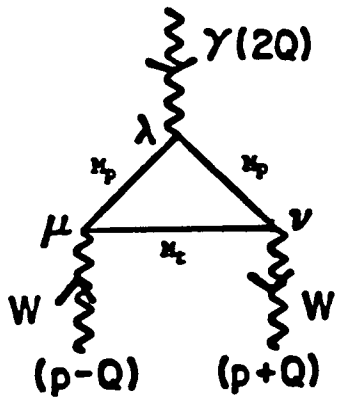

Heavy fermion loop contribution to $\Delta\kappa$ and ΔQ. We keep the terms that are proportional to the mass of the lepton. There will be three such loops: 1) electron-electron-neutrino loop, 2) bottom-bottom-top quarks loop, 3) top-top-bottom quarks loop. The integrals are the same but one has to redefine M_p and M_t for each type of loop. One must also take the charge and color factors into account for each different loop.

$\Delta\kappa$. However, as we saw in the first two chapters, one will measure κ rather than $\mathcal{M}$. Furthermore, as we will see later, the corrections from $\Delta\kappa$ are considerably larger than the corrections from ΔQ, generally speaking.

In calculating this diagram, one must make use of the following relations:

$$(p-Q)_\mu \cdot \varepsilon^\mu = (p+Q)_\nu \cdot \varepsilon^\nu = (2Q)_\lambda \cdot \varepsilon^\lambda \equiv 0 \tag{3.3}$$

where the ε are the polarization vectors in order to bring the whole diagram into the form

$$ap^\lambda g^{\mu\nu} + bQ^\nu g^{\lambda\mu} + cQ^\mu g^{\lambda\nu} + dp^\lambda Q^\mu Q^\nu. \tag{3.4}$$

However, the constants a, b, c all diverge. One then proceeds to rewrite the vertex as in eq. 3.2:

$$ap^\lambda g^{\mu\nu} + 2a(Q^\nu g^{\lambda\mu} - Q^\mu g^{\lambda\nu}) + (b-2a)Q^\nu g^{\lambda\mu} + (c+2a)Q^\mu g^{\lambda\nu} + dp^\lambda Q^\mu Q^\nu.$$

The power and beauty of a renormalizable model now appear. *The constants* $(b-2a)$ *and* $(c+2a)$ *are finite and opposite in sign!* This is exactly what one wants and what one needs. Therefore,

$$b - 2a \equiv (2ie)(\Delta\kappa) \tag{3.5}$$

Furthermore, our initial constant A will be used as a divergence "absorbant" and will have a contribution from the (diverging) constant a. Note however that in our specific case, the divergences absorbed by A from the leptons are exactly cancelled by the divergences coming from the quarks, so that A remains finite from the fermion sector. This is not to be taken as a general rule though; it will not occur for example in the gauge boson sector. For more details about the form of the vertex the reader is referred to Appendix V.

This important point being understood, the calculation is rather straightforward; albeit messy. We used dimensional regularization to manipulate the divergences.

In the calculation, we neglected Kobayashi-Maskawa-like terms, for two reasons. First, the terms that would enter in the calculation are very close to 1 and would not change the results significantly. Second, and more important, these terms lead to CP violation. We chose our vertex to be CP invariant; therefore, for consistency, we should not keep these terms since our vertex is not designed to take them into account. It is an interesting extension of this work to do the calculation in a CP non conserving model and see how different an answer one gets[42,48]. We will not worry about this question here.

3.3 Results.

The calculation is straightforward but tedious: we essentially carry out the work as outlined in the previous section. We shall not reproduce it here; a summary can be found in Appendix VI. Only the final results will be given.

For a loop of heavy fermions, where the notation is defined on fig. 18, one gets[74]:

$$(\Delta\kappa)_f = \mathcal{A}C \int_0^1 \frac{t^4 + (F-2)t^3 + (1+\epsilon-F)t^2}{t^2 - tF + \delta}\, dt \tag{3.6}$$

where:

$$\mathcal{A} \equiv g^2/96\pi^2 \approx 5 \times 10^{-4}$$

and is our standard unit for the remainder of the thesis. Besides,

$$\delta \equiv (M_t/M_W)^2, \epsilon \equiv (M_p/M_W)^2, F \equiv 1 + \delta - \epsilon$$

The constant C involves charge and color factors in the lepton and quark loops:

$$C = \quad 6 \text{ for the ttb loop,}$$

$$C = -3 \text{ for the bbt loop,}$$

$$C = -3 \text{ for the lepton loop.}$$

In the massless limit, all the integrals are the same and one easily sees that the quark contribution to $\Delta\kappa$ will be exactly cancelled by the lepton component. In the same limit, one easily calculates the integral to be 1/3, thereby recovering the results of ref. 68.

For the anomalous quadrupole moment, the calculation is simpler since no divergence occurs. We obtained[74]:

$$(\Delta Q)_f = (4/3)\mathcal{A}C \int_0^1 \frac{t^4 - t^3}{t^2 - Ft + \delta}\, dt \tag{3.7}$$

where the notation is the same as before. Again, the contribution of the quarks is cancelled by the contribution of the leptons in the massless limit. We also recover the results of ref. 68 in the massless limit.

On fig. 19, we show the contribution to $\Delta\kappa$ and ΔQ, for a complete fermion family (the lepton, ttb, and bbt loops) as a function of the mass of the top quark. The main features are clear: a very sizeable maximum occur for $\Delta\kappa$ at $M_{top} \approx M_W$.

Figure 19. $\Delta\kappa$ and ΔQ as a function of M_{top}.

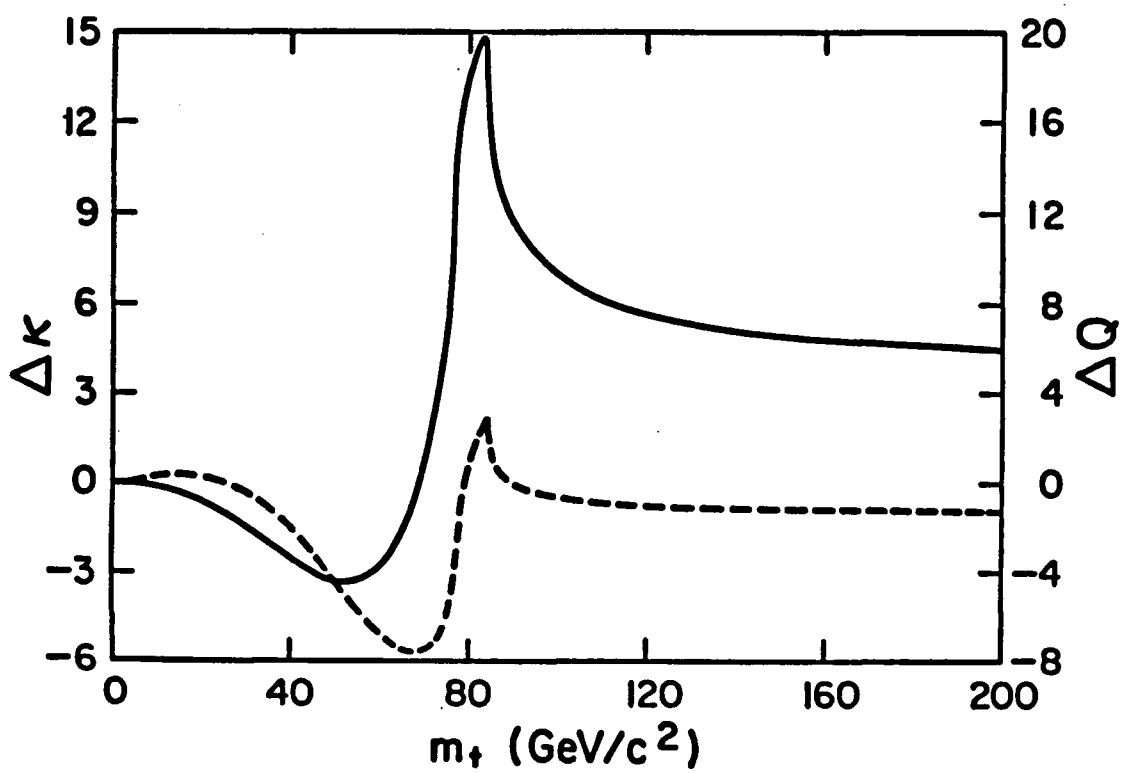

$\Delta\kappa$ (continuous line) and ΔQ (dotted line) as a function of M_{top} for a complete fermion family: we added the lepton loop and the 2 quark loops. The vertical scale is in units of $\mathcal{A} \equiv g^2/96\pi^2 \sim 5 \times 10^{-4}$. Note the very small values of ΔQ.

Note that this value for the mass of the top quark is close to the new experimental value from the ARGUS group[73]. Note also that for a small range of masses for the top quark, the value of $\Delta\kappa$ is negative. This value will be overcome by the contributions from the photon and neutral weak boson. There is also a "resonant" behaviour for values of M_{top} close to M_W. One would expect this kind of behaviour since the external particle is the W boson. Furthermore, it is interesting to note that even for very heavy loop particles, the contributions to $\Delta\kappa$ do not vanish. This is a property of SSB: all masses and couplings are very intimately connected to the vev acquired by the Higgs field. So, a decoupling theorem, as occurs in QCD, does not really apply here[75]. This nonzero value for large masses is the result of this intimate interplay. This does not mean that large mass limits will always be nonzero, merely that the limit is a little more subtle.

An extremum also occurs for ΔQ for such a top quark, but the value is rather small. Notice that for a small range of masses for the top quark, the sign of ΔQ can be positive.

For a very massive top quark one reads the limits as:

$$\Delta\kappa \rightarrow 4\mathcal{A},$$

$$\Delta Q \rightarrow -\mathcal{A}$$

The contributions from the boson loops have been calculated and verified in the past. For completeness, we give the Feynman diagrams in fig. 20 and results of the calculations[68,71]:

$$(\Delta\kappa)_{Z^0} = \frac{6\mathcal{A}}{R}\int_0^1 \frac{8(t^4 - t^3 + t^2) + R(t^4 - 5t^3 - 2t^2) - (1/2)R^2(t^3 - 5t^2 + 4t)}{t^2 - Rt + R}\, dt \quad (3.8)$$

Figure 20. Gauge boson loops involved in $\Delta\kappa$.

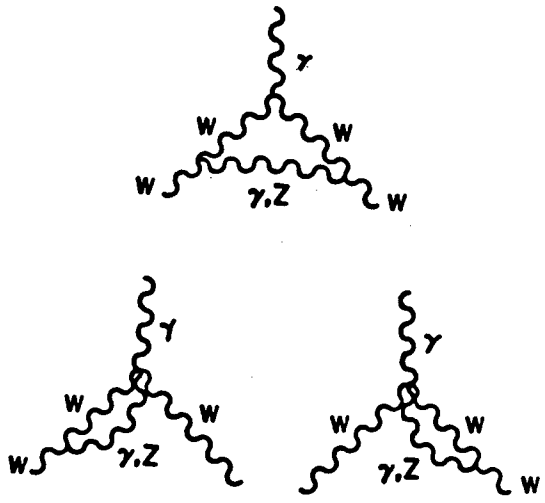

Photon and Z^0 gauge boson loop contribution to $\Delta\kappa$ in the SM. As the loops involved known particles, their contributions are very well defined. (i.e. one gets a number.)

Figure 21. Higgs boson loop involved in $\Delta\kappa$.

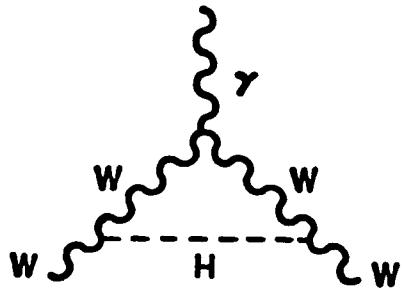

The Higgs particle will contribute to $\Delta\kappa$ through this loop. As the mass of the Higgs particle is not well defined, one has to consider it as a free parameter. One then obtains a graph of $\Delta\kappa$ as a function of the mass of the Higgs particle.

$$(\Delta Q)_{Z^0} = \frac{2\mathcal{A}}{R} \int_0^1 \frac{t^3(1-t)(8+R)}{t^2 - Rt + R}\, dt \tag{3.9}$$

$$(\Delta\kappa)_\gamma = (5/3)(\alpha/\pi) \qquad (\Delta Q)_\gamma = (1/9)(\alpha/\pi)$$

where $R \equiv (M_Z/M_W)^2$

Using these results, one gets:

$$(\Delta\kappa)_{Z^0} = -2\mathcal{A}, \qquad (\Delta\kappa)_\gamma = 8.6\mathcal{A}$$

and

$$(\Delta Q)_{Z^0} = 0.81\mathcal{A}, \qquad (\Delta Q)_\gamma = 0.57\mathcal{A}.$$

Note that the γ and the Z^0 compete in the $\Delta\kappa$ case but add in the ΔQ case. Although there is no profound meaning to this, it is worth mentioning.

As mentioned before, one of the big unknowns of the SM is the Higgs particle. Its contribution to $\Delta\kappa$ and ΔQ arises from the diagram on fig. 21 and is also taken from the literature[68]. It reads as follows:

$$(\Delta\kappa)_{Higgs} = 3\mathcal{A} \int_0^1 \frac{t^4 - t^3 + 2t^2 - (1/2)\rho^2 t^2 (t-1)}{t^2 + \rho^2(1-t)}\, dt \tag{3.10}$$

and

$$(\Delta Q)_{Higgs} = 2\mathcal{A} \int_0^1 \frac{t^3(1-t)}{t^2 + \rho^2(1-t)}\, dt \tag{3.11}$$

Figure 22. $\Delta\kappa$ and ΔQ as a function of the mass of the Higgs particle.

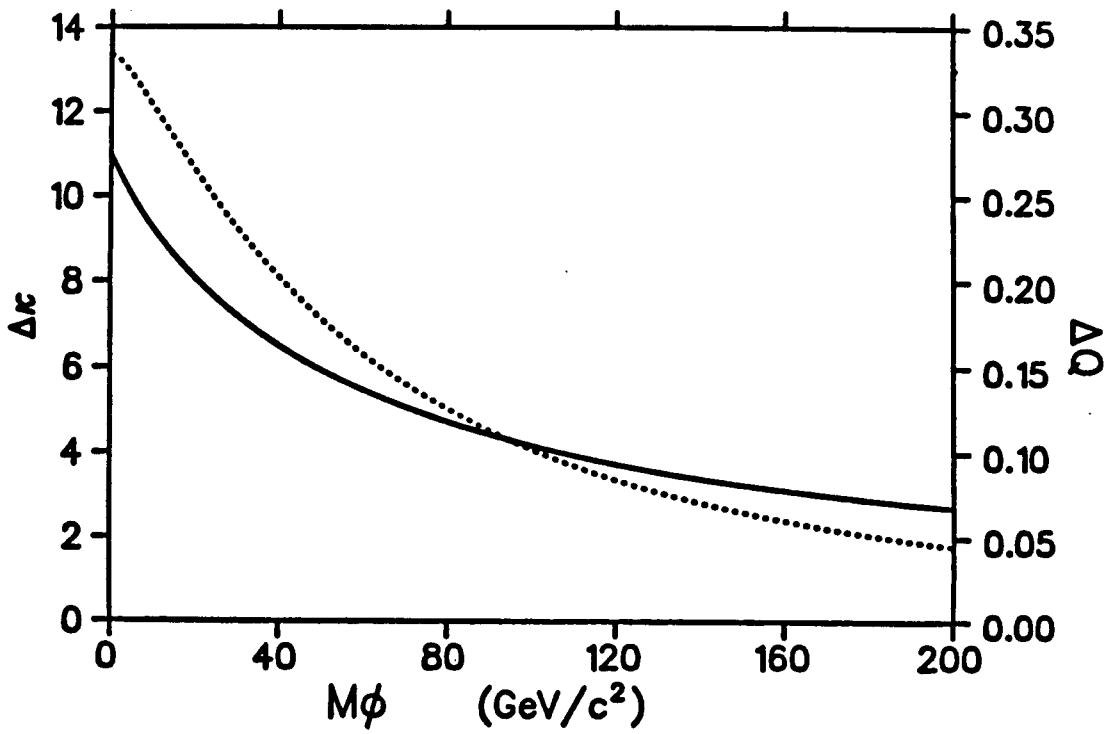

$\Delta\kappa$ (continuous line) and ΔQ (dotted line) as a function of the mass of the Higgs particle. The vertical scale is in units of $\mathcal{A}$. Note the small values of ΔQ.

where

$$\rho \equiv M_{Higgs}/M_W$$

The mass of the Higgs boson is unknown in the SM and the particle has not been observed yet. Some loose bounds can be obtained[62,76] but they still allow for a large mass range. We shall adopt the following range:

$$10GeV/c^2 \leq M_{Higgs} \leq 1000GeV/c^2.$$

See Appendix VIII for more details on the mass of the Higgs.

These functions are plotted in fig. 22 as a function of the mass of the Higgs for the range mentioned. The main points are that $(\Delta\kappa)_{Higgs}$ is monotonic and decreases rather quickly from 11 $\mathcal{A}$ for a massless Higgs particle to $1\mathcal{A}$ for a ultra massive one. On the other hand, $(\Delta Q)_{Higgs}$ is very small and one would not expect it to make any difference for the total value of the quadrupole moment. It is also monotonic in M_{Higgs}.

In order to give a good idea of $\Delta\kappa$ and ΔQ in the SM, we show on fig. 23 and fig. 24 three dimensional plots of $\Delta\kappa$ and ΔQ as a function of the mass of the top quark and the mass of the Higgs particle. Again, the main features are clear: a sizeable maximum occurs both for $\Delta\kappa$ and ΔQ when the mass of the top quark is approximately equal to the mass of the W boson, no matter what the mass of the Higgs is. Note that the contributions of the gauge bosons and the Higgs particle are sufficient to bring $\Delta\kappa$ in the positive range for any value of the masses covered here. Note also the relatively weak depenance on the mass of the Higgs particle as compared to the mass of the top quark. For ΔQ, there is practically no dependence at all on the mass of the Higgs particle. Note also that on a large portion of the mass range covered here, ΔQ can be negative. The values are very small on the whole range of masses covered here.

Figure 23. $\Delta\kappa$ as a function of M_{top} and M_{Higgs}.

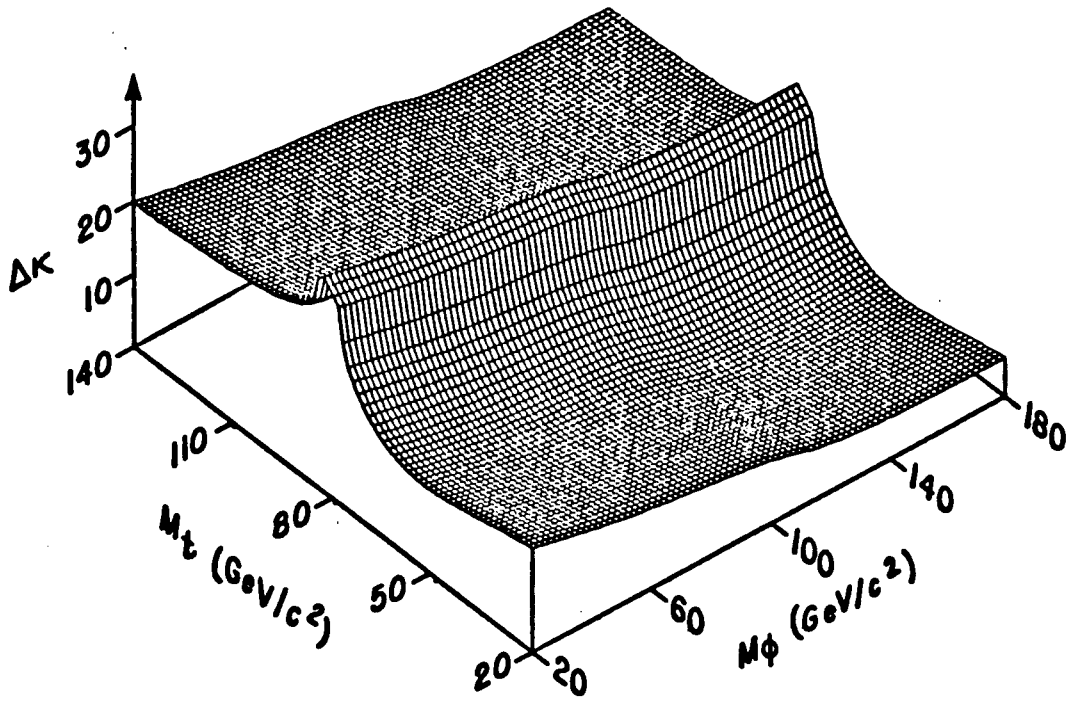

$\Delta\kappa$ as a function of M_{top} and M_{Higgs}. The vertical scale is in units of $\mathcal{A}$. Note the peak that occurs for $M_{top} \sim M_W$ for any value of M_{Higgs}

Figure 24. ΔQ as a function of M_{top} and M_{Higgs}.

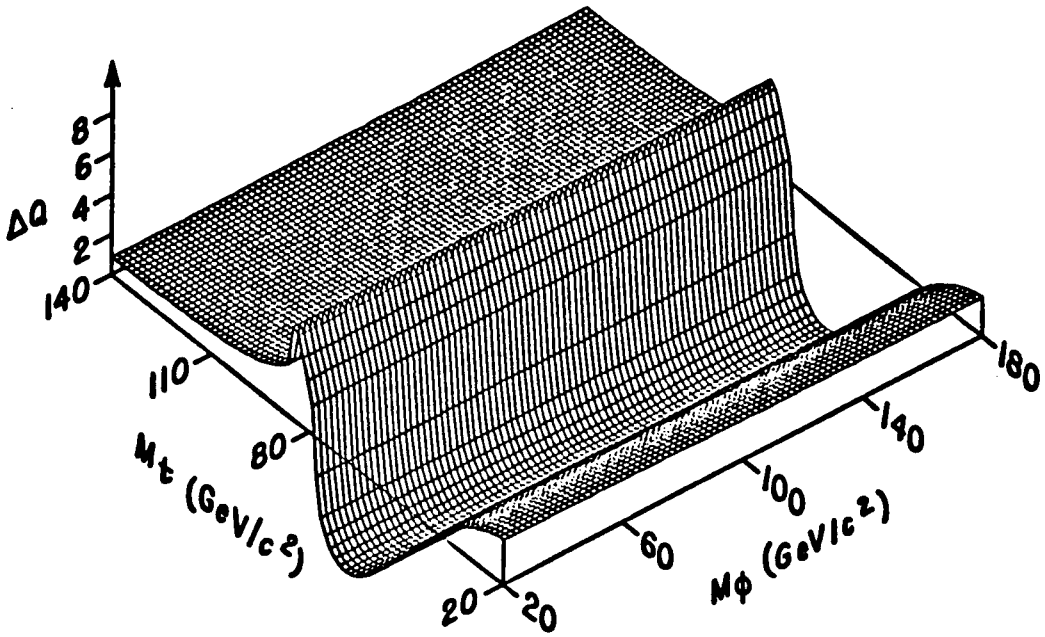

ΔQ as a function of M_{top} and M_{Higgs}. The scale is in units of $\mathcal{A}$. Note the small values of the scales and the rapid change of ΔQ for values of $M_{top} \sim M_W$.

From these graphs, we can set an upper limit on these parameters:

$$\Delta\kappa_{max} \approx 30\mathcal{A}$$
$$\approx 1.5 \times 10^{-2}$$

and

$$\Delta Q_{max} \approx 4.5\mathcal{A}$$
$$\approx 0.25 \times 10^{-2}$$

These are the maximal values allowed by the minimal SM.

For completeness, we give values of $\Delta\kappa$ and ΔQ over an interesting range of M_{top} and M_{Higgs} in Table III.

A somewhat relevant point regards neutral particles. From the previous discussion, one would be tempted to conclude that any neutral particle can acquire an effective magnetic moment via loop corrections. This is partly correct and...partly wrong. For example, in the SM framework the fact that the neutrino is massless forces its magnetic moment to vanish identically[77]. However, if its mass is not zero, it will acquire a magnetic moment proportional to its mass. This mass dependence reflects the facts that a Majorana neutrino cannot have any moment and that the difference between a Dirac neutrino and a Majorana neutrino vanishes as the mass goes to zero[78]. Recently, it has been suggested that such a magnetic moment could be responsible for the solar neutrino problem[79]. In going through the magnetic field of the sun as they escape from it, they would precess from the left-handed state to the right-handed state and would not trigger the detectors when they reach the earth. This certainly goes beyond the SM since it allows a nonzero mass for the neutrino. Thus, if the neutrino were to be massive it would acquire a magnetic moment at loop-level only; at tree-level, it would still be zero.

TABLE III

$\Delta\kappa$ and ΔQ for different $M_{top}$and M_{Higgs}.

$M_\phi \setminus M_t$	20	50	83	100	150	500
20	$\begin{pmatrix}14.0\\1.9\end{pmatrix}$	$\begin{pmatrix}11.4\\-2.8\end{pmatrix}$	$\begin{pmatrix}29.5\\4.1\end{pmatrix}$	$\begin{pmatrix}21.6\\1.1\end{pmatrix}$	$\begin{pmatrix}19.5\\0.5\end{pmatrix}$	$\begin{pmatrix}18.8\\0.3\end{pmatrix}$
50	$\begin{pmatrix}11.9\\1.8\end{pmatrix}$	$\begin{pmatrix}9.2\\-2.9\end{pmatrix}$	$\begin{pmatrix}27.3\\4.0\end{pmatrix}$	$\begin{pmatrix}19.4\\0.9\end{pmatrix}$	$\begin{pmatrix}17.4\\0.4\end{pmatrix}$	$\begin{pmatrix}16.6\\0.2\end{pmatrix}$
100	$\begin{pmatrix}10.1\\1.8\end{pmatrix}$	$\begin{pmatrix}7.4\\-3.0\end{pmatrix}$	$\begin{pmatrix}25.5\\3.9\end{pmatrix}$	$\begin{pmatrix}17.7\\0.8\end{pmatrix}$	$\begin{pmatrix}15.6\\0.3\end{pmatrix}$	$\begin{pmatrix}14.8\\0.2\end{pmatrix}$
150	$\begin{pmatrix}9.2\\1.7\end{pmatrix}$	$\begin{pmatrix}6.5\\-3.0\end{pmatrix}$	$\begin{pmatrix}24.6\\3.9\end{pmatrix}$	$\begin{pmatrix}16.8\\0.8\end{pmatrix}$	$\begin{pmatrix}14.7\\0.3\end{pmatrix}$	$\begin{pmatrix}13.9\\0.1\end{pmatrix}$
500	$\begin{pmatrix}7.6\\1.7\end{pmatrix}$	$\begin{pmatrix}4.8\\-3.1\end{pmatrix}$	$\begin{pmatrix}23.0\\3.8\end{pmatrix}$	$\begin{pmatrix}15.1\\0.8\end{pmatrix}$	$\begin{pmatrix}13.0\\0.2\end{pmatrix}$	$\begin{pmatrix}12.2\\-0.1\end{pmatrix}$

Values of $\begin{pmatrix}\Delta\kappa\\\Delta Q\end{pmatrix}$ for different values of the mass of the top quark (M_t) and the mass of the Higgs particle (M_ϕ). All the masses are in GeV/c^2 and the numbers are in units of $\mathcal{A} \sim 5 \times 10^{-4}$.

If the particles are composites, they can have large magnetic moments. For example, the large magnetic moment of the neutron was an early clue to its compositeness. In the same way, if the Z^0 were to have a large moment it would indicate most likely compositeness and would go far beyond the SM. From classical analogy, since a multipole expansion does not make sense for a neutral particle, one must go to the loop level, beyond classical physics, in order to get the magnetic moment. On the other hand a multipole expansion makes perfect sense for a neutral charge distribution and such a composite particle could acquire a large magnetic moment.

3.4 Conclusions.

The main conclusions of this chapter are the limits obtained for $\Delta\kappa$ and ΔQ. We stress again that those are the absolute maximum values allowed by the minimal SM. Again:

$$\Delta\kappa_{max} \approx 1.5\%$$

$$\Delta Q_{max} \approx 0.25\%$$

This means that a measurement of $\Delta\kappa$ of 3% for example would immediately imply that the minimal SM is incomplete. One would have to add at least one family of fermions: adding approximately 1% on the peak value. However, one could argue that this extra family could have a very heavy bottom-like quark. We have verified that a light bottom-like particle gives the largest contribution to $\Delta\kappa$ or ΔQ; we assumed the top-like particle to be heavier than the bottom-like. We have also verified that decreasing the mass of the bottom quark from 5 GeV to 2 GeV does not increase $\Delta\kappa$ by more than 20% at the peak. The goal of these tests was to take into account the new mass limits from the ARGUS collaboration: $m_{top} > 50GeV/c^2$ and $m_{bottom} < 5GeV/c^2$. [ref. 73] This strengthens our conclusions that each fermion family contributes at best 1.5% to $\Delta\kappa$ and 0.25% to ΔQ.

It is also expected that the introduction of Kobayashi-Maskawa-like terms will not change these results since the new factors that one would introduce are very close to one.

Chapter IV
Loop Corrections to κ
in a
Two-Higgs-Doublet Model.

4.1 Introduction

In the SM, one really needs only one Higgs doublet to break the symmetry and give masses to the fermions and gauge bosons. However, there exists no real argument (theoretical or experimental) to limit the number of doublets to one. The addition of extra Higgs doublets is the simplest extension to the minimal SM. It is natural to study it and see its consequences. By adding a doublet, one has another "source" of mass for the fermions and the gauge bosons. It has been argued in the past[80] that one could give one of the vev's (see Appendix I for definition.)a large value and use it to generate mass for the heavy gauge bosons while the other vev is small and gives mass to the lighter fermions. This, of course, does not explain satisfactorily the big mass difference between the fermions and gauge bosons; since the question now regards the big difference between the vev's. This mass question essentially requires a greater unification to have any answer. The extra doublet will also give rise to many new interaction terms that will open new channels for processes. As we will explain later, these new channels can lead to unwanted processes. One then has to put some constraints on the model. We will merely limit ourselves to new interactions involved in the magnetic moment of the W boson.

All these considerations make multi-Higgs-doublet models interesting in their own right. Besides, most new theories require more than one Higgs doublet in order to be consistent, or phenomenologically acceptable. Supersymmetric models, for

example, require at least two Higgs doublets in order to give masses to all quarks[20].

In this chapter, we will investigate a two-Higgs-doublet model. In a first section, we will study some possible problems that one can encounter by such extensions. Even though one has a large freedom in the new sectors of the model, there exist some "no-go" theorems that one must respect in order to agree with known phenomenology. These will slightly constrain the model. In a second section we will describe the model in some details. This part will be rather technical, but the details we give will help understand the SM, which we briefly explain in Appendix I. Once the physics of the model is explained, we will proceed to calculate the corrections to κ that arise in this model. This will be our third section. A fourth section will contain our conclusions.

4.2 Constraints on the Possible Extensions.

A – The ρ Parameter.

One of the constraints of possible extensions to the SM regards the ratio

$$\rho \equiv M_W^2/M_Z^2 cos^2(\theta_W)$$

which has been measured to be $\rho \approx 0.992 \pm 0.020$. Recall that this parameter is exactly one in the SM [ref. 29, 81] One must then build the model to preserve this ratio. There are several ways to insure that this will be so:

(i) One can choose the Higgs multiplets such that the following relation is satisfied:

$$I(I+1) = (3/4)Y^2$$

where Y is the hypercharge and I is the isospin. This relation is sufficient to ensure that ρ will be one[82]. One simple way to implement this is to work with Higgs doublets with $Y \pm 1$; although an infinite number of solutions are possible (e.g. I=3; Y=4).

(ii) One can choose arbitrary Higgs multiplets and fine-tune the parameters such that $\rho \equiv 1$ is preserved. Certainly, this way of doing things is valid but not nearly as "elegant" as the previous one where the ratio is preserved "per se".

In what follows, we shall adopt the simplest and more "natural" possibility and use two Higgs doublets with Y=+1 for each one.

B – Flavor Changing Currents (FCC).

Any model that contains several Higgs particles faces the problem of unsuppressed flavor changing couplings which lead directly to larger than acceptable rates for processes like:

$$\mu \to e\ \gamma \qquad \mu \to 3\ e$$

$$K \to \mu\ \mu \qquad K \to \mu\ e$$

In the SM, FCC are "naturally" suppressed by the GIM mechanism[83] so that the rates agree with experiments. The same FCC will also lead to a value of $\Delta M_K \equiv M_{K_L} - M_{K_S}$ that is far too large[84]. One then has to suppress or eliminate FCC. In a multi-doublet model, two directions can be used to do so:

(i) One can choose the masses of the Higgs particles large enough so that FCC induced by Higgs exchange are very suppressed. However, one can run into some problems with very large masses for the Higgs particles. (See Appendix VIII for more details.)

(ii) Another, more subtle, way to deal with this problem is to constrain the form of the Lagrangian. Glashow and Weinberg[85] showed that tree-level FCC via Higgs exchange will be absent *only* if all fermions of a given charge couple to no more than one Higgs doublet. One simple way to achieve this is to impose the following symmetry on the Lagrangian: we want $\mathcal{L}$ to be invariant under

$$\Phi_2 \to -\Phi_2 \qquad d_r \to -d_r$$

$$\Phi_1 \to -\Phi_1 \qquad u_r \to -u_r$$

where the Φ_i are the Higgs fields and d, u refer to quarks. In what follows, we shall not be concerned with the quarks but the symmetry imposed on the Lagrangian

will constrain the form of the Higgs potential we will use later.

C – Mass of the Higgs Particles.

Several investigations[86] concern the limits on the mass of the Higgs particles in multi-Higgs-doublet models. The reader is referred to Appendix VIII for more details. In this chapter, we will set our limits at:

$$50GeV/c^2 \leq M_\phi \leq 1000GeV/c^2$$

for all Higgs particles.

So we will work with two Higgs doublets of hypercharge +1. The particle content of this model is very similar to the SM. We simply add a few scalars; the fermionic and bosonic sectors are unchanged from the SM. Therefore, as we start with eight degrees of freedom in the Higgs sector and will loose three to the weak bosons, we will be left with five scalars: two of them will be charged (conjugate of each other), two will be neutral scalars and one will be a neutral pseudo-scalar.

The interaction Lagrangian is profoundly modified by this addition; but the new couplings relevant to the calculation of $\Delta\kappa$ all come from the covariant derivative terms. The Higgs potential will also be relevant to us in order to get some mass terms and mixings. We will then limit ourselves to these two components of the Lagrangian.

4.3 Description of the Model.

We work with two Higgs doublets, which we can write as

$$\Phi_1 = \begin{pmatrix} \phi_1^+ \\ \phi_1^0 \end{pmatrix} \qquad \Phi_2 = \begin{pmatrix} \phi_2^+ \\ \phi_2^0 \end{pmatrix}$$

Both of these fields can acquire a vev. The vev's are set by the weak scale such that

$$\sum_i (vev)_i^2 \approx (250GeV)^2.$$

In principle, one could be left with a phase between the vev's. For simplicity, we will set this phase to 0. We then have:

$$\langle \Phi_1 \rangle = \begin{pmatrix} 0 \\ a/\sqrt{2} \end{pmatrix} \qquad \langle \Phi_2 \rangle = \begin{pmatrix} 0 \\ b/\sqrt{2} \end{pmatrix}$$

The goal now is to "transfer" the vev of one field to the other. In order to do so, we define new fields:

$$\Phi_1' = \Phi_1 cos(\alpha) + \Phi_2 sin(\alpha)$$

and

$$\Phi_2' = -\Phi_1 sin(\alpha) + \Phi_2 cos(\alpha)$$

which leads directly to

$$\langle \Phi_1' \rangle = \frac{a}{\sqrt{2}} cos(\alpha) + \frac{b}{\sqrt{2}} sin(\alpha)$$

$$\langle \Phi_2' \rangle = -\frac{a}{\sqrt{2}} sin(\alpha) + \frac{b}{\sqrt{2}} cos(\alpha)$$

At that point, it is possible to impose $\langle \Phi_2' \rangle \equiv 0$, thereby defining $tan(\alpha) = b/a$ and obtaining:

$$\langle \Phi_1' \rangle = \begin{pmatrix} 0 \\ v/\sqrt{2} \end{pmatrix} \qquad \langle \Phi_2' \rangle = \begin{pmatrix} 0 \\ 0 \end{pmatrix}$$

where $v^2 \equiv a^2 + b^2$. The mixing angle α seems very arbitrary, but some considerations from $K_L - K_S$ mass difference impose the constraint[87]

$$(b/a)^2 \leq 2(M_{Higgs}/m_c)$$

Using $m_c \sim 1.6GeV/c^2$ and the maximum mass for the Higgs ($M_{Higgs} \sim 1TeV/c^2$) one gets:

$$tan(\alpha) \leq \ 40$$

This is a slight constraint on the model that will not affect us.

The point of the previous rotations becomes clear when one rewrites the doublets in terms of the physical and unphysical fields:

$$\Phi_1' = \begin{pmatrix} G^+ \\ (v + H_1^0 + iG^0)/\sqrt{2} \end{pmatrix} \qquad \Phi_2' = \begin{pmatrix} H^+ \\ (H_2^0 + iH_3^0)/\sqrt{2} \end{pmatrix}$$

It is now clear that the first doublet (Φ_1') is the same as the SM doublet where G^+ and G^0 are the would-be Goldstone bosons that will become the longitudinal component of the $W^\pm$ and the Z^0 bosons respectively and H_1^0 is the Higgs particle. However, we can expect mixing between particles of the first doublet and particles of the second doublet since, generally speaking, particles with the same quantum numbers mix. When masses differ by several orders of magnitude, one can expect the mixing to be small, but in our case one cannot really make this assumption. So, we expect mixing between $H_1^0 H_2^0$, $G^+ H^+$, $G^0 H_3^0$. However, recall that G^+, G^0 are would-be Goldstone bosons. On the grounds that mixing is physical, should therefore be gauge independant and that in the U-gauge these would-be Goldstone bosons simply do not appear, one concludes that the would-be Goldstone bosons cannot mix with any physical fields. Thus, one is left with mixing only between H_1^0 and H_2^0. A complete calculation will show this conclusion to be correct.

In order to calculate the corrections to κ, we need the fields that couple either to the photon or to the $W^{\pm}$ bosons. All these new couplings come from the covariant derivative terms, which now differ from the SM. Using the newly defined fields, we now proceed to calculate these terms. We shall also be interested in the Higgs potential in order to get mass terms for all these Higgs particles and the mixing between H_1^0 and H_2^0.

A – Covariant Derivative Terms.

These terms are written as:

$$\mathcal{L}_{CD} = (D_\mu \Phi_1)^\dagger (D_\mu \Phi_1) + (D_\mu \Phi_2)^\dagger (D_\mu \Phi_2) \tag{4.1}$$

where

$$D_\mu \equiv \partial_\mu - i\frac{g'}{2}B_\mu - i\frac{g}{2}\vec{\tau}\cdot\vec{A}_\mu$$

with $\vec{A}_\mu$ and B_μ being the SU(2) and U(1) generators, respectively and $\vec{\tau}$ the Pauli matrices. A very short calculation shows that:

$$\mathcal{L}_{CD} = (D_\mu \Phi_1')^\dagger (D_\mu \Phi_1') + (D_\mu \Phi_2')^\dagger (D_\mu \Phi_2') \tag{4.2}$$

It is worthwile to mention that it is always possible to get rid of the phase between the two vev's in $\mathcal{L}_{CD}$. This implies that one cannot get CP violation from $\mathcal{L}_{CD}$. However, this phase could appear in Yukawa terms and would then lead to CP violation in these terms. More generally, it can show up every time one has a vertex with an odd number of gauge fields; but those terms are of higher order and very small. We shall not pursue this avenue any further[88].

At this point, the most straightforward way to proceed is to rewrite all the fields in terms of the physical fields of the SM. The definitions of the gauge bosons will not change since the Higgs fields are not involved in those. Recall that[83]:

$$
\begin{aligned}
B_\mu &\equiv (g\mathcal{A}_\mu - g' Z_\mu)/\mathcal{G} \\
A^3_\mu &\equiv (g'\mathcal{A}_\mu + g Z_\mu)/\mathcal{G} \\
A^2_\mu &\equiv i(W^+_\mu - W^-_\mu)/\sqrt{2} \\
A^1_\mu &\equiv (W^+_\mu + W^-_\mu)/\sqrt{2}
\end{aligned}
$$

where $\mathcal{G}^2 \equiv g^2 + g'^2$ and $tan(\theta_W) \equiv g'/g$ and $\mathcal{A}_\mu$ is the real photon field. Then, one easily derives the following expression:

$$
D_\mu = \begin{pmatrix} \partial_\mu - i(\mathcal{G}/2)sin(2\theta_W)\mathcal{A}_\mu - (\mathcal{G}/2)cos(2\theta_W)Z^0_\mu & -i(g/\sqrt{2})W^+_\mu \\ -i(g/\sqrt{2})W^-_\mu & \partial_\mu + i(\mathcal{G}/2)Z^0_\mu \end{pmatrix}. \tag{4.3}
$$

Using this form of the covariant derivatives and the definitions of the fields, one expands $\mathcal{L}_{CD}$ in order to get interaction terms. However, a last problem encountered relates to terms of the form:

$$
-i(gv/2)\{(\partial_\mu G^-)W^+_\mu - W^-_\mu(\partial_\mu G^+)\} - i(gv/2)\partial_\mu(W^-_\mu \ G^+) \tag{4.4}
$$

The last term is a surface term (total divergence) and can be safely dropped. After a partial integration, one gets:

$$
iM_W\{G^-(\partial_\mu W^+_\mu) - G^+(\partial_\mu W^-_\mu)\}
$$

where the definition of the mass of the W boson has been used: $M_W \equiv (gv/2)$.

One wants to get rid of those terms because they correspond to a particle spontaneously decaying into another one without any other residue; which is difficult to make sense of. These terms involve only a gauge boson and its would-be Goldstone boson that will become its longitudinal component. The appearance of such terms

is a consequence of not having fixed the gauge yet; indeed we have not been working in any given gauge up to now.

In order to remedy this problem and get rid of the unwanted terms, we introduce, following 't Hooft[12], the gauge fixing Lagrangian:

$$\mathcal{L}_{GF} = \frac{-1}{\zeta}\left[\partial_\mu W_\mu^- + i\zeta M_W\ G^-\right]\left[\partial_\mu W_\mu^+ - i\zeta M_W\ G^+\right] \tag{4.5}$$

Note that this gauge fixing Lagrangian gives a mass to the would-be Goldstone boson (G^+) that is ζM_W. In fact, one would expect this result: since the would-be Goldstone bosons become the longitudinal component of the gauge bosons, they must have the same mass as their respective gauge boson (in the 't Hooft-Feynman gauge: $\zeta \to 1$). This mass term will have some effects in the potential.

We have similar terms for the Z^0, albeit a little easier. We want to get rid of terms like:

$$-\mathcal{G}v\ G^0(\partial_\mu Z_\mu) \tag{4.6}$$

and introduce the gauge fixing Lagrangian:

$$\mathcal{L}_{GF} = \frac{-1}{2\zeta}\left[\partial_\mu Z^\mu - \zeta\mathcal{G}v\ G^0\right]\left[\partial_\mu Z^\mu - \zeta\mathcal{G}v\ G^0\right] \tag{4.7}$$

Again, we assign a mass to the would-be Goldstone boson that is ζM_Z.

These gauge fixing Lagrangians involve only the would-be Goldstone bosons and will occur only in the first doublet; namely the Φ_1' fields. If one were to work in the unitarity gauge, obviously the gauge would be fixed, and such terms would not occur. In this gauge, the would-be Goldstone bosons do not exist as they are "gauged away" and absorbed by the gauge bosons. The gauge we chose here is known as renormalizable gauges because the high energy behaviour of the model is much easier to see in this gauge. The unitarity gauge is good to express the physical content of the model but makes the renormalizability of the theory quite

obscure. 't Hooft had the insight of using a gauge to show one facet of a theory and another one to prove another facet of the same theory. Since the theory we are working with is gauge invariant, this is all consistent.

In final form, one has:

$$
\begin{aligned}
\mathcal{L}_{CD} + \mathcal{L}_{GF} = \Bigg\{ . \Bigg\{ . \Big[. (\partial_\mu + i(\mathcal{G}/2) sin(2\theta_W) \mathcal{A}_\mu + i(\mathcal{G}/2) cos(2\theta_w) Z_\mu) G^- \\
+ (igW_\mu^- / \sqrt{2}) (\frac{v + H_1^0 - iG^0}{\sqrt{2}}) \Big] \times \Big[h.c. \Big] \\
+ \Big[(ig/\sqrt{2}) W_\mu^+ \; G^- + (\partial_\mu - i(\mathcal{G}/2) Z_\mu) (\frac{v + H_1^0 - iG^0}{\sqrt{2}}) \Big] \times \Big[h.c. \Big] \Bigg\} \\
+ \Big\{ G^- \to H^-, \; H_1^0 \to H_2^0, \; G^0 \to H - 3^0, \; v \to 0 \Big\} \; \Bigg\} \\
- \frac{1}{2\zeta} \Big[\partial_\mu W_\mu^- + ig\zeta G^- \Big] \times \Big[h.c. \Big] \\
- \frac{1}{2\zeta} \Big[\partial_\mu Z_\mu - \zeta \mathcal{G} v G^0 \Big] \times \Big[h.c. \Big]
\end{aligned}
\tag{4.8}
$$

All the new terms involving gauge bosons and Higgs particles are here! One simply has to expand the whole expression and read off the couplings when proper care is taken of the i's and momenta coming from the plane waves. We shall not expand this expression any further; neither will we list all the vertices here. In due time, we will list the vertices relevant for the calculation of $\Delta\kappa$.

B – Higgs Potential.

The only constraint on our potential comes from FCC that we want to suppress. One possible[76] way to implement this is to require

$$V(\Phi_1, \Phi_2) = V(-\Phi_1, -\Phi_2). \tag{4.9}$$

Then, the most general potential takes the form[80]:

$$\begin{aligned} V(\Phi_1, \Phi_2) = &- \mu_1^2(\Phi_1^\dagger \Phi_1) + \lambda_1(\Phi_1^\dagger \Phi_1)^2 - \mu_2^2(\Phi_2^\dagger \Phi_2) + \lambda_2(\Phi_2^\dagger \Phi_2)^2 \\ &+ \lambda_3(\Phi_1^\dagger \Phi_1)(\Phi_2^\dagger \Phi_2) + \lambda_4(\Phi_1^\dagger \Phi_2)^2 \\ &+ \frac{\lambda_5}{2}\left[(\Phi_1^\dagger \Phi_2)^2 + (\Phi_2^\dagger \Phi_1)^2\right] \end{aligned} \tag{4.10}$$

Then one proceeds to find the minimum of the potential:

$$\begin{aligned} \frac{\partial V}{\partial \Phi_1} &= -2\mu_1^2 \Phi_1 + 4\lambda_1 \Phi_1^3 + 2(\lambda_3 + \lambda_4 + \lambda_5)\Phi_1 \Phi_2^2 \\ &= 0 \end{aligned}$$

and

$$\begin{aligned} \frac{\partial V}{\partial \Phi_2} &= -2\mu_2^2 \Phi_2 + 4\lambda_2 \Phi_2^3 + 2(\lambda_2 + \lambda_4 + \lambda_5)\Phi_1^2 \Phi_2 \\ &= 0 \end{aligned}$$

which gives us:

$$\mu_1^2 = 2\lambda_1 \Phi_1^2 + (\lambda_3 + \lambda_4 + \lambda_5)\Phi_2^2$$

and

$$\mu_2^2 = 2\lambda_2\Phi_2^2 + (\lambda_3 + \lambda_4 + \lambda_5)\Phi_1^2.$$

As we break the symmetry in the form:

$$\langle\Phi_1\rangle = \begin{pmatrix} 0 \\ a/\sqrt{2} \end{pmatrix} \qquad \langle\Phi_2\rangle = \begin{pmatrix} 0 \\ b/\sqrt{2} \end{pmatrix}$$

we obtain

$$\mu_1^2 = \lambda_1 \ a^2 + (1/2)(\lambda_3 + \lambda_4 + \lambda_5)b^2 \qquad (4.11 - a)$$

$$\mu_2^2 = \lambda_2 \ b^2 + (1/2)(\lambda_3 + \lambda_4 + \lambda_5)a^2. \qquad (4.11 - b)$$

Now, we are ready to expand the potential! Recall:

$$\Phi_1 = \Phi_1' cos(\alpha) - \Phi_2' sin(\alpha)$$

$$\Phi_2 = \Phi_1' sin(\alpha) + \Phi_2' cos(\alpha)$$

The next step is now to substitute these expressions into eq. 4.10. It should be clear that we have to work with the "prime" fields since we rewrote our covariant derivatives in terms of these fields. They made the interpretation of the doublets easier, but they make the potential more complicated. After a lengthy algebraic manipulation, we obtained:

$$
\begin{aligned}
V(\Phi_1', \Phi_2') = & -\mu_1^2\left[\Phi_1'^\dagger\Phi_1' cos^2(\alpha) + \Phi_2'^\dagger\Phi_2' sin^2(\alpha)\right] \\
& -\mu_2^2\left[\Phi_1'^\dagger\Phi_1' sin^2(\alpha) + \Phi_2'^\dagger\Phi_2' cos^2(\alpha)\right] \\
& + \frac{\mu_1^2 - \mu_2^2}{2}\left[\Phi_1'^\dagger\Phi_2' + \Phi_2'^\dagger\Phi_1'\right] sin(2\alpha) \\
& + (\Phi_1'^\dagger\Phi_1')^2\left[\lambda_1 cos^4(\alpha) + \lambda_2 sin^4(\alpha) + (1/4)\Lambda sin^2(2\alpha)\right] \\
& + (\Phi_2'^\dagger\Phi_2')^2\left[\lambda_1 sin^4(\alpha) + \lambda_2 cos^4(\alpha) + (1/4)\Lambda sin^2(2\alpha)\right] \\
& + \left[(\Phi_1'^\dagger\Phi_2')^2 + (\Phi_2'^\dagger\Phi_1')^2\right]\left[(1/4)(\lambda_1 + \lambda_2 - \Lambda) sin^2(2\alpha) + (1/2)\lambda_5\right] \qquad (4.12) \\
& + \left[(\Phi_1'^\dagger\Phi_1')(\Phi_2'^\dagger\Phi_2')\right]\left[(1/2)(\lambda_1 + \lambda_2 - \Lambda) sin^2(2\alpha) + \lambda_3\right] \\
& + \left[(\Phi_1'^\dagger\Phi_1')(\Phi_1'^\dagger\Phi_2' + \Phi_2'^\dagger\Phi_1')\right] \times \\
& \quad \left[-\lambda_1 cos^2(\alpha) + \lambda_2 sin^2(\alpha) + (1/2)\Lambda cos(2\alpha)\right] sin(2\alpha) \\
& + \left[(\Phi_2'^\dagger\Phi_2')(\Phi_1'^\dagger\Phi_2' + \Phi_2'^\dagger\Phi_1')\right] \times \\
& \quad \left[-\lambda_1 sin^2(\alpha) + \lambda_2 cos^2(\alpha) - (1/2)\Lambda cos(2\alpha)\right] sin(2\alpha) \\
& + \left|\Phi_1'^\dagger\Phi_2'\right|^2\left[(1/2)(\lambda_1 + \lambda_2 - \Lambda) sin^2(2\alpha) + \lambda_4\right]
\end{aligned}
$$

where

$$\Lambda \equiv \lambda_3 + \lambda_4 + \lambda_5.$$

One would now proceed to expand this expression in terms of the components, using:

$$\Phi_1' = \begin{pmatrix} G^+ \\ (v + H_1^0 + iG^0)/\sqrt{2} \end{pmatrix} \qquad \Phi_2' = \begin{pmatrix} H^+ \\ H_2^0 + iH_3^0)/\sqrt{2} \end{pmatrix}.$$

It is out of the question to present all this algebra here: it is straightforward but very long. We will only give the results. Note that we are not interested in the interaction terms, since they do not involve gauge bosons and, as seen before, we need to couple our Higgs particles either to the photon or to the $W^\pm$ bosons. So, we look for mass terms and mixing. We find the following terms:

$$\begin{aligned}
&G^-G^+(\frac{1}{v^2})(-\mu_1^2a^2 - \mu_2^2b^2 + \lambda_1a^4 + \lambda_2b^4 + \Lambda a^2b^2), \\
&G^0G^0(\frac{1}{2v^2})(-\mu_1^2a^2 - \mu_2^2b^2 + \lambda_1a^4 + \lambda_2b^4 + \Lambda a^2b^2), \\
&H^-H^+(\frac{v^2}{2})(-)(\lambda_4 + \lambda_5), \\
&H_3^0H_3^0(-\lambda_5)(\frac{v^2}{2}), \\
&H_1^0H_1^0(\frac{1}{v^2})(\lambda_1a^4 + \lambda_2b^4 + \Lambda a^2b^2), \\
&H_2^0H_2^0(\frac{1}{4})sin^2(2\alpha)v^2(\lambda_1 + \lambda_2 - \Lambda), \\
&H_1^0H_2^0(\frac{2ab}{v^2})(-\lambda_1a^2 + \lambda_2b^2 + (1/2)\lambda(a^2 - b^2)).
\end{aligned} \tag{4.13}$$

From the definitions of μ_1^2 and μ_2^2 (eq. 4.11) one verifies easily that the first two expressions are identically 0. This is what one wants since G^+ and G^0 are would-be

Goldstone bosons and must have the mass of the $W^{\pm}$ and Z^0 bosons, respectively. They already acquired such a mass, through the gauge fixing conditions, from the covariant derivative terms. Therefore, these extra mass terms *must* vanish identically. This is a good intermediate verification for our calculation.

The third and fourth expressions imply that:

$$\lambda_5 \leq 0 \qquad\qquad \lambda_4 \leq \lambda_5.$$

The last three expressions tell us that there is mixing between H_1^0 and H_2^0. Recall that H_1^0 is the Higgs particle of the SM; it will therefore be modified by the diagonalization of the mass matrix. In order to get rid of this mixing, we define new fields such that:

$$\begin{aligned} H_1^0 &= \quad h_1^0 cos(\beta) + h_2^0 sin(\beta) \\ H_2^0 &= -h_1^0 sin(\beta) + h_2^0 cos(\beta) \end{aligned} \tag{4.14}$$

where h_1^0 and h_2^0 are the mass eigenstates (i.e. the physical particles.)

We can derive expressions for the masses of the new fields. They read as:

$$M_{\substack{h_1^0 \\ h_2^0}} = \lambda_1 a^2 + \lambda_2 b^2 \pm \sqrt{(\lambda_1 a^2 - \lambda_2 b^2)^2 + \Lambda^2 a^2 b^2} \tag{4.15}$$

and for the mixing angle:

$$sin^2(\beta) = \frac{1}{2}\left\{1 \pm \frac{(a^2 - b^2)(\lambda_1 a^2 - \lambda_2 b^2) + 2\Lambda a^2 b^2}{(a^2 + b^2)\sqrt{(\lambda_1 a^2 - \lambda_2 b^2) + \Lambda^2 a^2 b^2}}\right\}. \tag{4.16}$$

The lesson to learn here is that the mass expressions are rather involved and not very useful to set limits or constraints on the masses. Similar expressions have been used in the past[89] in attempts to limit the mass range of the Higgs but the constraints have been loose or controversial. Even though one would like all the λ's to be of the same order, there is nothing to guarantee it! One should then consider them as free parameters and try to constrain them from known phenomenology.

Unfortunately, this is impossible; there are too many of these! At best, one can get some broad limits on the ratio of the masses. We will then ignore the mass and mixing expressions and use the previous limits:

$$50GeV/c^2 \leq M_{Higgs} \leq 1000GeV/c^2.$$

The reader is referred to Appendix VIII for more details on the mass of the Higgs particles.

Besides, we shall assume that the neutral Higgs particles all have the same mass, M_0, and that all the charged ones have the same mass, M_+. As we will see later, the masses enter as M^2_{Higgs}/M^2_W, so that an average value does not introduce much inaccuracy, but will make the physics clearer. Furthermore, we will assume $cos^2(\beta) \equiv 1$, again to make the physics clearer. As we verified on the computer, this combination of masses and mixing gives us the largest possible value for $\Delta\kappa$; which is what we want.

This completes our description of the two-Higgs-doublet model. A lot of new interaction terms will arise in the fermionic sector but we will not worry about them, as they are not involved in the anomalous magnetic moment of the W-boson.

4.4 Calculation of $\Delta\kappa$.

We now have all that we need to calculate the new contributions to $\Delta\kappa$. The advantage of the rotations performed in section 4.3 is to see clearly where the new physics lies. It is clear now that we do not have to consider the would-be Goldstone bosons, G^+ and G^0, since they are part of the $W^\pm$ and Z^0 boson whose contributions have been calculated in Chapter III. The fermion sector is unchanged as far as κ is concerned. So we have to worry about H^+, H_3^0, h_1^0, h_2^0 only. All the new contributions to $\Delta\kappa$ from the THD model will involve these fields. We will assume that h_1^0 is the SM Higgs particle whose contribution to $\Delta\kappa$ remains as calculated in Chapter III. Our justification is that we look for a maximum value of κ.

The relevant couplings, that we derive from the covariant derivative, are shown on fig. 25. From these, one builds all the Feynman diagrams involved in the calculation of $\Delta\kappa$. These are given in fig. 26. A short calculation suffices to show that fig. 26-b to 26-d do not contribute to $\Delta\kappa$ but only the first one does. So we have to calculate only the triangle diagram shown on fig. 26-a, which is familiar by now! The calculation is easier with scalar loops than with fermion loops. We use the same techniques as before in regularizing the integrals and handling the divergences. The reader is referred to Appendix VII for some details of the calculation.

After a straightforward exercise, we obtained[90]:

$$\Delta\kappa = -3\mathcal{A}\int_0^1 \frac{-2t^4 + (2+F)t^3 - Ft^2}{t^2 - Ft + \delta}\, dt \tag{4.17}$$

and

$$\Delta Q = 2\mathcal{A}\int_0^1 \frac{t^3(t-1)}{t^2 - Ft + \delta}\, dt \tag{4.18}$$

where

$$F \equiv 1 + \delta - \epsilon, \delta \equiv (M_0/M_W)^2, \epsilon \equiv (M_+/M_W)^2$$

Figure 25. Vertices of gauge bosons and Higgs particles.

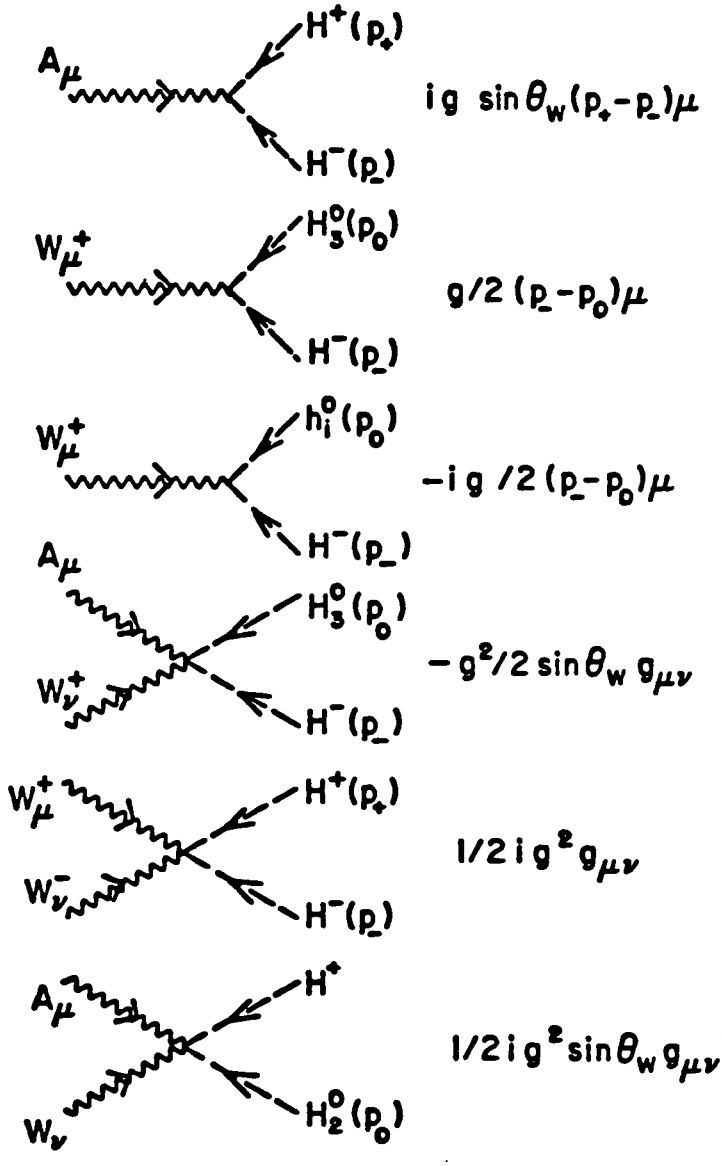

Extra Higgs-gauge boson vertices that arise in a two- Higgs-doublet model; these are all relevant to the calculation of $\Delta\kappa$.

Figure 26. Extra contributions to $\Delta\kappa$.

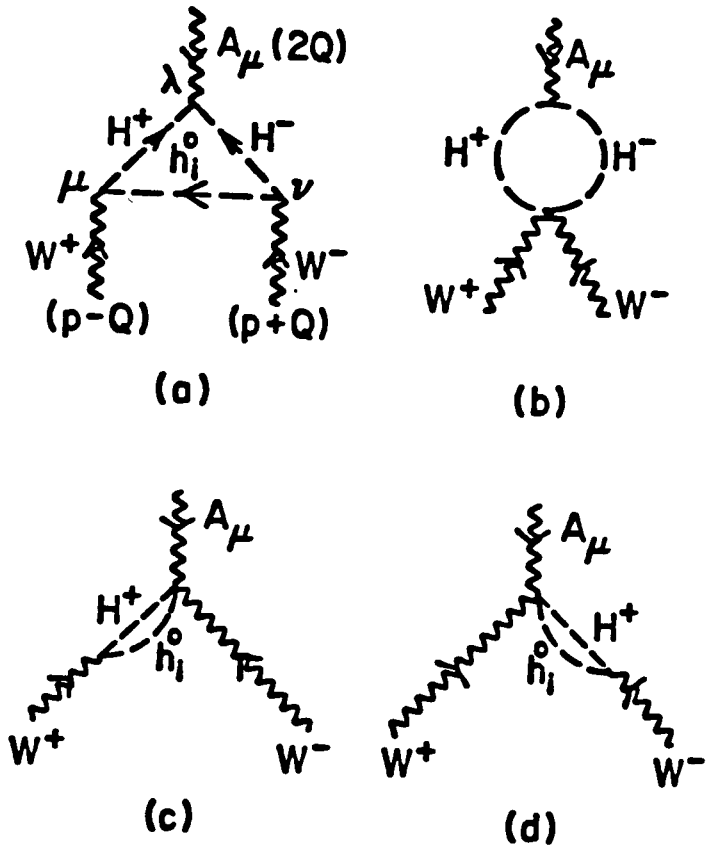

Extra Feynman diagrams that could contribute to $\Delta\kappa$ in a two-Higgs-doublet model. A short calculation shows that only the first one will effectively contribute; all the others being gauge terms.

As mentioned before, one has to sum over h_2^0 and H_3^0 in order to get the complete contribution to $\Delta\kappa$.

On fig. 27, we show $\Delta\kappa$ as a function of M_+ for different values of M_0; the analogue for ΔQ is on fig. 28. The first thing to notice is that the values are small over the wide range of masses studied. This means that the addition of a second Higgs doublet will not change the results much from the SM either for $\Delta\kappa$ or ΔQ. In order to give a better idea of what is happening, we give three-dimensional graphs of $\Delta\kappa$ and ΔQ as a function of M_0 and M_+ on fig. 29 and fig. 30 respectively. On both figures, the main features are clear. The maximum are easily picked up:

$$\Delta\kappa \rightarrow 2\mathcal{A}$$

in the limit of an infinitely massive neutral Higgs particle and a light charged one. When the limits are inverted, one gets:

$$\Delta\kappa \rightarrow -\mathcal{A}.$$

The anomalous quadrupole moment is essentially zero for the range of masses studied except when both Higgs particles are very light. It is interesting that $\Delta\kappa \rightarrow 0$ for both Higgs particles having identical and large masses.

From this, we can set limits on $\Delta\kappa$ and ΔQ in a THD model:

$$\Delta\kappa \leq 1.6 \times 10^{-2}$$

$$\Delta Q \leq 0.28 \times 10^{-2}$$

These are absolute limits in a two-Higgs-doublet model.

Figure 27. $\Delta\kappa$ as a function of M_+ for different values of M_0.

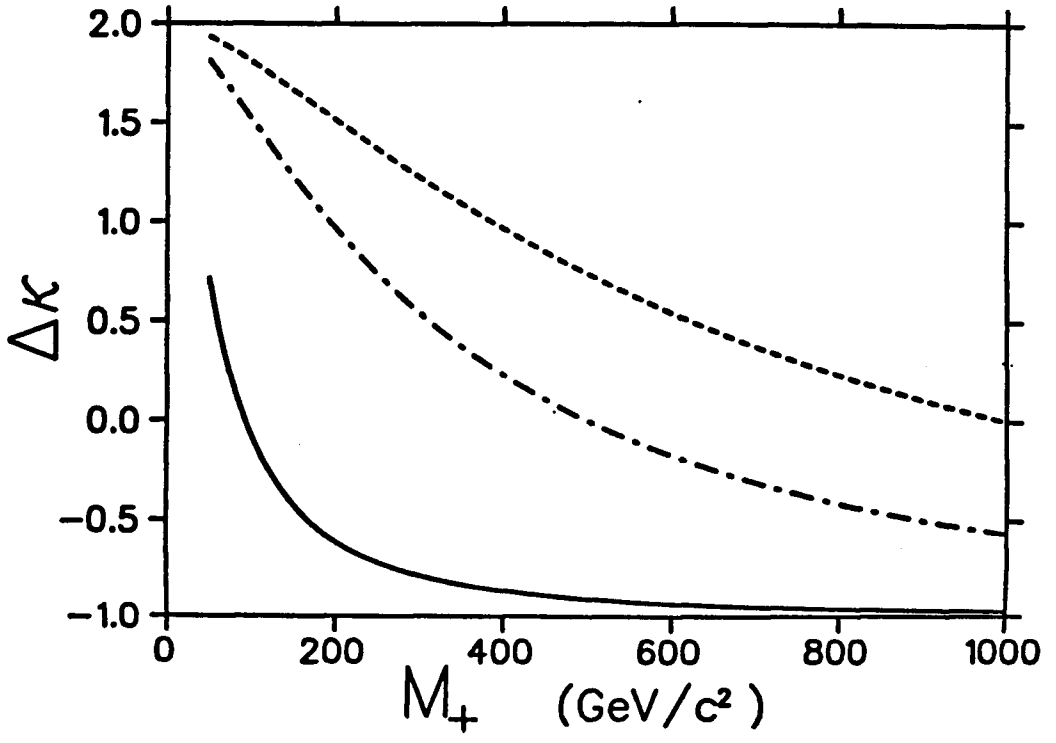

$\Delta\kappa$ as a function of M_+ for different values of M_0: 100 GeV/c^2 (continuous line), 500 GeV/c^2 (dash-dotted line), and 1000 GeV/c^2 (dotted line). The vertical scale is in units of $\mathcal{A} \equiv g^2/96\pi^2 \sim 5 \times 10^{-4}$.

Figure 28. ΔQ as a function of M_+ for different values of M_0.

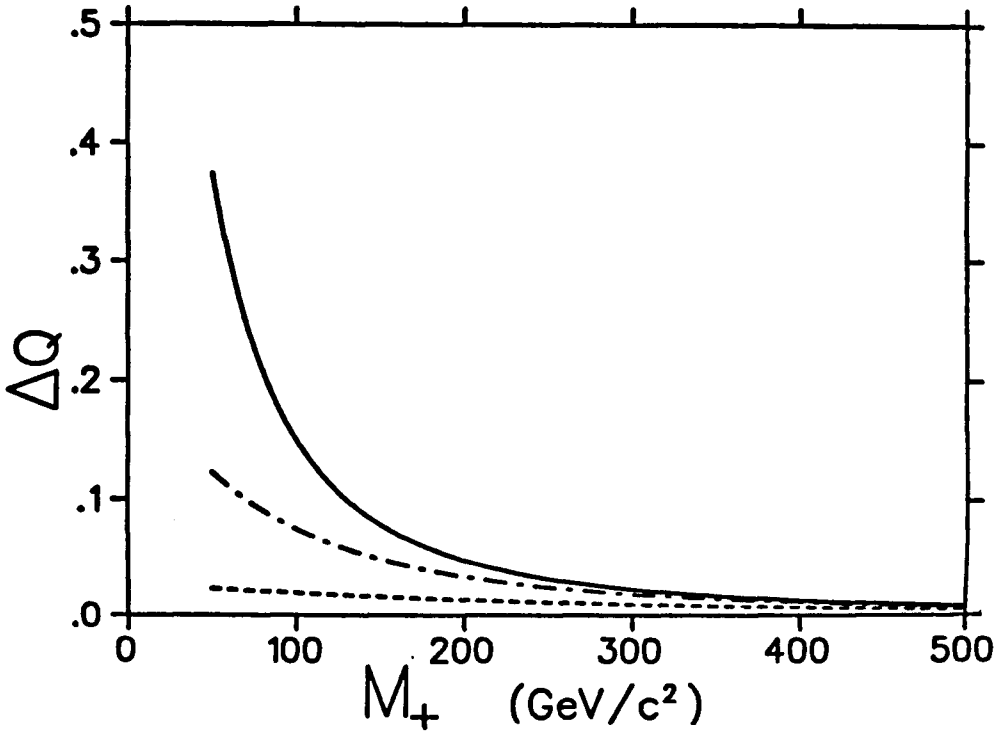

ΔQ as a function of M_+ for different values of M_0: 100 GeV/c^2 (continuous line), 200 GeV/c^2 (dash-dotted line), 500 GeV/c^2 (dotted line). The vertical scale is in units of $\mathcal{A}$.

Figure 29. $\Delta\kappa$ as a function of M_+ and M_0.

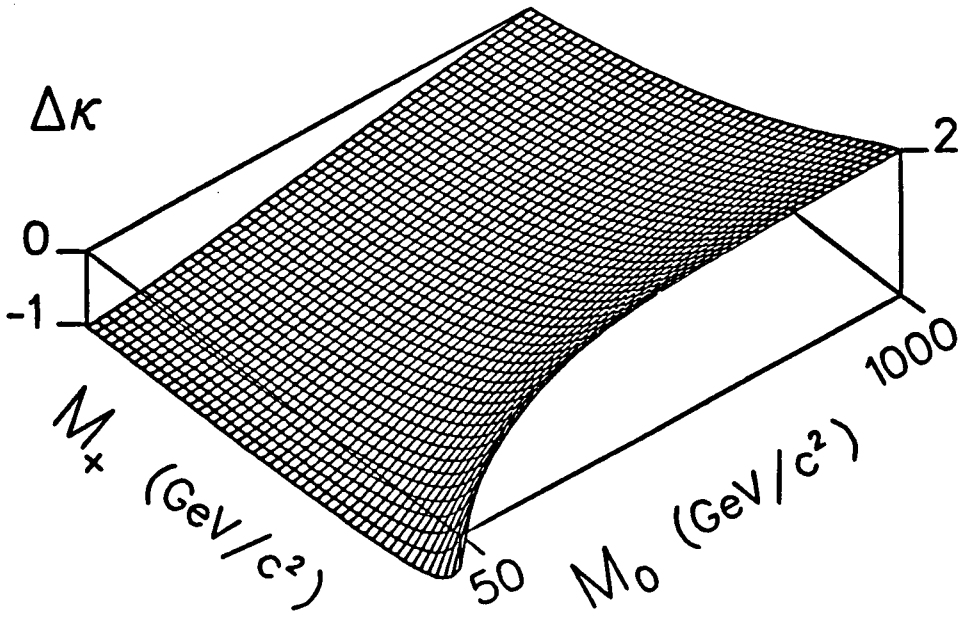

$\Delta\kappa$ as a function of M_+ and M_0. The vertical scale is in units of $\mathcal{A}$. Both horizontal axes are $50 - 1000$ GeV/c^2, the point (50,50) being the origin.

Figure 30. ΔQ as a function of M_+ and M_0.

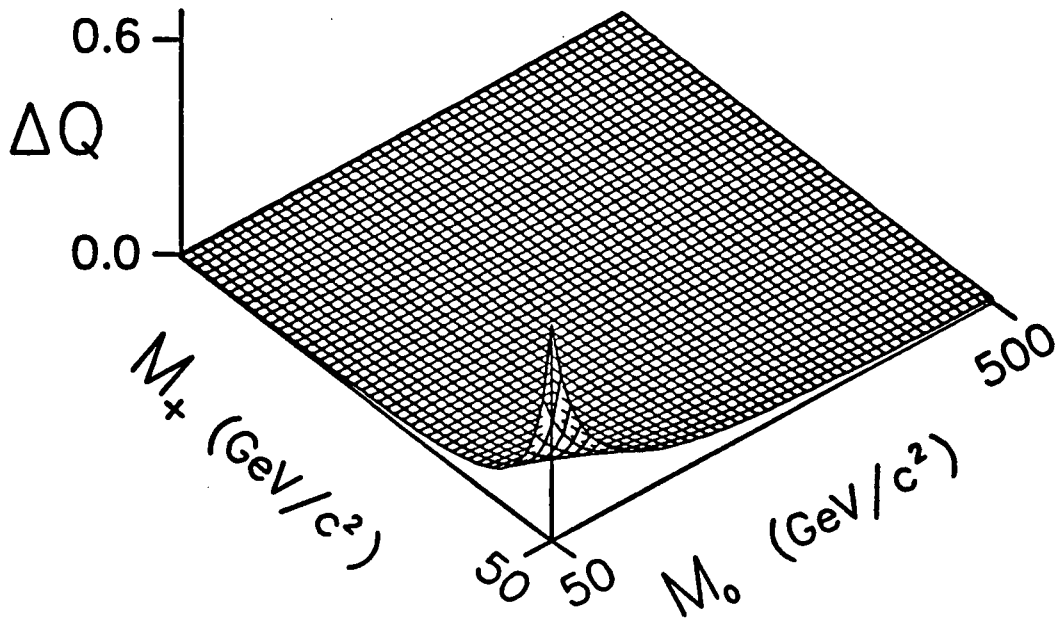

ΔQ as a function of M_+ and M_0. The vertical scale is in units of $\mathcal{A}$. Both horizontal axes are $50 - 500$ GeV/c^2, the point (50,50) being the origin.

4.5 Conclusions.

The conclusions of this calculation are clear, from fig. 29 and fig. 30

(i) Heavy Higgs particles will contribute very little to $\Delta\kappa$. If one of them is very light, the contribution is largest.

(ii) ΔQ is essentially unchanged by an extra Higgs doublet, except if both are very light.

More generally, even in the best cases, the extra contributions to $\Delta\kappa$ and ΔQ are very small and absolutely hopeless from an experimental point of view. Note also that the mass range studied here is as large as possible, if one wishes to avoid the " strong regime problems."

The main point is that two-Higgs-doublet models cannot increase $\Delta\kappa$ to 10% for example. Therefore, if such a measurement were performed, in a multi-Higgs-doublet context it would imply a very large number of extra Higgs particles in a narrow mass ratio; this would then be difficult to explain.

Again, in a two-Higgs-doublet model:

$$\Delta\kappa \leq 1.6 \times 10^{-2}$$

$$\Delta Q \leq 0.28 \times 10^{-2}$$

Conclusions.

In this thesis, we have been concerned mainly with the anomalous magnetic moment, κ, of the W-boson. In a first step we have looked at some processes where this parameter could be measured with reasonable accuracy using technologies available in the near future. In a second step, we have calculated loop corrections to κ that will arise in the SM; in a third step, we have extended these corrections to a two-Higgs-doublet model. The point of the last two sections was to set constraints on κ so that possible experimental discrepancies can be rightfully gauged.

From the experimental point of view, we have seen that the most promising experiment to measure κ is the two boson production. Namely:

$$e^+ \; e^- \rightarrow W^+ \; W^-.$$

This process enjoys a large cross-section and a strong κ dependance. However, in order to obtain a single value for κ, one must either go to large energies or look at the angular distribution. Over a range of 45 degrees, one would be able to determine κ within 30% or so, with sufficient statistics. Near threshold, this process can also lead to very useful information on the width of the W-boson. The amplitude of the tail that occurs near threshold is proportional to the width of the W; therefore the rate is a direct measure of the width.

The drawback of this process is that all three-boson vertices enter in the calculation: the process goes via the γW^+W^- and the $Z^0W^+W^-$ vertices so that the relative strengths of the vertices will be very difficult to extract. We have seen that the relative strength of the vertices is also an excellent probe of the SM.

Single-W-production processes have very small cross-sections. These small rates make them hopeless for a 30% measurement of κ in the near future. On

the other hand, some of them involve a single boson vertex and can be used to determine the strength of a particular coupling. This is clearly an advantage over the double-boson-production process. In the future, when the luminosities are improved by two orders of magnitude or so, these processes could become very useful for a precise determination of κ and of the ratio of the neutral and charged three-boson vertices. Indeed, we have seen that the cross-sections have a very strong dependence on κ and a single data point with reasonable error bars can lead easily to a 50% measurement. The most difficult obstacle is to bring a data point on any of the graphs of these processes.

On the other hand, single W production via a photon beam has also a large cross-section and a strong κ dependence. It also involves only one three-boson vertex. The main problem of this process is that multi-GeV photon beams will probably not be available for many years.

In contrast,radiative zeros do not appear to be of much use in the experimental determination of κ. In processes where they involve large cross-sections they are plagued by large backgrounds which make a determination of $\kappa \leq 5$ very unlikely. We know that if the SM is anywhere close to nature, values of $\kappa \sim 5$ are unthinkable. So, if, in these processes, one observes some signal above the background, it means that the SM is very wrong in its gauge sector.

The main conclusion from this section of the thesis, was that an order of magnitude estimate of κ will be possible to obtain in the near future at SLC or LEPI but that a 30% measurement has to wait for LEPII. The 10% measurement that we really need to rule out models or confirm the SM in a nontrivial manner will be extremely difficult at LEPII. It also appears that the relative strength of the charged and neutral gauge vertices will be impossible to measure appropriately at LEP or SLC.

We also investigated composite models. We found that such models can mimic very well the SM on a narrow range of energies, so that it is essentially impossible to distinguish between the two. However, by narrow range we mean approximately 100 GeV's; which means that the energies that could distinguish between the models will not be available in the near future. The main point here is that the measurement of κ besides requiring an enormous amount of data, would not be a good way to rule out composite models. It could, however, help to constrain the parameters of these models on non overlapping ranges, thereby ruling them out.

Chapters III and IV were concerned with theoretical limits on κ in the SM and beyond. The minimal SM with three fermion families is rather constrictive. We have calculated that the absolute maximum value that κ can have in the SM is 1.015. This means that if a value of 1.08 or even 1.05 were measured the SM could certainly not account for it. Note also that this maximum value occurs for a very specific value of the mass of the top quark (i.e. $m_{top} \sim 80GeV/c^2$.)and that it will decrease rather quickly if the mass of the top quark does not have this value. It is also interesting to note that the new lower bound for the mass of the top quark from the ARGUS collaboration[73] is getting close to the critical value. In the same way, the maximum value of the anomalous quadrupole moment of the W boson is 0.25%, which is rather small and hopeless to measure in the near future.

Then, we extended the model by adding one Higgs doublet. These multi-Higgs-doublet models are the first extension of the SM and a good verification of the ill-understood Higgs sector. By allowing more Higgs particles in the model, one opens new channels for processes and the goal is to try and find some experimental constrainsts to limit the number or couplings of those particles. It was the hope that κ could also limit the number of Higgs bosons. We found, however, that the contributions to $\Delta\kappa$ and ΔQ from those models are very small and absolutely hope-

less from the experimental point of view. We calculated that the absolute maximum value of κ in the two-Higgs-model that we studied is 1.016 and the maximum value of ΔQ is 0.28%. Theses values are far too close to their SM counterparts to have any hope to set any constraints on the number of Higgs bosons or the couplings involved; unless one has excellent statistics, which is not expected for many years. Again, in this context, if one would measure κ to be 1.08 for example, such a model could not explain this value, unless one is willing to have a large number of Higgs bosons.

As mentioned before, supersymetric models are very popular now-a-days. An ongoing calculation of similar loop corrections in a supersymmetric model indicates that here again the corrections will be rather small[91]. As of now, the results indicate that the maximum values that the contributions to κ can have are approximately 0.4%; most contributions are more like 0.1% and only one loop can have this large value. Of course, this is for a very specific choice of masses. Furthermore, some calculations with an E_6 model show[74] that the contributions from the heavy leptons arising in these models have a maximum contribution of 0.4% or so. From these results, one can see that none of the models could add significantly to the SM value. So, it remains that the main contribution to $\Delta\kappa$ or ΔQ comes from a fermion loop with a light b-quark and a t-quark whose mass is equal to the mass of the W-boson within a few GeV's. All the models investigated were of the weakly interacting type.

This shows that the maximum value of $\Delta\kappa$ allowed in weakly interacting models is at best 3%. Since it is impossible to use this parameter to distinguish between models one can invert the argument and say that if an anomalous magnetic moment of 1.1 were measured, most likely it would indicate that non-perturbative physics is at work. This could be either compositeness of the gauge bosons, strongly in-

teracting Higgs particles or others. It would certainly be interesting to calculate the contribution to $\Delta\kappa$ from a strongly interacting Higgs sector but the methods of calculation are deficient when a strong interaction comes into play.

This is the strongest statement that can be drawn from this work: an anomalous magnetic moment of 1.1 clearly indicates nonperturbative physics, while a value of 1.05 is very difficult to accommodate in any weakly interacting model and can be considered as a clue towards stongly interacting models or many extra weakly interacting families. On the other hand, a value of 1.02 could be accounted for in the minimal SM.

References.

1. S. L. Glashow, Nucl. Phys. **22**, (1961) 579.

2. S. Weinberg, Phys. Rev. Lett. **19**, (1967) 1264.

3. A. Salam in *Elementary Particle Theory, Proc. of the Eight Noble Symposium.*, ed. N. Svartholm, Wiley, New-York (1968).

4. T. P. Cheng, L. -F. Li, *Gauge Theory of Elementary Particle Physics.*, Oxford University Press, Oxford (1984).

5. M. B. Green, J. H. Schwartz, E. Witten, *Superstring Theory, Vol.I & Vol.II*, Cambridge University Press, Cambridge (1987).

6. D. Perkins, *Introduction to High Energy Physics.*, Addison-Wesley, London (1982).

7. F. Halzen, A. D. Martin, *Quarks and Leptons: an Introductory Course in Modern Particle Physics.*, John Wiley and Sons, New-York (1984).

8. S. C. Wu *et al.*, Phys. Rev. **105**, (1957) 1413.

9. T. D. Lee, C. N. Yang, Phys. Rev. **104**, (1956) 254.

10. J. Goldstone, Nuovo Cimento **19**, (1961) 154.

11. P. W. Higgs, Phys. Lett. **12**, (1964) 132; T. W. B. Kibble, Phys. Rev. **155**, (1967) 1554.

12. G. 't Hooft, Nucl. Phys. **B 35**, (1971) 167.

13. M. Kobayashi, T. Maskawa, Prog. Theor. Phys. **49**, (1973) 652.

14. F. J. Hasert *et al.*, Phys. Lett. **B 46**, (1973) 138.

15. P. Q. Hung, J. J. Sakurai *Ann. Rev. Nucl. Part. Sci.* **31**, (1983) 375.

16. G. Arnison *et al.*, Phys. Lett. **B 122**, (1983) 103;

G. Banner *et al.*, Phys. Lett. **B 122**, (1983) 476.

17. The AGS proposal.

18. For reviews on composite models, see M. E. Peskin, in *Proc. of 1981 Int. Symposium on Lepton and Photon Interactions.*, Bonn, (1981); H. Terazawa, in *Proc. of XXII Int. Conf. on High Energy Physics*, Leipzig, (1984).

19. L. O'Raifeartaigh, *Group Structure of Gauge Theories.*, Cambridge University Press, Cambridge, (1986).

20. See for example H. E. Haber, G. L. Kane, Physics Report **117**, (1985) 75.

21. J. H. Christenson *et al.*, Phys. Rev. Lett. **13**, (1964) 138.

22. S. Weinberg, Phys. Rev. Lett. **37**, (1976) 657.

23. L. Wolfenstein, Preprint, CMU-HEP-86-3.

24. D. V. Nanopoulos, Comm. Nucl. Part. Phys. **15**, (1986) 161.

25. T.K. Kuo, J. Pantaleone, Preprint, PURD-TH-86-20.

26. T. Ohshima, Preprint, INS-REP.-598.

27. E. Kolb, A. J. Stebbins, M. S. Turner, Phys. Rev. **D 35** (1987) 3598.

28. W. Wetzel, Z. Phys. **C 11**, (1981) 117.

29. W. J. Marciano, A. Sirlin, Phys. Rev. **D 29**, (1984) 945; Err. W. J. Marciano, A. Sirlin, Phys. Rev. **D 31** (1985) 213.

30. F. Olness, W.-K. Tung, Phys. Lett. **B 179**, (1986) 269.

31. Y. Y. Reznikiv, V. V. Skalozub, Sov. J. Nucl. Phys. **40** (1984) 802.

32. L. Schiff, *Quantum Mechanics.*, McGraw-Hill, New-York, (1955).

33. H. Aronson, Phys. Rev. **186**, (1969) 1434.

34. T. D. Lee, C. N. Yang, Phys. Rev. **128**, (1962) 885.

35. P. B. Schwinberg *et al.*, Phys. Rev. Lett. **47**, (1981) 1679.

36. R. S. VanDyck *et al.*, Phys. Rev. Lett. **38**, (1977) 310.

37. T. G. Rizzo, M. A. Samuel, Phys. Rev. **D 35**, (1987) 403.

38. J. D. Bjorken, S. D. Drell, *Relativistic Quantum Mechanics.*, McGraw-Hill, New-York, (1964).

39. G. Couture, J. N. Ng, Z. Phys. **C 32**, (1986) 579.

40. W. Alies, Ch. Boyer, A. J. Buras, Nucl. Phys. **B 119**, (1977) 125.

41. D. Dicus, K. Kallianpur, Phys. Rev. **D 32**, (1985) 35.

42. K. F. J. Gaemers, G. J. Gounaris, Z. Phys. **C 1**, (1979) 259.

43. M. J. Duncan, Preprint, UPR-0299-T.

44. F. Herzog, Phys. Lett. **B 148**, (1984) 355; Err. F. Herzog Phys. Lett. **B 155**, (1985) 468.

45. I. F. Ginzburg, G. L. Kotkin, U. G. Serbo, V. I. Telnov, Nucl. Inst. Method **205**, (1983) 47.

46. I. F. Ginzburg, G. L. Kotkin, S. L. Panfil, U. G. Serbo, Nucl. Phys. **B 228**, (1983) 285.

47. O. Cheyette, Phys. Lett. **B 137**, (1984) 431.

48. K. Hagiwara, R. D. Peccei, D. Zeppenfeld, Preprint, DESY 86-058.

49. M. Kuroda, J. Maalampi, K.H. Schwarzer, D. Schildknecht, Preprint, BI-TP 86/12.

50. J. Rohlf in *Proceedings of the Oregon Meeting of the APS, DPF*, ed. R. C. Hwa, World Scientific, Singapore (1986).

51. G. Barbiellini *et al.* in *Physics at LEP.*, eds. J. Ellis, R. D. Peccei, Report CERN 86-02 vol. 2.

52. *Proceedings of the SLC Workshop on Experimental Use of the SLC Linear Collider.*, SLAC-Report-247, SLAC, (1982).

53. K. O. Mikaelian, M. A. Samuel, Phy. Rev. Lett. **43**, (1979) 746.

54. R. W. Brown, D. Sadhev, K. O. Mikaelian, Phys. Rev. **D 20**, (1979) 1164.

55 S. J. Brodsky, R. W. Brown, Phy. Rev. Lett. **49**, (1982) 966.

56 R. W. Brown, K. L. Kowalski, S. J. Brodsky, Phys. Rev. **D 28**, (1983) 624.

57. J. Cortes, K. Hagiwara, F. Herzog, Nucl. Phys. **B 278**, (1984) 26.

58 M. A. Samuel, J. Reid, Phys. Rev. **D 35**, (1987) 3505.

59. M. Suzuki, Phys. Lett. **B 153**, (1985) 289.

60. I. Bars, M. Yoshimura, Phys. Rev. **D 6**, (1972) 374.

61. J. J. van der Bij, Preprint, Fermilab-Pub-86/129.

62. B. W. Lee, C. Quigg, H. B. Thacker, Phys. Rev. Lett. **38**, (1977) 883.

63. J. Maalampi, D. Schildnecht, K. H. Schwarzer, Phys. Lett. **B 166**, (1986),361.

64. C. L. Bilchak, J. D. Stroughair, Preprint BI-TP 87/02.

65. C. L. Bilchak, J. D. Stroughair, Phys. Rev. **D 30**, (1984) 1881.

66. P. Q. Hung, J. J. Sakurai, Nucl. Phys. **B 143**, (1978) 81.

67. J. D. Bjorken, Phys. Rev. **D 19**, (1979) 335.

68. W. A. Bardeen, R. Gastmans, B. Lautrup, Nucl. Phys. **B 46**, (1972) 319.

69. D. Barua, S. N. Gupta, Phys. Rev. **D 15**, (1977) 509.

70. L. L. DeRaad, K. A. Milton, W.-Y. Tsai, Phys. Rev. **D 12**, (1975) 3972.

71. C. L. Bilchak, R. Gastmans, A. van Proeyen, Preprint, KUL-TF-8611.

72. S. Yamada in *Proceedings of the 1983 International Symposium on Lepton and Photon at High Energies.*, eds. D. G. Cassel, D. L. Kreinick, Cornell University, Ithaca, N.Y. (1983).

73. H. Albrecht *et al.*, Phys. Lett. **B 192**, (1987) 245.

74. G. Couture, J. N. Ng, Preprint, TRI-PP-86-108.

75. T. Appelquist, J. Carazzone, Phys. Rev. **D 11**, (1974), 2856.

76. S. Weinberg, Phys. Rev. Lett. **36**, (1976) 294.

77. J. Liu, Preprint, CMU-HEP 86-15.

78. B. Kayser, Comm. Nucl. Part. Phys. **14**, (1985) 69.

79. M. B. Voloshin, M. I. Vysotsky, Preprint, ITEP-1 (1986).

80. H. E. Haber, G. L. Kane, T. Sterling, Nucl. Phys. **B 161**, (1979) 493.

81. J. J. van der Bij, F. Hoogeveen, Nucl. Phys. **B 283**, (1987) 477.

82. H. Haber. invited talk at the *SSC Workshop.*, 4/6/87. To appear in the proceedings.

83. See for example C. Quigg, *Gauge Theories of the Strong, Weak and Electromagnetic Interactions.*, Benjamin/Cummings, New-York, (1983).

84. T. P. Cheng, M. Sher, Preprint, WU-TH-87-1.

85. S. L. Glashow, S. Weinberg, Phys. Rev. **D 15**, (1976) 1958.

86. R. A. Flores, M. Sher, Annals of Physics **148**, (1983) 95.

87. L. F. Abbott, P. Sikivie, M. B. Wise, Phys. Rev. **D 21**, (1980) 1393.

88. J. L. Liu, L. Wolfenstein, Preprint, CMU-HEP-86-21.

89. K. S. Babu, E. Ma, Phys. Rev. **D 31**, (1985) 2861.

90. G. Couture, J. N. Ng, J. L. Hewett, T. G. Rizzo, To appear in Phys. Rev. **D**, Aug. (1987).

91. G. Couture, J. N. Ng, J. L. Hewett, T. G. Rizzo, manuscript in preparation.

92. See for example, P. Becher, M. Böhm, H. Joos, *Gauge Theories of Strong and Electroweak Interactions.*, John Wiley and Sons, New-York, (1984).

93. I. M. Sobol, *The Monte Carlo Method.*, MIR, Moscow, (1975).

94. E. Bickling, K. Kajantie, *Particle Kinematics.*, Wiley & Sons, New-York, (1973).

95. P Zakarauskas, Ph. D. Thesis, University of British Columbia, (1984), unpublished.

96. C. F. von Weiszäcker, Z. Phys. **88**, (1934) 612.

97. E. J. Williams, Phys. Rev. **45**, (1934) 729.

98. M.-S. Chen, P. Zerwas, Phys. Rev. **D 12**, (1975) 187.

99. A. Kamal, J. N. Ng, H. C. Lee, Phys. Rev. **D 34**, (1981) 2842.

100. C. Cohen-Tannoudji, B. Diu, F. Laloë, *Quantum Mechanics.* Herman, Paris, (1973).

101. I. I. Bigi, A. I. Sanda, Preprint, SLAC-PUB-4157.

102. J. D. Jackson, *Classical Electrodynamics.*, Wiley, New-York, (1972).

103. K. J. Kim, Y.-S. Tsai, Phy. Rev. **D 7**, (1973) 3710.

104. C. Itzikson, J.-B. Zuber, *Quantum Field Theory.*, McGraw-Hill, New-York (1980)

105. R. Jackiw in *Lectures on Current Algebra and its Applications.*, Princeton University Press, Princeton, N.J. (1972)

106. P. Ramond, *Field Theory, a Modern Primer.*, Benjamin/Cummings, New-York, (1981).

107. E. Eichten *et al.*, Rev. Mod. Phys. **56**, (1984) 633.

108. M. S. Chanowitz, M. K. Gaillard, Preprint, UCB-PTH-85/19.

109. J. Ellis, M. K. Gaillard, D. V. Nanopoulos, Nucl. Phys. **B 106**, (1976) 292.

110. S. Weinberg, Phys. Rev. Lett. **36**, (1976) 294.

111. S. McWilliams, L.-F. Li, Nucl. Phys. **B 179**, (1981) 62.

APPENDIX I

Electro-Weak Interactions.

In this appendix, we will give a brief review of the electro-weak part of the Standard Model; which is what we referred to as the SM in the thesis. This unification of the EM and weak interactions had been thought of as early as 1961 by Glashow but Weinberg in 1967 and Salam in 1968 finished the consistent, renormalizable model that we use today. This was accomplished through the use of the Goldstone and Higgs-Kibble mechanisms. As mentioned in the Introduction, the initial Lagrangian cannot have any explicit mass terms because they spoil gauge invariance and renormalizability; features that we want to keep at any cost!. So, one starts with massless generators or gauge bosons and use the combination of the above-mentioned processes to generate masses for the gauge bosons. In this process, one ends up with an extra particle, remnant of the scalar doublet that breaks the symmetry: the Higgs boson. There is a very abundant literature on this subject[4,92]; we will follow closely Quigg[83].

It was found experimentally that the weak interaction violates parity conservation: only left-handed particles take part in the weak interaction. We will group left-handed particles into weak isospin doublets; this is to say that one member of the doublet can turn itself into the other member via the weak interaction. Right-handed particles on the other hand will remain singlet under the weak isospin. That is:

$$L = \begin{pmatrix} e \\ \nu_e \end{pmatrix}_L$$

with

$$e_L = (1/2)(1-\gamma_5)e \qquad \nu_L = (1/2)(1-\gamma_5)\nu$$

while

$$R = e_R = (1/2)(1+\gamma_5)e$$

Before symmetry breaking, the electron and its neutrino are the same particle; with same the mass and the same charge. This initial charge is called the weak hypercharge Y and is obtained by the Gell-Mann-Nishijima relation: $Y = 2(Q - T_3)$ where Q is the electric charge and T_3 is the isospin eigenvalue. Then $Y_L = -1$ and $Y_R = -2$. One chooses this hypercharge to be the generator of the $U(1)_Y$ transformation.

We want to unify transformations generated by Y and those generated by τ (Pauli matrices of $SU(2)_L$). We use the product group $SU(2)_L \otimes U(1)_Y$ with coupling constants g and $g\prime/2$ respectively. We then need four generators or gauge bosons:

$$b^1_\mu, b^2_\mu, b^3_\mu \quad \text{for} \quad SU(2)_L$$

$$A_\mu \quad \text{for} \quad U(1)_Y$$

In order to have a complete Lagrangian, we include all terms of order four or less; higher order terms are nonrenormalizable. They read as:

$$L = L_{gauge} + L_{lepton} + L_{scalar} + L_{Yukawa}$$

$$L_{gauge} = -(1/4)F^l_{\mu\nu}F^{l\mu\nu} - (1/4)f_{\mu\nu}f^{\mu\nu}$$

$$\begin{aligned} L_{lepton} =& \bar{R}i\gamma^\mu(\partial_\mu + i\frac{g'}{2}A_\mu Y)R \\ &+\bar{L}i\gamma^\mu(\partial_\mu + i\frac{g'}{2}A_\mu Y + i\frac{g}{2}\vec{\tau}\cdot\vec{b}_\mu)L \end{aligned} \qquad (A-I.1)$$

$$L_{scalar} = (D_\mu\phi)^\dagger(D_\mu\phi) - V(\phi^\dagger\phi)$$

$$L_{Yukawa} = -G_e[\bar{R}\phi^\dagger L + \bar{L}\phi R]$$

where

$$F^l_{\mu\nu} \equiv \partial_\nu b^l_\mu - \partial_\mu b^l_\nu + g\epsilon_{jkl}b^j_\mu b^k_\nu$$

$$f_{\mu\nu} \equiv \partial_\nu A_\mu - \partial_\mu A_\nu$$

$$D_\mu \equiv \partial_\mu + i\frac{g'}{2}A_\mu Y + i\frac{g}{2}\vec{\tau}\cdot\vec{b}_\mu \qquad (A-I.2)$$

$$V(\phi^\dagger\phi) \equiv \mu^2(\phi^\dagger\phi) + |\lambda|(\phi^\dagger\phi)^2$$

$$\phi \equiv \begin{pmatrix} \phi^+ \\ \phi^0 \end{pmatrix}$$

The index l runs from 1 to 3 and refers to the isospin indices. The ϕ doublet is a doublet of complex scalar fields whose hypercharge is +1. Note that L_{lepton} shows explicitly that the right-handed leptons do not participate in the weak interaction.

This Lagrangian is invariant under local $SU(2)_L \otimes U(1)_Y$ gauge transformations. Now we let $\mu^2 < 0$ and break the symmetry through a vacuum expectation value (vev). This vev means that some field operators acting on the vacuum have a nonvanishing result. This is to say:

$$\langle 0|\phi|0\rangle \equiv \langle\phi\rangle_0 \neq 0.$$

We choose the vev to have the following form:

$$\langle\phi\rangle_0 \equiv \begin{pmatrix} 0 \\ \frac{v}{\sqrt{2}} \end{pmatrix}$$

so that the vacuum is neutral.

One easily verifies that:

$$\tau_i\langle\phi\rangle_0 \neq 0 \qquad Y\langle\phi\rangle_0 \neq 0$$

$$Q\langle\phi\rangle_0 = (1/2)(\tau_3 + Y)\langle\phi\rangle_0 = 0$$

This is what we want because the original four generators are broken but the combination that corresponds to the electric charge is not. Therefore the photon will remain massless but the other three generators will not. The vev breaks the symmetry according to:

$$SU(2)_L \otimes U(1)_Y \longrightarrow U(1)_{EM}$$

Furthermore, according to the Goldstone theorem, we can expect three massless spin-0 particles. They are the would-be Goldstone bosons that will be absorbed by the $W^{\pm}$ and Z^0 bosons when they acquire masses. The next steps are to expand the Lagrangian about the minimum of the Higgs potential. This is done by:

$$\phi \rightarrow \exp\left(\frac{i\vec{\zeta}\cdot\vec{\tau}}{2v}\right)\begin{pmatrix} 0 \\ (v+\eta)/\sqrt{2} \end{pmatrix} \qquad (A-I.3)$$

One can transform immediately to the unitarity gauge and rewrite:

$$\phi \rightarrow \phi' = \exp(\frac{-i\vec{\zeta}\cdot\vec{\tau}}{2v})\phi$$

$$= \begin{pmatrix} 0 \\ (v+\eta)/\sqrt{2} \end{pmatrix}$$

$$L \rightarrow L' = (\frac{-i\vec{\zeta}\cdot\vec{\tau}}{2v})L$$

while

$$R \rightarrow R, \quad A_\mu \rightarrow A_\mu, \quad \vec{\tau}\cdot\vec{b}_\mu \rightarrow \vec{\tau}\cdot\vec{b}'_\mu.$$

The next step is to rewrite the initial Lagrangian in terms of these new fields. The Yukawa term for example will become:

$$L_{Yukawa} = -G_e\frac{(v+\eta)}{\sqrt{2}}(\bar{e}_R e_L + \bar{e}_L e_R)$$

$$= -\frac{G_e v}{\sqrt{2}}\bar{e}e - \frac{G_e \eta}{\sqrt{2}}\bar{e}e \qquad (A-I.4)$$

where we recognize the first term as a mass term for the electron, with a mass $G_e v/\sqrt{2}$ and the second term as an interaction term. By the same procedure, one gets:

$$L_{scalar} = (1/2)(\partial_\mu\eta)(\partial_\mu\eta) - \mu^2\eta^2$$

$$+ \frac{v^2}{8}\left[g^2|b^1_\mu - ib^2_\mu|^2 + (g'A_\mu - gb^3_\mu)\right] \qquad (A-I.5)$$

$$+ \text{ interactions terms.}$$

So the η field has acquired a mass term:

$$M_H^2 = -2\mu^2 > 0. \qquad (A-I.6)$$

This is the Higgs particle.

The charged weak bosons are defined as linear combinations of the original generators:

$$W^{\pm} \equiv \frac{b_\mu^1 \mp i b_\mu^2}{\sqrt{2}} \qquad (A-I.7)$$

and the associated mass term is:

$$\frac{g^2 v^2}{8}\left[(W_\mu^+)^2 + (W_\mu^-)^2\right] \Rightarrow M_W^{\pm} = \frac{gv}{2}$$

For the neutral gauge boson and the photon the following orthogonal combinations lead to the correct result:

$$Z_\mu \equiv \frac{g b_\mu^3 - g' A_\mu}{\sqrt{g^2 + g'^2}} \qquad \mathcal{A}_\mu \equiv \frac{g A_\mu + g' b_\mu^3}{\sqrt{g^2 + g'^2}} \qquad (A-I.8)$$

with masses:

$$M_{Z^0} = \sqrt{g^2 + g'^2}(v/2) \qquad M_{\mathcal{A}_\mu} = 0.$$

which is what we want.

This is the particle spectrum and as we have seen before, all the couplings predict results that agree very well with experiments. In order for this theory to agree with the low energy Fermi theory, one must require:

$$v = (G_F\sqrt{2})^{-1/2} \sim 250 \ GeV. \qquad (A-I.9)$$

Given this, one tunes the Yukawa couplings to get the correct masses for the fermions. Note however that the gauge boson masses are very well defined in

terms of the coupling constants and that the mass of the Higgs boson is completely arbitrary. From interaction terms, if one is to identify the $\mathcal{A}_\mu$ with the photon, one has to require:

$$\frac{gg'}{\sqrt{g^2+g'^2}} \equiv e \qquad (A-I.10)$$

where e is the electric charge. This leaves only one free parameter in the model: the relative strength of the coupling constants. One can parametrize this by an angle called the weak mixing angle or the Weinberg angle θ_W. It is defined as:

$$g' = g tan(\theta_W) \qquad (A-I.11)$$

Then the gauge bosons can be defined as:

$$Z_\mu \equiv - A_\mu sin(\theta_W) + b^3_\mu cos(\theta_W)$$

$$(A-I.12)$$

$$\mathcal{A}_\mu \equiv \ A_\mu cos(\theta_W) + b^3_\mu sin(\theta_W)$$

The mass terms now become:

$$M^2_W \equiv \frac{\pi\alpha}{G_F\sqrt{2}sin^2(\theta_W)}$$

$$\sim \frac{(37\text{GeV})^2}{sin^2(\theta_W)}$$

$$M^2_{Z^0} = \frac{M^2_W}{cos^2(\theta_W)}.$$

This completely determines the particle content of the model and the masses of the gauge bosons have been measured and agree very well with the predictions of the model for $sin^2(\theta_W) \sim 0.22$ which is the approximate experimental value.

The three- and four-boson vertices arise from the L_{gauge} part of the Lagrangian. Their derivation is straightforward and we list them here for completeness on fig. 31. Note that the arrows are very important.

Figure 31. Three- and four-boson couplings in the SM.

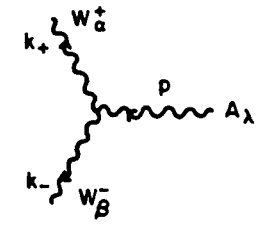

$$ie\left[g_{\alpha\beta}(k_+-k_-)_\lambda - g_{\alpha\lambda}(p+k_+)_\beta + g_{\beta\lambda}(p+k_-)_\alpha\right]$$

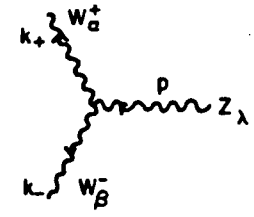

$$ie\cot\theta_W\left[g_{\alpha\beta}(k_+-k_-)_\lambda - g_{\alpha\lambda}(p+k_+)_\beta + g_{\beta\lambda}(p+k_-)_\alpha\right]$$

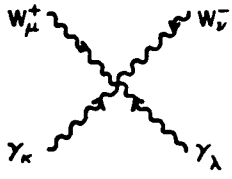

$$-ie^2(2g_{\kappa\lambda}g_{\mu\nu} - g_{\kappa\mu}g_{\lambda\nu} - g_{\kappa\nu}g_{\lambda\mu})$$

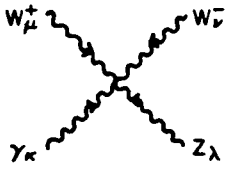

$$-ie^2\cot\theta_W(2g_{\kappa\lambda}g_{\mu\nu} - g_{\kappa\mu}g_{\lambda\nu} - g_{\kappa\nu}g_{\lambda\mu})$$

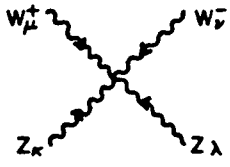

$$-ie^2\cot^2\theta_W(2g_{\kappa\lambda}g_{\mu\nu} - g_{\kappa\mu}g_{\lambda\nu} - g_{\kappa\nu}g_{\lambda\mu})$$

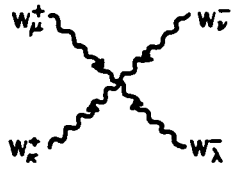

$$ig^2(2g_{\kappa\mu}g_{\lambda\nu} - g_{\kappa\lambda}g_{\mu\nu} - g_{\kappa\nu}g_{\lambda\mu})$$

This shows all three- and four-boson couplings that arise in the minimal SM.

APPENDIX II

Grouping of Feynman Diagrams.

In this short appendix, we will describe how the five diagrams of the process $e_R^- e^+ \rightarrow W^- e^+ \nu_e$ can be combined into three. It is clear that there is a big advantage in doing so. We will take for example the third diagram of fig. 2 which we reproduce here with relevant indices on fig. 32

Figure 32. Vertex in the process $e_r^- \; e^+ \rightarrow W^- \; e^+ \; \nu_e$.

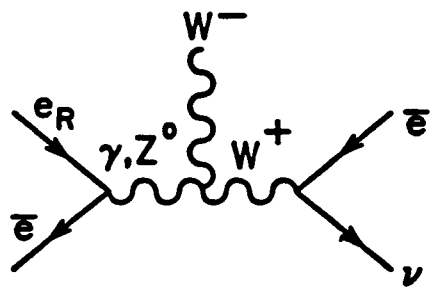

Two of the channels that occur in the process and that we can add up into one channel.

When we use the photon as one of the internal particles, we write this vertex as:

$$ie\bar{v}(\bar{p})\gamma^{\mu}u(p)(\frac{-ig^{\mu\mu'}}{s})\bar{u}(q)(-i)(\frac{G_F M_W^2}{\sqrt{2}})^{1/2}\gamma_{\alpha}(1-\gamma_5)v(\bar{q})$$

$$(-i)\left[\frac{g^{\alpha\alpha'} - \frac{(s-w)^{\alpha}(s-w)^{\alpha'}}{M_W^2}}{(s-w)^2 - M_W^2)}\right] \qquad (A-II.1)$$

$$ie\varepsilon_{\beta}\Big\{g_{\alpha'\beta}(-w^- + w^+)_{\mu'} - g_{\alpha'\mu'}(s+w^+)_{\beta} + g_{\beta\mu'}(s+w^-)_{\alpha'}\Big\}$$

The second half of the W-boson propagator can be dropped since it will lead, through the Dirac equation, to terms proportional to (m_e^2/M_W^2). These are very small and, as verified on the computer, are completely negligible. This very useful approximation can be made every time one has a line of massless fermions connected to the gauge boson. In our case, we are left with:

$$\frac{-ie^2\sqrt{G_F M_W^2/\sqrt{2}}}{s\left[(s-w)^2 - M_W^2\right]}\bar{v}(\bar{p})\gamma_{\mu}u(p)\bar{u}(q)\gamma_{\alpha}(1-\gamma_5)\varepsilon_{\beta}$$

$$\Big[g_{\alpha\beta}(q+\bar{q}-w)_{\mu} - g_{\alpha\mu}(p+\bar{p}+q+\bar{q})_{\beta} + g_{\beta\mu}(p+\bar{p}+w)_{\alpha}\Big] \qquad (A-II.2)$$

where we have used:

$$w^+ \equiv q+\bar{q} \qquad s \equiv p+\bar{p} \qquad w^- \equiv w$$

In the same way, when a Z^0-boson is the internal particle, the diagram becomes:

$$\frac{-ie^2\sqrt{G_F M_W^2/\sqrt{2}}}{s\left[(s-w)^2-M_W^2\right]}\left[\frac{s}{e(s-M_Z^2)}\right]\left[\frac{G_F M_Z^2}{2\sqrt{2}}\right]^{1/2} cotg(\theta_W)$$

$$\bar{v}(\bar{p})\gamma_\mu\left[R(1+\gamma_5)+L(1-\gamma_5)\right]u(p)\bar{u}(q)\gamma_\alpha(1-\gamma_5)\varepsilon_\beta v(\bar{q}) \qquad (A-II.3)$$

$$\left[g_{\alpha\beta}(q+\bar{q}-w)_\mu - g_{\alpha\mu}(p+\bar{p}+q+\bar{q})_\beta + g_{\beta\mu}(p+\bar{p}+w)_\alpha\right]$$

where we have dropped the second half of the heavy boson propagator.

We see that the tensor structure is essentially the same in the two cases. Therefore, by a judicious choice of couplings, it should be possible to group the two diagrams into a single one. Explicitly, we calculate, for the $(\gamma + Z^0)$ diagram:

$$\frac{ie^2\sqrt{G_F M_W^2/\sqrt{2}}}{s\left[(s-w)^2-M_W^2\right]}\bar{v}(\bar{p})\gamma_\mu\left[G_L\gamma_L+G_R\gamma_R\right]u(p)\bar{u}(q)\gamma_\alpha(1-\gamma_5)\varepsilon_\beta v(\bar{q}) \qquad (A-II.4)$$

$$\left[g_{\alpha\beta}(Q-w)_\mu - g_{\alpha\mu}(P+Q)_\beta + g_{\beta\mu}(P+w)_\alpha\right]$$

where

$$Q \equiv q+\bar{q} \qquad P \equiv p+\bar{p} \qquad \gamma_{\substack{R\\L}} \equiv (1\pm\gamma_5).$$

We have also defined the new couplings as:

$$G_L \equiv \frac{1}{2} - \left(\frac{s}{e}\right)\left(\frac{G_F M_Z^2}{2\sqrt{2}}\right)^{1/2}\left(\frac{cotg(\theta_W)L}{s-M_Z^2}\right)$$

$$(A-II.5)$$

$$G_R \equiv \frac{1}{2} - \left(\frac{s}{e}\right)\left(\frac{G_F M_Z^2}{2\sqrt{2}}\right)^{1/2}\left(\frac{cotg(\theta_W)R}{s-M_Z^2}\right)$$

Once this is done, one simply has to square the matrix element. This is a very lengthy enterprise because of the long tensor form of the vertex. Some symmetry arguments can be used to shorten the algebra by a fair amount.

APPENDIX III

Monte Carlo Method.

The Monte Carlo method of integration is a numerical method used to perform some complicated integrations that would be quite often impossible to do otherwise. The basic idea is rather simple and can be grasped through the following example. Suppose that one wants to find the area of a circle. One could proceed by dividing the circle into little squares and count how many little squares there are in the circle. Another way is to enclose the circle by a square and drop grains of sand onto the square at random. The ratio:

$$\frac{\text{number of grains in circle}}{\text{number of grains in square}}$$

is the same direct ratio of the areas. The same principle applies for more complicated functions. For example:

$$\int f(x)dx \quad = \quad \frac{\sum_{i=1}^{N} f(x_i)}{N}$$

where the x_i are picked at random on the interval we want to integrate. As the Monte Carlo method has been known for a long time[93,94], its properties are well known. Its error with respect to the "true" answer is known to decrease as $1/\sqrt{N}$. This is the main reason why the method was not used much before computers were available. Now-a-days, it is widely used and very useful.

In our specific decay processes, the method used to tackle the problem is the following. One considers the two incoming particles as forming one big particle with all the momentum. Then this big one decays into the first outgoing particle of the process and a not-so-big particle. Then this not-so-big particle decays into the second outgoing particle of the process and a not-so-so-big particle. Then this

not-so-so-big particle decays into the third outgoing particle of the process and a not-so-so-so-big particle...and so on until one has all the outgoing particles of the process. The last not-so-so-so-so-...-big particle of the chain is the last outgoing particle of the process. The Monte Carlo philosophy comes into play at the decay process. Each decay occurs in the rest frame of the decaying particle and the angles and energies of the decay products are random within the physically allowed range. One then boosts all the momenta of the outgoing particles to the lab. frame and these become the 4-vectors for the matrix element of the process that one has to input into the program. The cross-section is smaller or larger depending on the combination of 4-momenta we obtained from the decays. What we do is a multi-dimentional integration of the cross-section as a function of momenta. Essentially:

$$\text{cross} - \text{section} \quad = \quad \frac{\sum_{i=1}^{N} cross - section(p_i^1, p_i^2, ...p_i^n)}{N}$$

where n is the number of outgoing particles of the process and N is the number of events that we generate. For the processes that we calculated, N=50,000 was in general sufficient to have a stable answer. However, when a t-channel can proceed via photon exchange, we have a real pole and the program that we will list here cannot handle this. There might be some ways to do so by a change of variable, but this has not been tried yet with our routines. It would be a very useful extension, but it is far from trivial.

We list in the following pages the program that we used for the Monte Carlo integrations. The program we give is slightly modified to account for processes where some of the decaying particles are on-shell; this means that we let the decay products decay into other, lighter particles. The changes are shown clearly and the version for off-shell decaying particles is kept as "comments". This program is a generalisation of a program first developed in ref. 95.

```
C-----------------------------------------------------------------
C                        PROGRAM MONTE.FOR
C-----------------------------------------------------------------
C     FILE  5: INPUT FROM SOURCE
C     FILE  6: OUTPUT TO SINK
C     FILE 34: ANSWER EVERY 1000 PTS FOR DISPLAY
C     FILE 35: STORE LATEST ANSWER FOR RESTART
C     FILE 36: STORE MASSES FOR RESTART
C     FILE 37: MISCELLANEOUS FOR DISPLAY
C-----------------------------------------------------------------
C          DECLARE VARIABLES
C-----------------------------------------------------------------
C     II,JJ,KK ARE ABBREVIATIONS FOR OFTEN USED INTEGER EXPRESSIONS
C     NPTS IS THE NUMBER OF POINTS TO BE USED IN THE MONTE CARLO
C     N IS THE NUMBER OF PARTICLES IN THE FINAL STATE
C     SEED IS A PARAMETER NEEDED BY RANDOM NUMBER GENERATOR GGUBFS
C     PP IS THE INITIAL PARTICLE MOMENTUM IN THE LAB CM FRAME
C     M(I) IS THE MASS OF PARTICLE I
C     M2(I) IS THE SQUARE OF M(I)
C     MSUM(I) IS THE SUM OF M(J) FOR J=I TO N
C     MX(I) IS THE MASS OF THE VIRTUAL PARTICLE ABOUT TO DECAY INTO
C                                                M(I) AND MX(I+1)
C     MX2(I) IS THE SQUARE OF MX(I)
C     THE MATRIX B(4,4,I) BOOSTS THE MX(I) CM FRAME ONE BACK
C     LAMBDA(I) IS THE MAGNITUDE OF THE MOMENTUM OF PARTICLE I IN C.M
C     STOT IS THE CM ENERGY SQUARED OF THE PROCESS IN LAB CM FRAME
C     X1,X2 ARE THE USUAL PARTON MOMENTUM FRACTIONS
C     CME IS THE CM ENERGY SQUARED OF THE SUBPROCESS
C     V,XI ARE VELOCITY AND RAPIDITY OF ONE FRAME W.R.T.  ANOTHER
C     THETA,PHI ARE THE USUAL ANGLES
C     K4V(4,I) IS THE MOMENTUM 4-VECTOR OF PARTICLE I
C     LK4V(4,I) IS K4V(4,I) AFTER BOOSTING TO LAB FRAME
C     DV1 IS A DUMMY 4-VECTOR USED FOR PROGRAMMING EASE
C     A IS THE SUBPROCESS AMPLITUDE SUPPLIED BY THE USER
C     PXS IS THE PARTIAL X-SECTION CALCULATED ON EACH LOOP PASS
C     SUMW IS THE SUM OF THE PARTIAL PXS FOR ALL LOOP PASSES
C     JAC IS THE JACOBIAN FACTOR FROM THE INTEGRALS
C     KAP IS THE MAGNETIC MOMENT OF THE VECTOR BOSONS
C     INTEGRAL IS THE FINAL ANSWER
C-----------------------------------------------------------------
      IMPLICIT REAL*8(A-Z)
      INTEGER II,JJ,KK,NPTS,START,N,RAT,IJ,IK,I,NEQ,K,L
      DIMENSION M(9),M2(9),MSUM(9),MX(9),MX2(9),B(4,4,9),LAMBDA(8)
      DIMENSION K4V(4,9),LK4V(4,9),DV1(4)
      DIMENSION BTH(9,201),BPL(9,201),BPT(9,201)
C-------------COMMON BLOCKS-------------------------------------
      COMMON/AMP/AMPLITUDE
      COMMON/AAA/SEED
      COMMON/B1B/LK4V,PP,M
      COMMON/C1C/ALPHA,SINSQ,COSQAL,MZ,WZ,BRZ,ME,WE,BRE
      COMMON/LLL/L
C-----------------------------------------------------------------
C          PROGRAM SETUP
C-----------------------------------------------------------------
C     NEW CALCULATION OR RESTART, NUMBER OF EVENTS
C-----------------------------------------------------------------
      WRITE(6,10)
   10 FORMAT(' NEW CALCULATION (TYPE 0) OR RESTART (TYPE 1) ?')
      READ(5,11)JJ
   11 FORMAT(I1)
```

```
      IF(JJ.NE.0.AND.JJ.NE.1) THEN
      WRITE(6,12)
   12 FORMAT(' YOU MUST TYPE 0 OR 1')
      STOP
      END IF
      WRITE(6,13)
   13 FORMAT(' ENTER NUMBER OF EVENTS DESIRED  (I7)')
      READ(5,14)NPTS
   14 FORMAT(I7)
C-----------------------------------------------------------------
C     NEW: READ ENTRIES THROUGH TERMINAL
C-----------------------------------------------------------------
        IF(JJ.EQ.0) THEN
        START=1
        SEED=12345.0D0
        WRITE(6,510)
 510    FORMAT('-------------------------------------------------')
        WRITE(6,15)
  15    FORMAT(' E(6) AND Z ARE ON SHELL, MASS OF Z < MASS OF E(6) ')
        WRITE(6,511)
 511    FORMAT(' PP > HALF-MASS OF THE E(6) ' )
        WRITE(6,512)
 512    FORMAT(' OTHERWISE YOU GET X-SEC. << 0.0D0 ')
        WRITE(6,513)
 513    FORMAT('-------------------------------------------------')
        WRITE(6,16)
  16    FORMAT(' ENTER PP ')
        READ(5,30)PP
        WRITE(6,17)
  17    FORMAT(' ENTER NUMBER (3-9) OF PARTICLES  (I1)')
        READ(5,11)N
        IF(N.LT.3.OR.N.GT.9) STOP
        DO 19 I=1,N
          WRITE(6,18)I
  18      FORMAT(' ENTER M(',I1,')  (F15.8)')
          READ(5,30)M(I)
          M2(I)=M(I)**2
          WRITE(36,32)M(I),M2(I)
  19    CONTINUE
        END IF
        WRITE(6,20)
  20    FORMAT(' ENTER ALPHA  (F15.8)')
        READ(5,30)ALPHA
        WRITE(6,21)
  21    FORMAT(' ENTER SINSQ  (F15.8)')
        READ(5,30)SINSQ
        WRITE(6,22)
  22    FORMAT(' ENTER COSQ(ALPHA) FOR eEZ COUPLING  (F15.8) ')
        READ(5,30)COSQAL

        WRITE(6,23)
  23    FORMAT(' ENTER MASS OF Z-BOSON  (F15.8)')
        READ(3,30)MZ
        WRITE(6,530)
 530    FORMAT('-------------------------------------------------')
        COSQ=1.0D0-SINSQ
        PWZ=MZ/(24.0D0*ALPHA*COSQ*SINSQ)
        WRITE(6,531)PWZ
 531    FORMAT(' WIDTH FROM MASSLESS LEPTONS IS ',D15.6)
        WRITE(6,532)
```

```
532     FORMAT('-----------------------------------------------------')
        WRITE(6,24)
 24     FORMAT(' ENTER WIDTH OF THE Z-BOSON  (F15.8) ')
        READ(5,30)WZ
        WRITE(6,533)
533     FORMAT('-----------------------------------------------------')
        BRZ=PWZ/WZ
        WRITE(6,534)BRZ
534     FORMAT(' THE B. RATIO IS THEN ',D15.6)
        WRITE(6,535)
535     FORMAT('-----------------------------------------------------')

        WRITE(6,25)
 25     FORMAT(' MASS OF THE E(6) MUON ')
        READ(5,30)ME
        WRITE(6,520)
520     FORMAT('-----------------------------------------------------')
        SINSQAL=1.0D0-COSQAL
        COSQ=1.0D0-SINSQ
        R=(ME/MZ)**2
        PART1=(R-1.0D0)*(R**2+R-2.0D0)*ME/R**2
        PART2=SINSQAL*COSQAL/(32.0D0*ALPHA*SINSQ*COSQ)
        PARTIAL=PART1*PART2
        WRITE(6,27)PARTIAL
 27     FORMAT(' WIDTH FROM THE Z BOSON IS ',D12.4)
        WRITE(6,521)
521     FORMAT('-----------------------------------------------------')
        WRITE(6,28)
 28     FORMAT(' BRANCHING RATIO ')
        READ(5,30)BRE
        WRITE(6,522)
522     FORMAT('-----------------------------------------------------')
        WRITE(6,26)PARTIAL/BRE
 26     FORMAT(' THE TOTAL WIDTH IS THEN ',D15.6)
        WRITE(6,523)
523     FORMAT('-----------------------------------------------------')

        WE=PARTIAL/BRE

 30     FORMAT(F13.8)
        IF(ME-MZ.LE.0.0D0)THEN
        WRITE(6,524)
524     FORMAT(' I TOLD YOU THESE MASSES WOULD GIVE YOU NEG. X-SECS. ')
        WRITE(6,525)
525     FORMAT(' I MUST STOP. BETTER LUCK NEXT TIME! ')
        STOP
        END IF
        IF(PP-ME/2.0D0.LE.0.0D0)THEN
        WRITE(6,526)
526     FORMAT(' YOU DO NOT HAVE ENOUGH ENERGY TO CREATE THE E(6) ')
        WRITE(6,527)
527     FORMAT(' PARTICLE. I MUST STOP. TYPE BETTER NEXT TIME! ')
        STOP
        END IF
        IF((ME/2.0D0)-WE.LE.0.0D0.OR.(MZ/2.0D0)-WZ.LE.0.0D0)THEN
        WRITE(6,528)
528     FORMAT(' THE WIDTH IS LARGE FOR THE N.W. APPROXIMATION.... ')
        END IF
        WRITE(6,529)
529     FORMAT(' O.K. THESE ENERGIES AND MASSES SEEM TO BE SENSIBLE ')
```

```
C-----------------------------------------------------------------
C     RESTART: READ ENTRIES FROM FILES
C-----------------------------------------------------------------
      IF(JJ.EQ.1) THEN
        READ(35,31)START,N,SEED,SUMW,PP,DUMMY
  31    FORMAT(I7,I2,4D18.10)
        START=START+1
        IF(START.GE.NPTS) STOP
        DO 33 I=1,N
        READ(36,32)M(I),M2(I)
  32    FORMAT(2D18.10)
  33    CONTINUE
      END IF
C-----------------------------------------------------------------
C          INITIALIZE VARIABLES
C-----------------------------------------------------------------
         NEG=0
         MSUM(1)=M(1)+ME
         MSUM(2)=M(2)+MZ
         MSUM(3)=M(3)+M(4)
         MSUM(4)=M(4)
         SUMW=0.0D0
C-----------------------------------------------------------------
C        DO 42 I=1,N
C        MSUM(I)=0.0D0
C        DO 41 J=I,N
C  41    MSUM(I)=MSUM(I)+M(J)
C  42    CONTINUE
C-----------------------------------------------------------------
        KK=N-1
        II=3*N-4
        STOT=4.0D0*PP*PP
        IF((2.0D0*PP).LE.MSUM(1)) THEN
        WRITE(6,43)
  43    FORMAT(' OUPS! NOT ENOUGH ENERGY FOR REACTION')
        STOP
        END IF
C-----------------------------------------------------------------
      PI=3.14159265358979323B
      TRA=0.3893857D09
      WRITE(6,48)
  48  FORMAT(' BEGINNING MAIN MONTE CARLO LOOP',/)
C-----------------------------------------------------------------
C     CALCULATE (VERY ROUGHLY)THE MAXIMUM MOMENTUM OF THE PARTICLE
C-----------------------------------------------------------------
      SSTOT=4.0D0*PP**2
      DIFF1=DSQRT(SSTOT-ME**2)
      DIFF2=DSQRT(ME**2-MZ**2)+MZ/2.0D0
      IF(DIFF1.GE.DIFF2)PPMAX=DIFF1*0.7D0
      IF(DIFF1.LT.DIFF2)PPMAX=DIFF2*0.7D0
      IF(PPMAX.LT.60.0D0)PPMAX=60.0D0
C-----------------------------------------------------------------
C          BEGIN MAIN MONTE CARLO LOOP
C-----------------------------------------------------------------
      DO 999 IJ=START,NPTS
C-----------------------------------------------------------------
C     GENERATE X1,X2 AND CHECK IF ENOUGH ENERGY
C     AS IT IS, HAVE COLLISIONS BETWEEN TWO IDENTICAL PARTICLES
C     OF SAME HIGH ENERGY.(I.E.  X1=X2)
C-----------------------------------------------------------------
```

```
 50     X1=1.0D0
        X2=1.0D0
        CME=X1*X2*STOT
        MX(1)=DSQRT(CME)
        MX2(1)=CME
        IF(MX(1).LE.MSUM(1)) GO TO 50
        MX(N)=M(N)
        MX2(N)=M(N)**2
C-----------------------------------------------------------------
C     GENERATE VIRTUAL PARTICLE MASSES
C-----------------------------------------------------------------
C          DO 65 I=2,KK
C          MX(I)=(MX(I-1)-MSUM(I-1))*GGUBFS(SEED)+MSUM(I)
C          MX2(I)=MX(I)**2
C   65     CONTINUE
C-----------------------------------------------------------------
C       SPECIAL CASE WHEN THE E(6) AND Z BOSON ARE ON SHELL
C-----------------------------------------------------------------
         MX(2)=ME
         MX2(2)=ME**2
         MX(3)=MZ
         MX2(3)=MZ**2
C-----------------------------------------------------------------
C    SPECIALIZE THE PROGRAM TO THE CASE WHEN THE E(6) ELECTRON
C    IS ON SHELL                                  &
C    LOOK ONLY TO:                              &
C                                          &                 &&&  NEUTRINO
C      %                        @ ********                  %%%  ELECTRON
C        %                 @      #      &                  ***  Z BOSON
C          %            @            #     &                @@@  E(6) MUON
C            %**********                #    &              ###  MUONS
C          %             #
C        %                  #
C      %                        #
C
C     NO T-CHANNEL DIAGRAM...IF WE LOOK FOR A MUON AND A BIG E(6) MUON.
C-----------------------------------------------------------------
C     FIND BOOST MATRIX FROM SUBPROCESS CM TO LAB FRAME
C-----------------------------------------------------------------
        V=(X1-X2)/(X1+X2)
        XI=DLOG((1.0D0+V)/(1.0D0-V))/2.0D0
        COSTHETA=2.0D0*GGUBFS(SEED)-1.0D0
        THETA=DACOS(COSTHETA)
        PHI=2.0D0*PI*GGUBFS(SEED)
        CALL BOOST(B(1,1,1),XI,THETA,PHI)
C-----------------------------------------------------------------
C     LET THE PARTICLES DECAY, GET THE BOOST MATRICES AND 4-VECTORS
C-----------------------------------------------------------------
        DO 71 I=1,KK
 71     CALL DECAY(MX(I),MX(I+1),M(I),K4V(1,I),B(1,1,I+1))
        K4V(1,N)=MX(KK)-K4V(1,KK)
        K4V(2,N)=-K4V(2,KK)
        K4V(3,N)=-K4V(3,KK)
        K4V(4,N)=-K4V(4,KK)
C-----------------------------------------------------------------
C     BOOST 4-MOMENTA TO LAB FRAME
C-----------------------------------------------------------------
        DO 88 I=1,N
        DO 81 K=1,4
 81     DV1(K)=K4V(K,I)
```

```
      DO 84 JK=1,I
      J=I-JK+1
      IF(I.EQ.N) J=I-JK
      IF(J.EQ.0) GO TO 84
      CALL MULT(B(1,1,J),DV1,LK4V(1,I))
      DO 83 K=1,4
 83   DV1(K)=LK4V(K,I)
 84   CONTINUE
 88   CONTINUE
C-----------------------------------------------------------------
C     CALL AMPLITUDE -- MUST BE LINKED TO, OR PART OF THE PROGRAM
C-----------------------------------------------------------------
      CALL BIGMUAMPL
      A=AMPLITUDE
C-----------------------------------------------------------------
C     CALCULATE PHASE SPACE DENSITY AND ELEMENT OF INTEGRAL
C-----------------------------------------------------------------
      PXS=1.0D0
      DO 92 I=1,KK
      LAMBDA(I)=-4.0D0*M2(I)*MX2(I+1)+(MX2(I)-M2(I)-MX2(I+1))**2
      LAMBDA(I)=DSQRT(LAMBDA(I))/(2.0*MX(I))
      PXS=PXS*LAMBDA(I)
 92   CONTINUE
      JAC=(4.0D0*PI)**KK
C-----------------------------------------------------------------
C       DO 93 I=1,KK-1
C 93    JAC=JAC*(MX(I)-MSUM(I))
C-----------------------------------------------------------------
      FLUX=1.0D0/(2.0D0*CME)
C-----------------------------------------------------------------
C       FACTOR=DSQRT(CME)*(2.0D0*PI)**II
C-----------------------------------------------------------------
      FACTOR=(2.0D0**N)*(2.0D0*PI)**II
      PXS=PXS*A*JAC*FLUX*ME*MZ/(FACTOR*DSQRT(STOT))
      SUMW=SUMW+PXS
C-----------------------------------------------------------------
C     WRITE OUT THE FIRST TEN EVENTS
C-----------------------------------------------------------------
      IF(PXS.LT.0.0D0)NEG=NEG+1
      IF(IJ.LE.10.OR.PXS.LT.0.0D0)THEN
        WRITE(37,101)
101     FORMAT('  IJ      I      LK4V(1,I)',10X,'2',14X,'3',14X,'4')
        DO 103 I=1,N
        WRITE(37,102)IJ,I,LK4V(1,I),LK4V(2,I),LK4V(3,I),LK4V(4,I)
102     FORMAT(I9,1X,I2,4D15.6)
103     CONTINUE
        WRITE(37,104)
104     FORMAT('   IJ          A              PXS')
        WRITE(37,105)IJ,A,PXS*TRA
105     FORMAT(I9,2D15.6)
        END IF
C-----------------------------------------------------------------
C     BIN THE ANGULAR, MOMENTUM AND TRANSVERSE MOMENTUM DISTRIBUTIONS
C-----------------------------------------------------------------
        PMAX=PPMAX
        DO 200 L=1,N
        PL=DSQRT(LK4V(2,L)**2+LK4V(3,L)**2+LK4V(4,L)**2)
        TH=DACOS(LK4V(4,L)/PL)*180.0D0/3.14159265358979323B
        PT=DSQRT(LK4V(2,L)**2+LK4V(3,L)**2)
        CALL BIN(TH,BTH,0.00,180.00,PXS*TRA)
```

```
          CALL BIN(PL,BPL,0.00,PMAX,PXS*TRA)
          CALL BIN(PT,BPT,0.00,PMAX,PXS*TRA)
 200      CONTINUE
C-----------------------------------------------------------------
C     STORE ANSWER EVERY 1000 EVENTS FOR RESTART IF SYSTEM CRASHES
C-----------------------------------------------------------------
        RAT=MOD(IJ,1000)
        IF(RAT.EQ.0) THEN
        WRITE(34,111)IJ,N,PP,SUMW*TRA/FLOAT(IJ)
 111    FORMAT(I9,2X,I2,2X,D9.3,2X,D12.5)
        WRITE(6,112)IJ
 112    FORMAT(' FINISHED ',I7,' POINTS')
        END IF
C-----------------------------------------------------------------
CC          END MAIN MONTE CARLO LOOP
C-----------------------------------------------------------------
 999  CONTINUE
C-----------------------------------------------------------------
CC          CALCULATE THE INTEGRAL AND OUTPUT
C-----------------------------------------------------------------
      INTEGRAL=SUMW/FLOAT(NPTS)
      WRITE(37,123)NPTS,PP,NEG
 123  FORMAT(' NPTS= ',I9,4X,' PP= ',D15.6,2X,' NEG= ',I7)
      WRITE(37,125)MZ,WZ,ME,WE
 125  FORMAT(' MZ,WZ,ME,WE ',4D13.5)
      WRITE(37,126)SINSQ,COSQAL
 126  FORMAT(' SINSQ,COSQAL ',2D13.5)
      WRITE(37,124)INTEGRAL*TRA
 124  FORMAT(' X-SECTION= ',D15.6)
C-----------------------------------------------------------------
C   EMPTY THE BINS INTO SOME FILES
C-----------------------------------------------------------------
      WRITE(30,300)
      WRITE(31,301)
      WRITE(32,302)
 300  FORMAT(' ANGULAR DISTRIBUTION ')
 301  FORMAT(' MOMENTUM DISTRIBUTION ')
 302  FORMAT(' TRANSVERSE MOMENTUM DISTRIBUTION ')
      WRITE(30,350)INTEGRAL*TRA
      WRITE(31,350)INTEGRAL*TRA
      WRITE(32,350)INTEGRAL*TRA
 350  FORMAT(' X-SECTION 'D15.6)
      WRITE(30,303)NPTS,NEG
      WRITE(31,303)NPTS,NEG
      WRITE(32,303)NPTS,NEG
 303  FORMAT(' # OF EVENTS',I6,3X,'# OF NEG.  X-SECTIONS',I5)
      WRITE(30,304)PP,SINSQ,COSQAL
      WRITE(31,304)PP,SINSQ,COSQAL
      WRITE(32,304)PP,SINSQ,COSQAL
 304  FORMAT(' BEAM ',D11.3,4X,' SINSQ ',D11.3,4X,' COSQAL ',D11.3)
      WRITE(30,305)MZ,WZ,BRZ
      WRITE(30,306)ME,WE,BRE
      WRITE(31,305)MZ,WZ,BRZ
      WRITE(31,306)ME,WE,BRE
      WRITE(32,305)MZ,WZ,BRZ
      WRITE(32,306)ME,WE,BRE
 305  FORMAT(' Z MASS     ',D10.3,3X,' WIDTH ',D10.3,3X,'B.  RATIO',D10.
 306  FORMAT(' E(6) MASS ',D10.3,3X,' WIDTH ',D10.3,3X,'B.  RATIO',D10.
      THETAP=0.0D0
      PTP=0.0D0
```

```
      PLP=0.0D0
      DO 400 K=1,201
      THETAP=THETAP+180.0/201.0
      WRITE(30,401)THETAP,BTH(1,K),BTH(2,K),BTH(3,K),BTH(4,K)
      PLP=PLP+PMAX/201.00
      WRITE(31,401)PLP,BPL(1,K),BPL(2,K),BPL(3,K),BPL(4,K)
      PTP=PTP+PMAX/201.00
      WRITE(32,401)PTP,BPT(1,K),BPT(2,K),BPT(3,K),BPT(4,K)
 401  FORMAT(5D14.4)
 400  CONTINUE
      END
C-----------------------------------------------------------------
C--------       MUST LINK TO RTNS.OBJ FOR SUBROUTINES       ----------
C-----------------------------------------------------------------
```

```
      SUBROUTINE DECAY2(M1,M2,M3,BM2,BM3)
      REAL*8 M1,M2,M3,V2(4),V3(4),BM2(4,4),BM3(4,4)
      REAL*8 COSTHETA,THETA,PHI,V,PI,XI
      REAL*8 SEED
      COMMON/AAA/SEED
      EXTERNAL GGUBFS,BOOST
      PI=3.14159265358979323B
      V3(1)=(M1*M1+M3*M3-M2*M2)/(2.0*M1)
      V3(4)=DSQRT(V3(1)*V3(1)-M3*M3)
      V2(1)=M1-V3(1)
      V2(4)=-V3(4)
      V=V2(4)/V2(1)
      IF(V.EQ.-1.0D0) STOP
      XI=DLOG((1.0D0+V)/(1.0D0-V))/2.0D0
      COSTHETA=2.0*GGUBFS(SEED)-1.0D0
      THETA=DACOS(COSTHETA)
      PHI=2.0*PI*GGUBFS(SEED)
      CALL BOOST(BM2,XI,THETA,PHI)
      V=V3(4)/V3(1)
      IF(V.EQ.-1.0D0) STOP
      XI=DLOG((1.0D0+V)/(1.0D0-V))/2.0D0
      COSTHETA=2.0D0*GGUBFS(SEED)-1.0D0
      THETA=DACOS(COSTHETA)
      PHI=2.0D0*PI*GGUBFS(SEED)
      CALL BOOST(BM3,XI,THETA,PHI)
      RETURN
      END

      SUBROUTINE BOOST(B,XI,THETA,PHI)
      REAL *8 B(4,4),XI,THETA,PHI
      B(1,1)= DCOSH(XI)
      B(1,2)= -DSINH(XI)*DSIN(THETA)
      B(1,3)= 0.0D0
      B(1,4)= DSINH(XI)*DCOS(THETA)
      B(2,1)= 0.0D0
      B(2,2)= DCOS(PHI)*DCOS(THETA)
      B(2,3)= -DSIN(PHI)
      B(2,4)= DSIN(THETA)*DCOS(PHI)
      B(3,1)= 0.0D0
      B(3,2)= DSIN(PHI)*DCOS(THETA)
      B(3,3)= DCOS(PHI)
      B(3,4)= DSIN(THETA)*DSIN(PHI)
      B(4,1)= DSINH(XI)
      B(4,2)= -DCOSH(XI)*DSIN(THETA)
      B(4,3)= 0.0D0
      B(4,4)= DCOSH(XI)*DCOS(THETA)
      RETURN
      END

      SUBROUTINE BIN(F,AR,INF,SUP, W)
C-----------------------------------------------------------------------
C        CLASSES F INTO ONE OF 201 BINS BETWEEN INF AND SUP AND PUT
C                                  IT INTO ARRAY AR
C-----------------------------------------------------------------------
      REAL*8 F,AR(9,201),INF,SUP,W
      COMMON/LLL/L
      INTEGER POS,L
      POS=DINT(200.0*(F-INF)/(SUP-INF))+1
      IF (POS .GT. 201) POS = 201
      IF (POS .LT. 1) POS = 1
```

```
      AR(L,POS)=AR(L,POS)+W
      RETURN
      END
      SUBROUTINE BINN(F,AR,INF,SUP,W)
      REAL*8 F,AR(201),INF,SUP,W
      INTEGER POS
      POS=DINT(200.0*(F-INF)/(SUP-INF))+1
      IF (POS .GT. 201) POS = 201
      IF (POS .LT. 1) POS = 1
      AR(POS)=AR(POS)+W
      RETURN
      END

      SUBROUTINE SCALP3(V1,V2,VSV)
      REAL*8 V1(4), V2(4), VSV
      VSV = V1(2)*V2(2) + V1(3)*V2(3) + V1(4)*V2(4)
      RETURN
      END

      SUBROUTINE MULT(B,V1,V2)
C-----------------------------------------------------------------------
C             CALCULATES THE PRODUCT BETWEEN THE MATRIX B AND
C                 VECTOR V1 AND PUTS RESULT INTO V2
C-----------------------------------------------------------------------
      REAL*8 B(4,4), V1(4), V2(4), PH
      DO 300 I=1,4
      PH=0.0D0
      DO 301 J=1,4
301   PH = B(I,J) * V1(J) + PH
      V2(I) = PH
300   CONTINUE
      RETURN
      END

      SUBROUTINE DIST(X,SC,UP,DN)
C-----------------------------------------------------------------------
C     DUKE AND OWENS VALENCE QUARK DISTRIBUTIONS IN PROTON (SET 1)
C-----------------------------------------------------------------------
      REAL*8 X,SC,UP,DN,N1,N2,N3,N4,NUD,ND,GUD,GD,SC2,B
      EXTERNAL BETA
C-----------------------------------------------------------------------
C     SET UP PARAMETERS
C-----------------------------------------------------------------------
      SC2=SC**2
      N1=0.419D0+0.004D0*SC-0.007D0*SC2
      N2=3.46D0+0.724D0*SC-0.066D0*SC2
      GUD=4.40D0-4.86D0*SC+1.32D0*SC2
      N3=0.763D0-0.237D0*SC+0.026D0*SC2
      N4=4.00D0+0.627D0*SC-0.019D0*SC2
      GD=-0.421D0*SC+0.033D0*SC2
      CALL BETA(N1,N2+1.0D0,B)
      NUD=3.0/(B*(1.0D0+GUD*N1/(N1+N2+1.0D0)))
      CALL BETA(N3,N4+1.0D0,B)
      ND=1.0D0/(B*(1.0D0+GD*N3/(N3+N4+1.0D0)))
C-----------------------------------------------------------------------
C     FIND DISTRIBUTION VALUES AT X
C-----------------------------------------------------------------------
      DN=ND*(1.0D0+GD*X)*(1.0D0-X)**N4
      DN=DN*X**(N3-1.0D0)
      UP=NUD*(1.0D0+GUD*X)*(1.0D0-X)**N2
```

```
      UP=UP*X**(N1-1.0D0)-DN
      RETURN
      END

      SUBROUTINE BETA(X,Y,B)
C-----------------------------------------------------------------------
C     CALCULATES THE EULER BETA FUNCTION IN DOUBLE PRECISION
C-----------------------------------------------------------------------
      REAL*8 X,Y,B,DGAMMA
      EXTERNAL DGAMMA
      B=DGAMMA(X)*DGAMMA(Y)/DGAMMA(X+Y)
      RETURN
      END

      SUBROUTINE DECAY(M1,M4,M3,V3,M)
C-----------------------------------------------------------------------
C
C    FOR DECAY OF M1 INTO M2 AND M3, CALCULATE THE 4-VECTOR V3
C    OF PARTICLE 3 IN M1 REST FRAME, THEN CALCULATE BOOST MATRIX
C    FROM M2 TO M1 REST FRAME
C-----------------------------------------------------------------------
      REAL*8 M1,M4,M3,V3(4),M(4,4),COSTHETA,THETA,PHI,V,PI,XI
      REAL*8 SEED,PX2,EX2,VV
      COMMON/AAA/SEED
      EXTERNAL GGUBFS,BOOST
      VV=1.0D0
      PI= 3.14159265358979323 8
      V3(1) = (M1*M1+M3*M3-M4*M4)/(2.0D0*M1)
      V3(2) = 0.0D0
      V3(3) = 0.0D0
      V3(4) = DSQRT(V3(1)*V3(1) - M3*M3)
      PX2 = -V3(4)
      EX2 = M1-V3(1)
C-----------------------------------------------------------------------
C            COMPOSE BOOST MATRIX BETWEEN QUARKS CM AND X CM
C-----------------------------------------------------------------------
      V = PX2/EX2
      IF(V.LE.-VV) RETURN
      IF(V.NE.-VV) XI= DLOG((VV+V)/(VV-V))/2.
      COSTHETA =2.0D0*GGUBFS(SEED)-1.0D0
      THETA =DACOS(COSTHETA)
      PHI =2.0D0*PI*GGUBFS(SEED)
      CALL BOOST(M, XI, THETA, PHI)
      RETURN
      END

      SUBROUTINE SCALP(V1,V2,V1SV2)
C-----------------------------------------------------------------------
C     TAKE THE SCALAR PRODUCT OF THE TWO 4-VECTORS V1
C     AND V2 AND PUT THE RESULT INTO V1SV2
C-----------------------------------------------------------------------
      REAL*8 V1(4),V2(4),V1SV2
      V1SV2 = V1(1)*V2(1) - V1(2)*V2(2) - V1(3)*V2(3) - V1(4)*V2(4)
      RETURN
      END
```

APPENDIX IV

Weiszäcker-Williams Approximation.

This approximation method, also known as the equivalent-photon approximation, was first elaborated in 1933-1935. [ref. 96, 97] It relates the high-energy photon-induced cross-section of a given process, $\sigma_{\gamma X \to Y}$, to the corresponding cross-section induced by a charged particle,$\sigma_{eX \to Y}$ through the relation:

$$\sigma_{eX \to Y} = \int dk N(k) \sigma_{\gamma X \to Y} \qquad (A - IV.1)$$

where X is the initial state and Y is the final one. The quantity N(k) is the spectrum of equivalent photons. The method assumes that the intermediate photon is on-shell by neglecting the contributions of the longitudinal component of the photon. In our case, it translates into small angles of emission of the electron since this gives rise to a pole in the photon propagator; the 4-momentum of the photon is 0, which is the characteristic of a real photon. The main advantage of the method lies in the fact that the subprocess $\sigma_{\gamma X \to Y}$ is most often much simpler to calculate than the total process. This allows one to do complete analytical calculations which otherwise would be impossible. The problem now is to obtain the photon spectrum. In the early work of Weiszäcker and Williams, the spectrum was obtained by a semi-classical picture as:

$$N(k) = \frac{2\alpha}{\pi} ln(b_M/b_m) \qquad (A - IV.2)$$

where b_M and b_m are the largest and smallest impact parameters, respectively. Later work[98] generalized the method to three types of processes:

1)an electron radiates a photon which then interacts with the system

2)an electron radiates a photon and interacts itself with the system

3)a photon decays into a lepton pair and one of the leptons interacts with the system.

The essential point is that in order to get the spectrum of the interacting particle, one integrates over the momentum of the outgoing particle of the radiative process. One approximation is usually made in order to get simple expressions for the spectrum: one assumes that the mass of the radiating and radiated particles (i.e. these that do not interact with the system) are very small compared with their momentum. In our case, as we deal with electrons, this condition is easily met. In the case of heavy bosons, for example, one would have to be very careful in using this approximation.

When the conditions are met, one calculates the spectrum to be, for each of the three cases:

$$1) \qquad N(k) = \frac{\alpha}{\pi}\frac{1+(1-x)^2}{x} \quad ln(E/m_e)$$

$$2) \qquad N(k) = \frac{\alpha}{\pi}\frac{1+x^2}{1-x} \quad ln(E/m_e) \qquad (A-IV.3)$$

$$3) \qquad N(k) = \frac{\alpha}{\pi}(x^2+(1-x)^2) \quad ln(E/m_e)$$

where E is the energy of the radiating particle and x is the fraction of this energy carried away by the interacting particle; the photon in our case. Note that a factor 1/2 has been dropped in the log terms[98]: they should read as $ln((E/m_e)+(1/2))$. In most cases $E \gg m_e$ so that one does not loose anything by dropping it; at low energy, one should remember it; although the whole scheme would not work

too well at very low energy.

Then

$$\sigma_{eX\to Y}(E) = \int_{k_{min}}^{k_{max}} N(k)\sigma_{\gamma X\to Y}(k) \qquad (A-IV.4)$$

Instead of working with the energy of the photon as such, one might prefer to work with the s-variable of the sub-process $\gamma X \to Y$. In that case, the form of the spectrum does not change[99]. One replaces:

$$E^2 \to s_{tot} \qquad x \to \frac{s}{s_{tot}} \qquad dx \to \frac{ds}{s_{tot}}.$$

In this way, one gets:

$$1) \qquad N(s) = \frac{\alpha}{\pi}\frac{s_{tot}}{s}\Big(1 - \frac{s}{s_{tot}} + \frac{s^2}{2s_{tot}^2}\Big) ln\Big(\frac{s_{tot}}{m_e^2}\Big)$$

$$2) \qquad N(s) = \frac{\alpha}{\pi}\Big(\frac{1}{2s_{tot}}\Big)\Big(\frac{s_{tot}^2 - s^2}{s_{tot} - s}\Big) ln\Big(\frac{s_{tot}}{m_e^2}\Big) \qquad (A-IV.5)$$

$$3) \qquad N(s) = \frac{\alpha}{\pi}\Big(\frac{1}{2} + \frac{s^2}{s_{tot}^2} - \frac{s}{s_{tot}}\Big) ln\Big(\frac{s_{tot}}{m_e^2}\Big)$$

In the process that we studied before, the first case applies and we have:

$$\sigma_{eX\to Y}(s) = \frac{\alpha}{\pi} ln\Big(\frac{s_{tot}}{m_e^2}\Big) \int_{M_W^2}^{s_{tot}} \Big(1 - \frac{s}{s_{tot}} + \frac{s^2}{2s_{tot}^2}\Big)\big(\sigma_{\gamma x\to Y}(s)\big)\frac{ds}{s}. \qquad (A-IV.6)$$

which is the equation that we used in our calculation. After a change of variable, one recovers the equation given in Chapter I. Again, we emphasize that

there are some constraints to this approximation and that in some cases one must be careful in using it. Furthermore it is interesting to note that in a strongly interacting Higgs boson system, this approximation will break down since the longitudinal components of the gauge bosons are very important.

APPENDIX V

General Form of the γW^+W^- Vertex.

The general form of the vertex that we used in Chapters III and IV seems rather obscure. The goal of this appendix is to explain and justify this specific form. Furthermore, we will also define precisely what is meant by magnetic dipole and electric quadrupole moments of a particle.

Before we turn to these topics, it is worthwhile to go back to classical electromagnetism (EM) and quantum mechanics. We will start with a classical system of charges[100]: we have a system of N charges and want to calculate the potential, $W(\vec{\rho})$ created by these charges at point $\vec{\rho}$. This vector $\vec{\rho}$ is the vector from a given point on the charge distribution to the point of observation. We also define the vectors $\vec{r}_n$ as the vectors from each charge "n" of the distribution to this given point. Then, the potential at $\vec{\rho}$ is given by:

$$W(\vec{\rho}) \equiv \frac{1}{4\pi\epsilon_0}\sum_{n=1}^{N}\frac{q_n}{|\vec{\rho}-\vec{r}_n|}$$

Then, one expands $\frac{1}{|\vec{\rho}-\vec{r}_n|}$ in terms of Legendre polynomials as:

$$\frac{1}{|\vec{\rho}-\vec{r}_n|} \equiv \frac{1}{\rho}\sum_{l=0}^{\infty}\left(\frac{r_n}{\rho}\right)^l P_l\big(cos(\alpha_n)\big).$$

Expanding the Legendre polynomials in terms of spherical harmonics according to:

$$P_l\big(cos(\alpha_n)\big) \equiv \frac{4\pi}{2l+1}\sum_{m=-l}^{+l}(-1)^m Y_l^{-m}(\theta_m,\phi_m)Y_l^m(\Theta,\Phi),$$

the potential can be written as:

$$W(\vec{\rho}) = \frac{1}{4\pi\epsilon_0} \sum_{l=0}^{\infty} \sum_{m=-l}^{l} \sqrt{\frac{4\pi}{2l+1}} (-1)^l Q_l^{-m} \frac{1}{\rho^{l+1}} Y_l^m(\Theta, \Phi)$$

where Θ and Φ are the polar angles related to $\vec{\rho}$.

We have defined $Q_l^m(r_1, r_2, ...r_N)$ as

$$Q_l^m(r_1, r_2, ...r_N) \equiv \sum_{n-1}^{N} \sqrt{\frac{4\pi}{2l+1}} (r_n)^l Y_l^m(\theta_m, \phi_m).$$

The $Q_l^m(r_1, r_2, ...r_N)$ are the electric multipole moments of the charge distribution. This expansion shows clearly that the potential created by a system of charges is completely determined by its multipole expansion. One can verify that:

$W_0(\vec{\rho})$ *is the potential due to the net charge,*

$W_1(\vec{\rho})$ *is the potential due to the net dipole moment,*

$W_2(\vec{\rho})$ *is the potential due to the net quadrupole moment,*

and so on.

Therefore,

Q_0^0 *is the total charge of the system,*

Q_1^m *is the dipole moment of the system,*

Q_2^m *is the quadrupole moment of the system.*

Certainly one can do a similar decomposition for magnetic moments. The magnetic field due to a system of moving charges is well defined by its magnetic multipole expansion. Note however that the parity of the magnetic moments is opposite to those of electric moments: electric moments of order l have parity $(-1)^l$ and magnetic moments of order l have parity $(-1)^{l+1}$. This is due to the vectorial nature of the electric field and to the axial-vectorial nature of the magnetic field.

One can translate these results in quantum mechanics and calculate the matrix elements of the moments, which are now tensorial operators. One calculates the expectation value of the moments between two states of the system. As the wave function associated with the ket $|\Xi_{n_1,l_1,m_1}\rangle$ can be split in a radial part and an angular part described by the spherical harmonics, one can write:

$$\langle \Xi_{n_1,l_1,m_1}|Q_l^m|\Xi_{n_2,l_2,m_2}\rangle = \langle Q_l^m\rangle$$

$$=q\int_0^\infty r^2 R^*_{n_1,l_1} R_{n_2,l_2} dr$$

$$\int_0^\pi sin(\theta)d\theta \int_0^\pi Y_{l_1}^{m_1}{}^* Y_l^m Y_{l_2}^{m_2} d\phi$$

Using the Wigner-Eckart theorem for spherical harmonics, one can rewrite the angular integrals into Clebsh-Gorden coefficients. The angular integrals look like:

$$\langle l_2, l; 0, 0|l_1, 0\rangle\langle l_2, l; m_2, m|l_1, m_1\rangle$$

where we have dropped some normalisation constants. The physics we are interested in comes from the properties of the C.-G. coefficients. Using

$$\langle J_1, J_2, ; -m_1, -m_2 | J, -m \rangle = (-1)^{(J_1+J_2-J)} \langle J_1, J_2; m_1, m_2 | J, m \rangle$$

we get:

$$\langle l_2, l; 0, 0 | l_1, 0 \rangle = 0 \text{ if } l_1 + l_2 + l \text{ is odd}$$

and

$$\langle l_2, l; m_2, m | l_1, m_1 \rangle \neq 0 \text{ if } m_1 = m_2 + m \text{ and } |l_1 - l_2| \leq l \leq l_1 + l_2$$

Because of the inverse parity of the magnetic moments, one gets:

$$\langle l_2, l; 0.0 | l_1, 0 \rangle = \text{ if } l_1 + l_2 + l \text{ is even}$$

while the second condition remains the same.

Therefore, $\langle Q_l^m \rangle$ will not vanish only if:

$$m = 0 \quad \text{and} \quad 0 \leq l \leq 2l_1$$

Recall that l is even for electric moments and odd for magnetic moments. Therefore:

1) a spinless particle cannot acquire any moment

2) a spin $-$ 1/2 particle can acquire a magnetic dipole moment

3) a spin $-$ 1 particle can acquire a magnetic dipole moment and an electric quadrupole moment

and so on.

Here we went from a distribution to a particle state; associating l_1 with the spin of the particle. We are justified in doing so because we started with the potential *due* to the distribution. Clearly, we can reduce this to a particle since the multipole moments of a particle cannot depend on the potential we put the particle in. In the same way, this multipole expansion of the distribution is independent of the potential we put it in. In going to quantum mechanics, all the arguments applied for a distribution apply as well for a particle.

So, as we consider the W boson as a spin-1 particle, it will interact via its charge, its magnetic dipole moment and its electric quadrupole moment only.

One should say a word here about composite objects. If one has an extended composite object (proton or neutron for example) the argument still holds because the only vector available is the spin of the particle. Therefore, in spite of its compositeness, the system can still be considered as a particle as far as this argument goes. This is why it is so important[101] to measure the electric dipole moments of particles: they are supposed to be 0 in exact symmetries! If one allows the breaking of CP or T symmetries, the particles can acquire such moments. So the neutron is allowed to gain an electric dipole moment that will arise from weak interaction effects where both C and P are violated.

Furthermore, one sees that the classical multipole expansion is senseless for a neutral particle but perfectly correct for a neutral distribution. Therefore, at tree level, one expects all moments of a neutral particle to vanish. The fact that the neutron has a large magnetic moment uncovers its compositeness. At loop level, a neutral particle can acquire small magnetic dipole and electric quadrupole moments. Some other symmetries can forbid it though. For example, the photon will not acquire any moment to any order, while the neutrino can have a magnetic moment to the loop level if it is allowed to have a mass.

These considerations explain why we mention only the magnetic dipole moment and the electric quadrupole moment in the thesis. We consider CP and T as exact symmetries. Since there is no confusion possible, we will loosely use magnetic moment and quadrupole moment to designate magnetic dipole moment and electric quadrupole moment respectively.

We now justify the specific form of the vertex that we used. Again we will start from quantum mechanics. In QM, the magnetic and quadrupole operators of a system are defined as[33]:

$$\mu_i = \frac{1}{2}\epsilon_{ijk}\int d^3x \;\; x_j J_k(x)$$

$$Q_{i,j} = \int d^3x(3x_i x_j - x^2\delta_{i,j})\rho(x)$$

where $\rho(x)$ and $J(x)$ are charge and current densities respectively. The intrinsic magnetic moment $\mathcal{M}$ and quadrupole moment Q_E of a particle are defined as the matrix element of the operators for a positively charged particle at rest with the spin eigenstate $S_3 = +1$. This is to say:

$$\mathcal{M} \equiv \langle p = 0, S_3 = 1|\mu_3|p = 0, S_3 = 1\rangle$$

$$Q_E \equiv \langle p = 0, S_3 = 1|Q_{3,3}|p = 0, S_3 = 1\rangle.$$

Note that $Q_{3,3}$ is the Q_2^0 of the previous notation; recall that m had to be zero for the matrix element to not vanish.

Going back to classical EM, we recall that the magnetic moment of a system will interact with the magnetic field through $\vec{\mathcal{M}}\cdot\vec{B}$. The electric quadrupole moment will interact with the electric field gradient through $Q_{i,j}(\partial E_i/\partial x_j)$.[ref. 102] In

deriving the equations of interactions, terms proportional to these forms will give the magnetic moment and quadrupole moment.

It is a nontrivial matter to go from these nonrelativistic relations to the field theoretic forms of the vertices. The reader is referred to the literature for the details of the calculations[103]. We will merely show an argument due to Cheng and Li[4]. We will calculate the magnetic moment of the W boson at tree level. We use the γW^+W^- vertex as defined in fig. 3.1. The vertex reads:

$$\Gamma^{\mu\nu\lambda} = ie\Big\{(k_1 - k_2)_\nu g^{\lambda\mu} + (k_2 - k_3)_\lambda g^{\mu\nu} + (k_3 - k_1)_\mu g^{\lambda\nu}\Big\}.$$

Using the on-shell condition and $k_1 + k_2 + k_3 = 0$, one can rewrite this vertex as:

$$\Gamma^{\lambda\mu\nu} = ie\Big\{2(k_1^\nu g^{\lambda\mu} - k_1^\mu g^{\lambda\nu}) + (k_2 - k_3)^\lambda g^{\mu\nu}\Big\}$$

As the moments are defined in the 0-momentum limit, we can use the following 4-vectors:

$$k_2^\mu \approx (M, -\frac{\vec{k}}{2}) \quad k_3^\nu \approx (-M, -\frac{\vec{k}}{2}) \quad k_1 \approx (0, \vec{k})$$

for $M \gg |\vec{k}|$. We assumed that k_1 is the photon momentum. The polarisation vectors for the charged particles are:

$$\varepsilon_2^\mu = (-\frac{\vec{k}\cdot\vec{e}_2}{2M}, \vec{e}_2) \quad \varepsilon_3^\nu = (\frac{\vec{k}\cdot\vec{e}_3}{2M}, \vec{e}_3)$$

where $\vec{e}_i$ are unit vectors. These obeys the conditions $\varepsilon_2 \cdot k_2 \approx 0 \approx \varepsilon_3 \cdot k_3$

Now we let the W boson interact with the photon: we contract $\Gamma^{\lambda\mu\nu}\varepsilon_2^\mu\varepsilon_3^\nu A^\lambda$ and obtain an expression that looks like:

$$\sim ie\{-2\frac{(\vec{k}\times\vec{A})\cdot(\vec{e}_2\times\vec{e}_3)}{2M} - A^0(\vec{e}_2\cdot\vec{e}_3)\}.$$

So we can identify the second term with the charge of the particle and the first one with the magnetic moment; with a gyromagnetic ratio, g_V, of 2. This is in agreement with the general result that the tree level of any non-strongly interacting particle will have a magnetic moment given by[103]:

$$\mathcal{M}_0 = s\frac{e}{m}$$

where s and m are the spin and mass of the particle, respectively.

If we had kept an anomalous term, following Lee and Yang[43], the vertex would have read:

$$\Gamma^{\lambda\mu\nu} = ie\Big\{(1+\kappa)(k_1^\nu g^{\lambda\mu} - k_1^\mu g^{\lambda\nu}) + (k_2 - k_3)^\lambda g^{\mu\nu}\Big\}$$

and

$$\mathcal{M} \equiv (1+\kappa)\frac{e}{2M_W}$$

The name "anomalous" associated to κ refers to the fact that the loop corrections are shuffled into this parameter in the same way that the "anomalous magnetic moment" of the electron refers to the higher order corrections being absorbed into $(g-2)_e$.

This explains that we have, at tree level:

$$\mathcal{M} \equiv (1+\kappa)\frac{e}{2M_W}$$

The calculation of the quadrupole moment is more involved; one would associate the term coupled with $\vec{k}^2 A^0$ with the quadrupole moment since the second

spacial derivative of the potential is the field gradiant; which is coupled to the quadrupole moment. One can derive the expression to be, at tree level with an anomalous term:

$$Q_E \equiv \frac{-e\kappa}{M_W^2}.$$

We emphasize again that $\kappa \equiv 1$ at tree level in the SM. In going to higher orders, we want to add to our tree level vertex. We will then have some corrections to κ, which we call $\Delta\kappa$. As this variable occured in front of the photon momentum, we would like the correction to this parameter to appear also in front of the photon momentum. The fact that κ occured in front of the photon momentum gave this nice interpretation that we have; if it were to occur elsewhere, it would not lead to the same interpretation. So, we would like to add a term like:

$$\Delta\kappa(k_1^\nu g^{\lambda\mu} - k_1^\mu g^{\lambda\nu}).$$

There exists another kernel of momentum that is also gauge- and CP- invariant and did not appear at tree level. Namely:

$$\Delta Q(k_2 - k_3)^\lambda \frac{k_1^\mu k_1^\nu}{M_W^2}$$

where the denominator is simply to keep the units straight so that the parameter ΔQ is also dimensionless. So we write our vertex as:

$$\Gamma^{\lambda\mu\nu} = ie\Big\{A\{2(k_1^\nu g^{\lambda\mu} - k_1^\mu g^{\lambda\nu}) + (k_2 - k_3)^\lambda g^{\mu\nu}\}$$

$$+ \Delta\kappa(k_1^\nu g^{\lambda\mu} - k_1^\mu g^{\lambda\nu})$$

$$+ \frac{\Delta Q}{2M_W^2}(k_2 - k_3)^\lambda k_1^\mu k_1^\nu\Big\}$$

where the factor of 2 in the last term is a matter of definition.

To see how these terms will change $\mathcal{M}$ and Q_E one has to do the same type of calculations we sketched before. The result is that $\mathcal{M}$ and Q_E now become:

$$\mathcal{M} \rightarrow \frac{e}{2M_W}(1 + (\kappa + \Delta\kappa) + \frac{\Delta Q}{2})$$

$$Q_E \rightarrow -\frac{e}{M_W^2}((\kappa + \Delta\kappa) - \frac{\Delta Q}{2})$$

These are the corrections that we can expect in a CP-invariant theory. It certainly is possible to work with more general vertices[42,48] and allow CP- and T-violation. In these models, particles can acquire electric dipole and magnetic quadrupole moments besides the ones they have here. If one assumes that these symmetries are exact as we did here, the vertex we used is the most general.

APPENDIX VI

Calculation of $\Delta\kappa$ and ΔQ in the SM Framework.

In this appendix, we will show briefly how the calculation of $\Delta\kappa$ and ΔQ is performed in the SM framework. The couplings are given in Appendix IV. We will concentrate on the fermion loop contribution shown on fig. 18 and reproduced here with internal momenta and indices on fig. 33.

Figure 33. Fermion loop correction to κ.

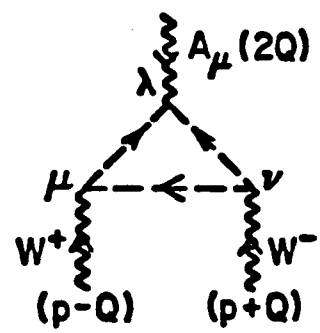

This defines the internal momenta that we used for the calculation of $\Delta\kappa$ and ΔQ in the SM.

Following Bardeen [68], we impose the on-shell condition and gauge invariance, which translate into:

$$(p-Q)^2 = M_W^2 \qquad (p+Q)^2 = M_W^2 \qquad 2Q^2 = 0$$

and

$$Q_\lambda = 0 \qquad (p-Q)_\mu = 0 \qquad (p+Q)_\nu = 0.$$

One must also remember the famous -1 amplitude factor for any fermion loop. This diagram then becomes, after a few lines of algebra:

$$\int \frac{d^4k}{(2\pi)^4} \frac{-2g^2e}{8\ \mathrm{DEN}} Tr\{(1+\gamma_5)\gamma_\mu(\not{p}-\not{k})\gamma\nu(\not{k}+\not{Q}-M_p)\gamma_\lambda(\not{k}-\not{Q}-M_p)\}$$

where

$$\mathrm{DEN} \equiv \left[(p-k)^2 - M_t^2\right]\left[(k+Q)^2 - M_p^2\right]\left[(k-Q)^2 - M_p^2\right].$$

We drop the γ_5 term because it is involved in the anomaly terms and will cancel exactly with the quarks contribution to the anomaly.

At this point, it is worthwhile to explain in some details what is meant by the anomaly. Anomalies are closely linked with renormalization and Ward-Takahashi (W-T) identities. Renormalization makes extensive use of the intricate cancellations of a gauge theory and the W-T identities preserve these cancellations to higher orders; thus preserving renormalizability to loop level. However, there are cases where conservation laws derived from gauge invariance through Noether's theorem are verified at tree level but violated at loop level. The terms that violate at loop level the tree level conservation laws are called anomalies. Anomalies will violate W-T identities and can spoil renormalizability of a model. Therefore, each anomaly term must vanish on its own or different anomaly terms must cancel identically for a model to be acceptable.

The anomalies were first investigated by Schwinger in 1951 and more extensively by Adler and by Bell and Jackiw in 1969; it is known as the ABJ anomaly.

What these authors found is that an axial current of interacting fields that is conserved at tree level ($\partial_\mu J^5_\mu = 0$) can be violated at loop level ($\partial_\mu J^5_\mu \neq 0$). They also found that anomalies can occur only as the result of 1-loop diagram and that diagrams without fermion cannot lead to an anomaly. This means that a triangle diagram with fermions and AAA or VVA couplings can lead to an anomaly. It is known that anomalies that might arise from higher order diagrams are related to the anomalies that arise from the triangle diagram: if there is no anomaly from the triangle diagram, the model is anomaly-free.[104] An explicit calculation of an anomaly term can be found in ref. 4 for example. It can be summarised as follows: some divergent integrals forbid a change of integration variable that would allow respect for both the vector and the axial W-T identities. Therefore it is impossible to respect both and this leads to the anomaly term. It was shown by Jackiw[105] that for divergent integrals a change of variable is illegitimate and in fact gives rise to a surface term which is essentially the anomaly.

In order to have an anomaly-free theory, each anomaly term must vanish or different anomaly terms must cancel. In the SM , it has been verified that the anomaly terms that arise from the leptons will exactly cancel the anomaly terms that arise from the quarks. These cancellations require three types of quarks for each lepton family and support strongly the concept of colour.[83]

In our case, we have a fermion loop and the couplings are of the form: (V-A)V(V-A); we will certainly have an anomaly term. The anomaly will arise from the AVV term and is represented by the γ_5 term. The term that we neglected is the contribution to the anomaly from the fermions and the lepton term will exactly cancel the quark term. This justifies the dropping of the γ_5 term.

At this point, we use the Feynman parameter[106] trick:

$$\frac{1}{ABC} \equiv 2\int_0^1 dx \int_0^{1-x} dy \frac{1}{\Big[Ax + By + C(1-x-y)\Big]^3}$$

which in our case translates into

$$A \equiv (k+Q)^2 - M_p^2 \qquad B \equiv (k-Q)^2 - M_p^2 \qquad C \equiv (p-Q)^2 - M_t^2$$

After some algebra, one brings the expression in the form:

$$\frac{-4eg^2}{8(2\pi)^4}\int_0^1 dx \int_0^{1-x} dy \int d^4k \frac{1}{\left[k^2 + 2k(xS + yD - p) + \tilde{M}^2(1-x-y) - M_p^2\right]^3}\Bigg\{$$

$$(1) \qquad Tr(\gamma_\mu \not{p}\gamma_\nu \not{k}\gamma_\lambda \not{k}) \quad - Tr(\gamma_\mu \not{k}\gamma_\nu \not{k}\gamma_\lambda \not{k}) \qquad (5)$$

$$(2) \quad - Tr(\gamma_\mu \not{p}\gamma_\nu \not{k}\gamma_\lambda \not{Q}) \quad + Tr(\gamma_\mu \not{k}\gamma_\nu \not{k}\gamma_\lambda \not{Q}) \qquad (6)$$

$$(3) \quad + Tr(\gamma_\mu \not{p}\gamma_\nu \not{Q}\gamma_\lambda \not{k}) \quad - Tr(\gamma_\mu \not{k}\gamma_\nu \not{Q}\gamma_\lambda \not{k}) \qquad (7)$$

$$(4) \quad + (M_p)^2 Tr(\gamma_\mu \not{p}\gamma_\nu\gamma_\lambda) \quad - (M_p)^2 Tr(\gamma_\mu \not{k}\gamma_\nu\gamma_\lambda) \quad (8)\Bigg\}$$

where

$$S \equiv p + Q \qquad D \equiv p - Q \qquad \tilde{M}^2 \equiv M_W^2 - M_t^2 + M_p^2$$

From power counting, one sees that terms (1),(5),(6) and (7) diverge. One has to handle these terms carefully as parts of them will diverge and parts will be finite. Using dimensional regularization, one then proceeds to do this part of

the integration program. One must also make extensive use of gauge invariance in order to bring all terms in one of the four forms:

$$p^\lambda Q^\mu Q^\nu, \quad p^\lambda g^{\mu\nu}, \quad Q^\mu g^{\lambda\nu}, \quad Q^\nu g^{\lambda\mu}.$$

Once the four-dimensional integrals are done, one should rewrite the denominator in the more handy form:

$$(x+y)^2 - F(x+y) + \delta$$

with

$$\delta \equiv (M_t/M_W)^2, \quad \varepsilon \equiv (M_p/M_W)^2 \quad \text{and} \quad F \equiv 1 + \delta - \varepsilon.$$

After a lengthy exercise of algebra, one gets the following contributions from *the finite parts of (1)-(8)*:

$$K \int_0^1 dx \int_0^{1-x} dy \frac{1}{M_W^2\Big[(x+y)^2 - F(x+y) + \delta\Big]} \Bigg\{$$

$$- 64 p^\lambda Q^\mu Q^\nu (x+y-1)(xy)$$

$$- 4 M_W^2 p^\lambda g^{\mu\nu} \Big[(x+y-1)^2(x+y) + (x+y)\varepsilon\Big]$$

$$- 8 M_W^2 (Q^\mu g^{\lambda\nu} - Q^\nu g^{\lambda\mu}) \Big[(x+y-1)(x+xy+x^2) - x\varepsilon\Big] \Bigg\}$$

where K is a constant.

As they stand now, these integrals are horrible to do. There is a nice substitution that one can perform to make life much easier:

$$x = ut \qquad y = (1-u)t$$

so that

$$(x+y)=t \qquad xy = ut^2 - u^2t^2$$

and the Jacobian is $-t$.

It so happens that the integrations on u are all very simple and one is left with the integrations over t. The expression now looks like:

$$K\int_0^1 \frac{dt}{M_W^2\left[t^2 - tF + \delta\right]}\Bigg\{$$

$$-\,64p^\lambda Q^\mu Q^\nu (1/6)(t^4 - t^3)$$

$$-\,4M_W^2 p^\lambda g^{\mu\nu}(t^4 - 2t^3 + t^2(1+\varepsilon))$$

$$-\,4M_W^2(Q^\mu g^{\lambda\nu} - Q^\nu g^{\lambda\mu})(t^4 - t^2(1+\varepsilon))\Bigg\}$$

The integrals are now much more managable; still not that easy...

The divergent parts arise from terms (1), (5), (6), (7). After some algebra, they will take the form:

$$J\int_0^1 dx \int_0^{1-x} \frac{\Gamma(\epsilon)\left[2p^\lambda g^{\mu\nu}(x-1) + 2(Q^\mu g^{\lambda\nu} - Q^\nu g^{\lambda\mu})(1+x)\right]}{\left[(x+y)^2 - F(x+y) + \delta\right]^\epsilon}$$

where Γ is the standard gamma function and the limit $\epsilon \to 0$ must be taken. Part of this expression will diverge as the limit is taken. However, the exponent at the denominator makes things not so clear.

One rewrites:

$$\frac{\Gamma(\epsilon)}{[\quad]^{\epsilon}} \equiv \Gamma(\epsilon)e^{-\epsilon ln[\quad]}$$

$$\equiv \Gamma(\epsilon)\big[1-\epsilon ln[\quad]\big]$$

$$\approx \Gamma(\epsilon) - ln[\quad]$$

where the approximation is exact when $\epsilon \to 0$. We used the fact that $\Gamma(\epsilon) \sim 1/\epsilon$ to reach the last line.

Using the same substitution as before: $x = ut,\ \ y = (1-u)t$ one ends up with the following expressions:

$$-\Gamma(\epsilon)\Big[(4/3)(Q^{\nu}g^{\lambda\mu} - Q^{\mu}g^{\lambda\nu}) + (2/3)p^{\lambda}g^{\mu\nu}\Big]$$

$$+\int_0^1 \Big[2(Q^{\nu}g^{\lambda\mu} - Q^{\mu}g^{\lambda\nu})(t+(1/2)t^2) + 2p^{\lambda}g^{\mu\nu}(t-(1/2)t^2)\Big] ln\big[t^2 - tF + \delta\big]dt$$

After some more algebra, one writes the expression as:

$$\Big[2p^{\lambda}g^{\mu\nu} + 4(Q^{\nu}g^{\lambda\mu} - Q^{\mu}g^{\lambda\nu})\Big]\Big[-(1/3)\Gamma(\epsilon) + (1/3)ln(\varepsilon)\Big]$$

$$+ 2p^{\lambda}g^{\mu\nu}\int_0^1 \frac{(F/2)t^2 - (1+(F/6))t^3 + (1/3)t^4}{t^2 - tF + \delta}dt$$

$$+ 2(Q^{\nu}g^{\lambda\mu} - Q^{\mu}g^{\lambda\nu})\int_0^1 \frac{(F/2)t^2 - (1-(F/6))t^3 - (1/3)t^4}{t^2 - tF + \delta}dt$$

Now we can put all things together. We start with the ΔQ term since it is easier:

$$\frac{-ieg^2}{6\pi^2 M_W^2}p^{\lambda}Q^{\mu}Q^{\nu}\int_0^1 \frac{t^4 - t^3}{t^2 - tF + \delta}dt = ie\Delta Q\frac{4}{M_W^2}p^{\lambda}Q^{\mu}Q^{\nu}$$

so that

$$\Delta Q = -3\frac{g^2}{72\pi^2}\int_0^1 \frac{t^4 - t^3}{t^2 - tF + \delta}$$

We now turn to the $\Delta\kappa$ term. This one is more involved. Adding all contributions, we get:

$$\frac{-ieg^2}{16\pi^2}\Bigg\{p^\lambda g^{\mu\nu}\Big[-(2/3)\Gamma(\epsilon) + (2/3)ln(\varepsilon)$$

$$+\int_0^1 \frac{t^2(F-1-\varepsilon) - (F/3)t^3 - (1/3)t^4}{t^2 - tF + \delta}dt\Big]$$

$$+2(Q^\nu g^{\lambda\mu} - Q^\mu g^{\lambda\nu})\Big[-(2/3)\Gamma(\epsilon) + (2/3)ln(\varepsilon)$$

$$+\int_0^1 \frac{(1/2)t^2(F-1-\epsilon) + t^3((F/6)-1) + (1/6)t^4}{t^2 - tF + \delta}dt\Big]\Bigg\}$$

which is :

$$\frac{-ieg^2}{16\pi^2}\Bigg\{\cdot\Big[p^\lambda g^{\mu\nu} + 2(Q^\nu g^{\lambda\mu} - Q^\mu g^{\lambda\nu})\Big]$$

$$\times\Big[-(2/3)\Gamma(\epsilon) + (2/3)ln(\varepsilon)$$

$$+\int \frac{t^2(F-1-\varepsilon) - (F/3)t^3 - (1/3)t^4}{t^2 - tF + \delta}dt\Big]$$

$$+2(Q^\nu g^{\lambda\mu} - Q^\mu g^{\lambda\nu})\times$$

$$\int_0^1 \frac{(1/2)t^4 + t^3((F/2)-1) - (1/2)t^2(F-1-\varepsilon)}{t^2 - tF + \delta}dt\Bigg\}$$

The first part will be absorbed into the constant A of the vertex and the second one is the $\Delta\kappa$ term that we want. More precisely:

$$2\Delta\kappa = \frac{-g^2}{16\pi^2}\int_0^1 \frac{t^4 + t^3(F-2) + t^2(1+\varepsilon - F)}{t^2 - tF + \delta}dt$$

so that

$$\Delta\kappa = -3\frac{g^2}{96\pi^2}\int_0^1 \frac{t^4 + t^3(F-2) + t^2(1+\varepsilon - F)}{t^2 - tF + \delta}dt$$

We have calculated the lepton loop only. Obviously, the integrals are the same for quark loops and only overall charge and colour factors will change. So this result stands for any massive fermion loop.

APPENDIX VII

Calculation of $\Delta\kappa$ and ΔQ in a Two-Higgs-Doublet Model.

In this appendix, we will outline the procedure to calculate $\Delta\kappa$ and ΔQ in a two-Higgs-doublet model (THD). We will concentrate on the triangle diagram of fig. 26-a that we reproduce here with internal momentum and indices on fig. 34. As the Higgs particles are scalars, their couplings are easier than fermionic ones and the calculation itself is shorter.

Figure 34. Higgs-boson loop correction to κ.

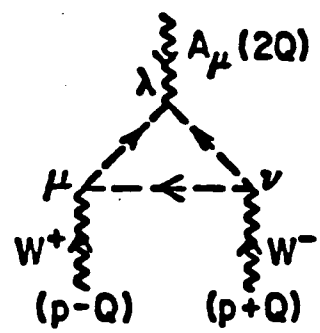

This defines the internal momenta that we used for the calculation of $\Delta\kappa$ and ΔQ in the THD model.

Again, we require on-shell condition and gauge invariance so that:

$$(p-Q)^2 = M_W^2 \qquad (p+Q)^2 = M_W^2 \qquad 4Q^2 = 0$$

and

$$Q^\lambda = 0 \qquad (p-Q)^\mu = 0 \qquad (p+Q)^\nu = 0.$$

After a few straightforward lines, we write this vertex as:

$$2g^2 e \int \frac{d^4k}{(2\pi)^4} \frac{(Q-k)^\mu \; k^\lambda \; (Q+k)^\nu}{\left[(k-Q)^2 - M_p^2\right]\left[(k+Q)^2 - M_p^2\right]\left[(k-p)^2 - M_t^2\right]} \qquad (A-VII.1)$$

Using the Feynman parameters, one quickly gets:

$$4g^2 e \int_0^1 dx \int_0^{1-x} dy \int \frac{d^4k}{(2\pi)^4} \frac{\left[Q^\mu Q^\nu k^\lambda + Q^\mu k^\nu k^\lambda - Q^\nu k^\mu k^\lambda - k^\mu k^\nu k^\lambda\right]}{\left[k^2 - 2k\cdot\left[p - xS - yZ\right] + \tilde{M}^2(1-x-y) - M_p^2\right]^3} \qquad (A-VII.2)$$

where

$$\tilde{M}^2 \equiv M_W^2 - M_t^2 + M_p^2 \qquad S \equiv p+Q \qquad Z \equiv p-Q.$$

These are all the terms involved!

Using the little table of 4-dimensional integrals, one obtains:

$$\int_0^1 dx \int_0^{1-x} dy \Big\{ p^\lambda Q^\mu Q^\nu \frac{(-4xy)(x+y-1)}{D}$$

$$+ Q^\nu \frac{\Gamma(\epsilon)}{D^\epsilon}(y g^{\mu\lambda}) - Q^\mu \frac{\Gamma(\epsilon)}{D^\epsilon}(x g^{\nu\lambda}) \qquad (A-VII.3)$$

$$- p^\lambda \frac{\Gamma(\epsilon)}{D^\epsilon}(1/2) g^{\mu\nu}(x+y-1)\Big\}$$

where we omitted a few constants and where

$$D \equiv (x+y-1)^2 + R^2(x+y-1) + \rho^2$$

with

$$R^2 \equiv \frac{\tilde{M}^2}{M_W^2} \qquad \rho^2 \equiv \frac{M_p^2}{M_W^2}.$$

Again, we can rewrite the denominator as we did in the SM case. Note also that the expression is symmetric in x and y, as it must be.

The anomalous quadrupole moment part can be calculated immediately since all terms are finite. We find:

$$\frac{16ieg^2}{32\pi^2 M_W^2}\int_0^1 dx \int_0^{1-x} dy \frac{(xy)(x+y-1)}{D} p^\lambda Q^\mu Q^\nu$$

$$= 4ie\frac{\Delta Q}{M_W^2} p^\lambda Q^\mu Q^\nu \qquad (A-VII.4)$$

so that:

$$\Delta Q = \frac{4g^2}{32\pi^2}\int_0^1 dx \int_0^{1-x} dy \frac{(xy)(x+y-1)}{D} \qquad (A-VII.5)$$

which, using the substitution $x = ut$ and $y = (1-u)t$ can be written as:

$$\Delta Q = \frac{g^2}{48\pi^2}\int_0^1 \frac{t^4 - t^3}{t^2 - tF + \delta} dt \qquad (A-VII.6)$$

with

$$\delta \equiv \frac{M_t^2}{M_W^2} \qquad \varepsilon \equiv \frac{M_p^2}{M_W^2} \qquad F \equiv 1 + \delta - \varepsilon$$

This is the expression that we gave in Chapter IV.

We now turn to the calculation of $\Delta\kappa$, which is a bit more involved.

By symmetry in x and y, the remaining terms can be written as:

$$\int_0^1 dx \int_0^{1-x} \frac{\Gamma(\epsilon)}{D^\epsilon}\Big[-(1/2)p^\lambda g^{\mu\nu}(2x-1) + (Q^\nu g^{\lambda\mu} - Q^\mu g^{\lambda\nu})x\Big] \qquad (A-VII.7)$$

where one must take the limit $\epsilon \to 0$. Again, we use

$$\frac{\Gamma(\epsilon)}{D^\epsilon} = \Gamma(\epsilon) - ln(D)$$

and we rewrite D as:

$$(x+y)^2 - (x+y)F + \delta$$

with the definitions as before.

After integration, the $\Gamma(\epsilon)$ term leads to:

$$(1/6)\Gamma(\epsilon)\Big[(1/2)p^\lambda g^{\mu\nu} + (Q^\nu g^{\lambda\mu} - Q^\mu g^{\lambda\nu})\Big] \qquad (A-VII.8)$$

which is absorbed into the constant A of the vertex. The log term, on the other hand, leads to:

$$-\Big\{ \cdot \int_0^1 dx \int_0^{1-x} dy\ ln(D)\ \left[p^\lambda g^{\mu\nu}(-1/2)(2x-1) - (2x-1)(Q^\nu g^{\lambda\mu} - Q^\mu g^{\lambda\nu})\right]$$

$$+ \int_0^1 dx \int_0^{1-x} dy\ ln(D)\ (Q^\nu g^{\lambda\mu} - Q^\mu g^{\lambda\nu})(3x-1)\Big\}$$

$$(A-VII.9)$$

The first part will again be absorbed into the constant A of the vertex and the second part leads to the $\Delta\kappa$ term that we want.

With all the constants, we have:

$$\Delta\kappa = \frac{g^2}{16\pi^2}\int_0^1 dx \int_0^{1-x} dy(3x-1)\ ln\left[(x+y)^2-(x+y)F+\delta\right] \qquad (A-VII.10)$$

Using the $u\ t$ transformation, one gets:

$$\Delta\kappa = \frac{g^2}{16\pi^2}\int_0^1 \left[(3/2)t^2-t\right]\ ln\left[t^2-tF+\delta\right]dt \qquad (A-VII.11)$$

which, by partial integrations can be brought in its final form:

$$\Delta\kappa = -3\frac{g^2}{96\pi^2}\int_0^1 \frac{-2t^4+(2+F)t^3-Ft^2}{t^2-tF+\delta}dt \qquad (A-VII.12)$$

This is the most "transparent" form of these expressions. In performing the integrals, it is better to integrate by parts first and bring the expressions to a few terms and two integrals that are in t^0 and t^1 over the denominator.

APPENDIX VIII

Constraints on the mass of the Higgs boson.

In this appendix, we will discuss some bounds that can be derived for the mass of the Higgs particle. As mentioned earlier, the mass of this particle is free in the SM, and it will remain so in any model that uses SSB and the Higgs mechanism to generate masses for the gauge-bosons. The discussion will be twofold: in the first part, we will discuss bounds that were derived in a SM context but have broader applications while in the second part we will discuss bounds dived in a multi-Higgs-doublet framework.

I Standard Model.

Starting from the famous mexican hat potential:

$$V = -\frac{\mu^2}{2}(\phi^\dagger\phi) + 1/4\lambda(\phi^\dagger\phi)^2 \qquad (A-VIII.1)$$

if $\mu^2 \geq 0$ the potential has a minimum at $\phi^2 = \mu^2/\lambda$. One then rewrites the vev of ϕ as:

$$\langle\phi\rangle = \begin{pmatrix} 0 \\ a/\sqrt{2} \end{pmatrix}$$

and one sees that $a^2 = 2\mu^2/\lambda$. The vev is well defined through the Fermi constant that has been measured precisely for a number of years. However, λ is undefined. As a result, the mass of the Higgs particle, $2\mu^2$, is undefined and one cannot relate it to any physical quantity measurable in the laboratory. Since the SM is known, physicists have tried to constrain this free parameter.

In the SM framework, all couplings involving the Higgs particle are well defined; all of them are proportional to the mass of the other particle at the vertex[4,92]. This

in itself is not a problem. It simply means that the Higgs will decay preferentially to heavy quarks if it is not very massive but will overwhelmingly decay into gauge bosons if its mass is above 200 GeV or so[107]. However, one can run into consistency problems by using the Higgs particle and its couplings as defined in the SM. Indeed, for large Higgs masses, the dominant decay modes are:

$$H \to W^+W^-, \qquad H \to Z^0Z^0.$$

As the mass of the Higgs increases, so does its width. Beyond a critical mass, M_c, the width approaches the mass; which is a feature of a strongly coupled theory. Which means that perturbation theory breaks down! Along this line of thought, it has been , and still is, very popular to do a partial wave analysis of some processes and to require unitarity to not be violated. This, sometimes, allows one to set reasonable bounds on the particles concerned. Lee, Quigg and Thacker did so for the Higgs in the SM context[62]. They performed a partial wave analysis on different processes:

$$W_l^+ \; W_l^- \to W_l^+ \; W_l^-$$

$$Z_l \; Z_l \to Z_l \; Z_l$$

$$Z_l \; Z_l \to W_l^+ \; W_l^-$$

where l stands for longitudinal.

They found that the most divergent contributions were from the longitudinal part of the bosons. This should not be too surprising since these components are the would-be Goldstone bosons and were part of the Higgs sector. Their partial wave analysis was defined as follows:

$$T(s,t) = 16\pi \sum_J (2J+1) a_J(s) P_J(cos(\theta)) \qquad (A-VIII.2)$$

and

$$a_J = A(q/M_W)^4 + B(q/M_W)^2 + C.$$

In this way, they calculated, for example:

$$a_0(W_l^+W_l^- \to W_l^+W_l^-) = \\ -\frac{G_F M_H^2}{8\pi\sqrt{2}}\left[2+\frac{M_H^2}{s-M_H^2}-\frac{M_H^2}{S}Ln(1+\frac{s}{M_H^2})\right] \qquad (A-VIII.3)$$

in the limit where $s, M_H^2 \gg M_W^2, M_Z^2$. In order to not violate unitarity, one requires $|a_0| \leq 1$. Assuming $s \gg M_W^2$, one obtains:

$$a_0 \to -\frac{G_F M_H^2}{4\pi\sqrt{2}} \qquad (A-VIII.4)$$

Therefore, one would like:

$$M_H^2 \leq \frac{4\pi\sqrt{2}}{G_F} \approx 1(TeV/c)^2 \qquad (A-VIII.5)$$

This bound is interpreted as the limit where perturbation theory is reliable. If the mass of the Higgs is larger than 1 TeV, perturbation theory breaks down and higher order effects will become more and more important. Of course, if the mass is slightly less than 1 TeV, higher order contributions will also be important, but unitarity will be preserved.

Recently, Gaillard and Chanowitz[108] inverted the argument and looked at a the effects of a very massive Higgs boson; they assumed $M_H^2 \gg s$. From this point of view, one sees that unitarity is violated for $\sqrt{s} \approx 2$ TeV, so that the tree approximation will not be reliable for $\sqrt{s} \geq 2$ TeV.

We used the result from Lee, Quigg, Thacker to set the upper limit of the mass of the Higgs at 1 TeV.

A lower bound on the mass can also be derived.[86,109] From the form of the potential, for appropriate values of μ^2 and λ, one gets the standard mexican hat. However,if one decreases the value of μ^2 sufficiently, one can change this potential into a less "binding" form, where the vev is now a relative minimum and the real minimum is a t the origin. Certainly, it is still possible for the fields to acquire

a vev, but one can argue that the vacuum is not stable since it is only a relative minimum and can tunnel to the origin. By requiring the vev to be an absolute minimum, one can derive a minimum value for the mass of the Higgs.

Through arguments along these and cosmological considerations, Coleman, Weinberg[110] and Linde derived a lower limit of 10 GeV for the mass of the Higgs. Note that this bound is beyond the Upsilon state. Thus the the Higgs cannot be observed in Upsilon decays, as was thought for a while.

II Multi-Higgs-Doublet Models.

We will describe two sources of constraints on the mass of the Higgs.

i) Flavour Changing Currents.

As mentioned before, any two Higgs doublet model faces large FCC and too large rates for rare processes like $\mu \rightarrow e\gamma, K \rightarrow \mu\mu, K \rightarrow \mu e$ and too large a value for the mass difference between K_L and K_S, which is approximately 10^{-5}ev experimentally. Of all these, it is generally recognised that the mass difference of the Kaon system is the more stringent.

Using a model with one doublet (coupling to all fermions) per generation, previous calculations[111] concluded that the mass of the FC Higgs had to be:

$$\begin{aligned} M_H^2 \geq & \frac{2\sqrt{2}G_F m_b^2}{\Delta M_K} \times 8.5 \times 10^{-2} GeV^3 \\ & \sim (150 TeV)^2 \end{aligned} \quad . \qquad (A-VIII.6)$$

However, a key assumption in this derivation was that all elements of the Yukawa-mass-matrix were comparable and of the same order of the heaviest fermion mass; thus the appearance of m_b only in the previous expression. This approxima-

tion has been challenged recently[84] and as a result, the mass of the FC Higgs has dropped to the order of 1 TeV and, given experimental uncertainties, it might very well be quite lower.

It is clear that these bounds involve many estimates of Yukawa mass matrix parameters and lead at the very best to estimates on the mass of the Higgs where the error is in the exponent!

ii) Renormalization Group Equations.

From a completely different point of view, renormalization group equations allowed to put some bounds on the masses of the different Higgs particles that arise in a multi-Higgs-doublet model. Starting fom a potential similar to the one we used, one can derive[89] renormalization group equations for the five coupling constants λ_i. These equations are dictated by the interaction structure of the model. At the one-loop level, one gets:

$$\begin{aligned} 8\pi^2 \frac{d\lambda_1}{dt} =& 6\lambda_1^2 + 2\lambda_3^2 + 2\lambda_3\lambda_4 + \lambda_4^2 + \lambda_5^2 \\ & - ((3/2)g_1^2 + (9/2)g_2^2)\lambda_1 \\ & + (3/8)g_1^4 + (3/4)g_1^2 g_2^2 + (9/8)g_2^4 \end{aligned} \qquad (A-VIII.7)$$

where

$$t \equiv 1/2 ln\left(\frac{-q^2}{M_W^2}\right)$$

and q^2 is the momentum transfer. Besides, g_1 and g_2 are the SU(2) and U(1) coupling constants respectively. Similar expressions hold for the other λ_i's.

The coupling constants will also evolve with energy:

$$8\pi^2 \frac{dg_1^2}{dt} = \left((20/9)N + (1/6)N_H\right)g_1^4$$
$$8\pi^2 \frac{dg_2^2}{dt} = \left((4/3)N + (1/6)N_H - (22/3)\right)g_2^4$$

where N is the number of quark and lepton families. (taken to be three.)

As we have shown in chapter IV, mass expressions can be obtained from the potential; explicitly, the authors find:

$$\begin{aligned} m_1^2 + m_3^2 &\leq 2(f_1 + f_3)M_W^2/g_2^2 \\ m_2^2 &= 2f_2 M_W^2/g_2^2 \\ m_3^2 &\leq 2min(f_1, f_2)M_W^2/g_2^2 \\ m_4^2 &= 2f_4 M_W^2/g_2^2 \end{aligned} \qquad (A-VIII.8)$$

where the f_i are combinations of the λ_i's and the couplings are evaluated at $t = 0$. By solving numerically the previous differential equations, one can get some limit on the masses m_i^2. The main results are the following upper bounds:

$$\begin{aligned} (m_1^2 + m_3^2)^{1/2} &\leq 122 \ GeV \\ m_2 &\leq 121 \ GeV \\ m_3 &\leq 86 \ GeV \\ m_4 &\leq 120 \ GeV \end{aligned}$$

These results are in marked contrast with the previous bounds. One should remain cautious since this is only a one-loop calculation. The fact that the values obtained are so different from the previous is sufficient to arise one's suspicion...

These two examples suffice to show our point: as of today, there are no precise, reliable upper bounds on the mass of the Higgs. The partial wave analysis performed by Lee, Quigg, Thacker seems reliable but gives an upper mass of 1 TeV within a factor 2 or so. On the other hand, the lower bound is now out of the hand of the theorists and stems from experiments at PETRA-HERA which should have seen the particles (at least the charged ones) if they were lighter than 25 GeV. Therefore we set our limits at 1 TeV as the upper bound and an optimistic lower bound at 50 GeV.